UNCLASSIFIED

AD 267 493

*Reproduced by the*

ARMED SERVICES TECHNICAL INFORMATION AGENCY
ARLINGTON HALL STATION
ARLINGTON 12, VIRGINIA

UNCLASSIFIED

NOTICE: When government or other drawings, specifications or other data are used for any purpose other than in connection with a definitely related government procurement operation, the U. S. Government thereby incurs no responsibility, nor any obligation whatsoever; and the fact that the Government may have formulated, furnished, or in any way supplied the said drawings, specifications, or other data is not to be regarded by implication or otherwise as in any manner licensing the holder or any other person or corporation, or conveying any rights or permission to manufacture, use or sell any patented invention that may in any way be related thereto.

ASTIA FILE COPY 267493

267 493

10

FILE COPY
Return to
ASTIA
ARLINGTON HALL STATION
ARLINGTON 12, VIRGINIA
Attn: TIRS

First Quarterly Report

Covering the Period

May 15, 1961 - August 15, 1961

# TEMPERATURE INSENSITIVE TRANSISTOR

Research and Development

Contract No. DA 36-039 SC-87276

File No. 40550-PM-61-93-91(4124)

U. S. Army

Signal Research and Development Laboratory

Fort Monmouth, New Jersey

Hoffman Electronics Corporation
Semiconductor Division
1001 N. Arden Drive
El Monte, California

ASTIA
DEC 12 1961

$10.50

P-136

First Quarterly Report

Covering the Period

May 15, 1961 - August 15, 1961

# TEMPERATURE INSENSITIVE TRANSISTOR

Research and Development

Contract No. DA 36-039 SC-87276

File No. 40550-PM-61-93-91(4124)

Report Prepared by:

John Spanos, Project Leader

Dr. R. Epple

Report Approved by:

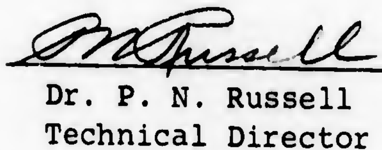

Dr. P. N. Russell
Technical Director

Hoffman Electronics Corporation
Semiconductor Division
El Monte, California

TABLE OF CONTENTS


| Section | Description | Page No. |
|---|---|---|
| | LIST OF ILLUSTRATIONS | iv |
| | PURPOSE | viii |
| | ABSTRACT | ix |
| | MEETINGS AND CONFERENCES | x |
| 1.0 | INTRODUCTION | 1 - 1 |
| 2.0 | THEORY | 2 - 1 |
| 2.1 | Temperature Dependence of Webster Equation | 2 - 1 |
| 2.2 | Dependency of W on Temperature | 2 - 2 |
| 2.3 | Emitter Region Conductivity | 2 - 3 |
| 2.4 | Base Region Mobility Ratio | 2 - 4 |
| 2.5 | Base Conductivity | 2 - 4 |
| 2.6 | Temperature Dependence of Z | 2 - 5 |
| 2.7 | Temperature Dependence of g(Z) | 2 - 6 |
| 2.8 | Electron Diffusion Coefficient in Base | 2 - 6 |
| 2.9 | Diffusion Length of Holes in Emitter | 2 - 7 |
| 2.10 | Diffusion Length of Electrons in Base | 2 - 7 |
| 2.11 | Diffusion Length of Holes in Base | 2 - 8 |
| 2.12 | The term $\frac{\partial}{\partial T}\left[\frac{s\ W\ A_s}{D_n\ A}\ g(Z)\right]$ | 2 - 9 |
| 2.13 | The term $\frac{\partial}{\partial T}\left[\frac{\sigma_B\ W}{\sigma_E\ L_E} + \frac{1}{2}\left(\frac{W}{L_B}\right)^2\right](1 + Z)$ | 2 - 11 |

TABLE OF CONTENTS (Continued)


| Section | Description | Page No. |
|---|---|---|
| 2.14 | Temperature Dependence of Z | 2 - 12 |
| 2.15 | Temperature Dependence of $h_{FE}$ | 2 - 12 |
| 2.16 | Discussion of Webster Equation | 2 - 12 |
| 2.17 | Fletcher Effect | 2 - 13 |
| 2.18 | Space Charge Recombination - Influence on $h_{FE}$ | 2 - 20 |
| 3.0 | DESIGN APPROACHES | 3 - 1 |
| 3.1 | Fletcher Effect - $h_{FE}$ Control | 3 - 1 |
| 3.2 | Fletcher Effect - High Injection Level | 3 - 3 |
| 3.3 | Fletcher Effect - Low Injection Level | 3 - 5 |
| 3.4 | Two Transistors in Parallel | 3 - 7 |
| 3.5 | Diode in Parallel to Emitter Junction | 3 - 9 |
| 3.6 | Controlled Surface Recombination | 3 - 13 |
| 4.0 | PRELIMINARY DESIGN CONSIDERATIONS | 4 - 1 |
| 4.1 | Determination of Background Resistivity | 4 - 1 |
| 4.2 | Device Geometry | 4 - 5 |
| 4.3 | Base Spreading Resistance | 4 - 11 |
| 4.4 | Boron Diffusion | 4 - 18 |
| 5.0 | EXPERIMENTAL | 5 - 1 |
| 5.1 | Test of Fletcher Effect | 5 - 1 |
| 5.2 | Two Transistors in Parallel Circuit | 5 - 12 |

TABLE OF CONTENTS (Continued)


| Section | Description | Page No. |
|---|---|---|
| 5.3 | Diode in Parallel With Emitter Junction . . . | 5 - 18 |
| 5.4 | Inverted Transistor Measurements . . . . . . | 5 - 23 |
| 6.0 | CONCLUSIONS . . . . . . . . . . . . . . . . . | 6 - 1 |
| 7.0 | PROGRAM FOR NEXT INTERVAL . . . . . . . . . . | 7 - 1 |
| 8.0 | LIST OF REFERENCES . . . . . . . . . . . . . | 8 - 1 |
| Appendix | | |
| I | Transistor Specifications . . . . . . . . . . | A - 1 |
| II | Two Transistors in Parallel Circuit - Gain Calculation . . . . . . . . . . . . . . . . | A - 3 |
| III | Diode Parallel to Emitter Junction - Circuit Calculation . . . . . . . . . . . . . . . . | A - 5 |
| IV | Emitter Efficiency - Calculation . . . . . . | A - 7 |
| V | Voltage Dependency on Impurity Concentration - Calculation . . . . . . . . . . . . . . . . | A - 10 |
| VI | Experimental Data for Section 3.5 . . . . . . | A - 13 |
| VII | Experimental Data for Section 3.4 . . . . . . | A - 23 |
| VIII | Identification of Key Personnel . . . . . . . | A - 28 |

## LIST OF ILLUSTRATIONS


| Figure | | Page No. |
|---|---|---|
| 2.17.1 | Current Density Under Emitter $I_E = 0.5$ ma | 2 - 17 |
| 2.17.2 | Current Density Under Emitter $I_E = 20$ ma | 2 - 18 |
| 2.17.3 | Current Density Under Emitter $I_E = 100$ ma | 2 - 19 |
| 3.1.1 | Split Base Configuration With Compensating Resistor | 3 - 2-A |
| 3.2.1 | Split Base Configuration With Compensating Resistor-High Injection Level Case | 3 - 6 |
| 3.2.2 | Split Emitter Configuration With Compensating Resistor | 3 - 6 |
| 3.4.1 | Positive Temperature Coefficient Resistor Circuit Diagram-2 Transistors in Parallel | 3 - 8 |
| 3.4.2 | Negative Temperature Coefficient Resistor Circuit Diagram-2 Transistors in Parallel | 3 - 8 |
| 3.5.1 | Minority Carrier Flow Map | 3 - 11 |
| 3.5.2 | Diode in Parallel Emitter Junction - Schematic | 3 - 12 |
| 3.5.3 | Diode in Parallel Emitter Junction - Pictorial | 3 - 12 |
| 3.5.4 | Diode in Parallel Emitter Junction - Single Substrate | 3 - 14 |
| 3.5.5 | Diode in Parallel Emitter Junction Built in Resistor Configuration - Single Substrate | 3 - 14 |
| 3.6.1 | Surface Tetrode | 3 - 16 |

LIST OF ILLUSTRATIONS (Continued)


| Figure | | Page No. |
|---|---|---|
| 3.6.2 | Tetrode Characteristics . . . . . . . . . . . | 3 - 16 |
| 3.6.3 | Surface Controlled $h_{FE}$ - Schematic . . . . . | 3 - 16 |
| 4.1.1 | Plot of $V_{CER}$ vs. Resistivity . . . . . . . . | 4 - 2 |
| 4.1.2 | Plot of Log $C_{OB}$ vs. Log $V_{CER}$ . . . . . . . . | 4 - 4 |
| 4.2.1 | Single Bar Emitter Base Configuration . . . | 4 - 7 |
| 4.2.2 | Double Bar Emitter Base Configuration . . . | 4 - 7 |
| 4.3.1 | Emitter Base Geometry Parameters . . . . . . | 4 - 13 |
| 4.3.2 | Emitter Base Geometry Parameters . . . . . . | 4 - 13 |
| 4.3.3 | Impurity Distribution in Base Region . . . . | 4 - 16 |
| 4.3.4 | Graphical Integration . . . . . . . . . . . | 4 - 17 |
| 4.4.1 | Relationship of Base Width to Surface Concentration . . . . . . . . . . . . . . . | 4 - 23 |
| 5.1.1 | Preliminary Device to Study Fletcher Effect on $h_{FE}$ . . . . . . . . . . . . . . . . . . . . | 5 - 2 |
| 5.1.2 | Curve Tracer Pictures: $I_C$ vs. $V_{CB}$, Parameter $I_b$ . . . . . . . . . . . . . . . . . | 5 - 3 |
| 5.1.3 | Curve Tracer Pictures: $I_C$ vs. $V_{CB}$, Parameter $I_b$ . . . . . . . . . . . . . . . . . | 5 - 4 |
| 5.1.4 | Curve Tracer Pictures: $I_C$ vs. $V_{CB}$, Parameter $I_b$ . . . . . . . . . . . . . . . . . | 5 - 5 |
| 5.1.5 | Curve Tracer Pictures: $I_C$ vs. $V_{CB}$, Parameter $I_b$ . . . . . . . . . . . . . . . . . | 5 - 6 |

LIST OF ILLUSTRATIONS (Continued)


| Figure | | Page No. |
|---|---|---|
| 5.1.6 | Curve Tracer Pictures: $I_C$ vs. $V_{CB}$, Parameter $I_b$ . . . . . . . . . . . . . . . . . | 5 - 7 |
| 5.1.7 | Curve Tracer Pictures: $I_C$ vs. $V_{CB}$, Parameter $I_b$ . . . . . . . . . . . . . . . . . | 5 - 8 |
| 5.1.8 | β vs. Collector Current . . . . . . . . . . . | 5 - 9 |
| 5.1.9 | β vs. Collector Current . . . . . . . . . . . | 5 - 10 |
| 5.1.10 | β vs. Collector Current . . . . . . . . . . . | 5 - 11 |
| 5.1.11 | Relative Change of β vs. Collector Current . | 5 - 11-A |
| 5.2.1 | Two Transistors in Parallel Circuit . . . . | 5 - 13 |
| 5.2.2 | Curve Tracer Pictures: $I_C$ vs. $V_{CB}$, Parameter $I_b$ . . . . . . . . . . . . . . . . . | 5 - 14 |
| 5.2.3 | Curve Tracer Pictures: $I_C$ vs. $V_{CB}$, Parameter $I_b$ . . . . . . . . . . . . . . . . . | 5 - 15 |
| 5.2.4 | β vs. Collector Current . . . . . . . . . . . | 5 - 16 |
| 5.2.5 | β vs. Collector Current . . . . . . . . . . . | 5 - 17 |
| 5.3.1 | Transistor With Diode Parallel Emitter Junction . . . . . . . . . . . . . . . . . . . . | 5 - 19 |
| 5.3.2 | Curve Tracer Pictures: $I_C$ vs. $I_{CB}$, Parameter $I_b$ . . . . . . . . . . . . . . . . . | 5 - 20 |
| 5.3.3 | Curve Tracer Pictures: $I_C$ vs. $I_{CB}$, Parameter $I_b$ . . . . . . . . . . . . . . . . . | 5 - 21 |
| 5.3.4 | β vs. Collector Current | 5 - 22 |
| AI | Curve of $h_{FE}$ vs. Collector Current . . . . . | A - 2 |

LIST OF ILLUSTRATIONS (Continued)


| Figure | | Page No. |
|---|---|---|
| V-1<br>V-2<br>V-3 | Plot of Impurity Concentration vs. Distance for Determination of tan ø to Impurity Distribution Curve . . . . . . . . . . . . . . . . | A - 11 |

DEFINITION OF SYMBOLS

$h_{FE}$ . . . . . . . . . . D.C. Current Gain

$\beta$ . . . . . . . . . . . D. C. Current Gain of a Transistor Combination with Resistors or Thermistors

s . . . . . . . . . . Surface Recombination Velocity

$\mu_n$ . . . . . . . . . Electron Mobility in Base Region

$\mu_p$ . . . . . . . . . Hole Mobility in Base Region

$\mu_{nL}$ . . . . . . . . . Lattice Mobility for Electrons

$\mu_{nI}$ . . . . . . . . . Electron Mobility Due to Coulomb Scattering

n . . . . . . . . . . Electron Concentration

p . . . . . . . . . . Hole Concentration

$\sigma_B$ . . . . . . . . . Conductivity of Base Region

$\sigma_E$ . . . . . . . . . Conductivity of Emitter Region

$\rho_S$ . . . . . . . . . Base Sheet Resistance

$\rho_{S_E}$ . . . . . . . . . Emitter Sheet Resistance

$\rho_s{}^*$ . . . . . . . . . Sheet Resistance Underneath Emitter

$D_n$ . . . . . . . . . Diffusion Constant of Electrons in Base Region

$L_E$ . . . . . . . . . Diffusion Length of Holes in Emitter Region

$L_B$ . . . . . . . . . Diffusion Length of Electrons in Base Region

v . . . . . . . . . . Electron Velocity

## DEFINITION OF SYMBOLS (Continued)

$W_d$ . . . . . . . . . Width of Depletion Layer

$W$ . . . . . . . . . . Base Width

$A_s$ . . . . . . . . . Effective Surface Area for Recombination

$A$ . . . . . . . . . . Cross Sectional Area of the Conduction Path

$Y_1$ . . . . . . . . . Effective Conduction Path Width at Collector Junction Due to Base Fringing

$\ell_E$ . . . . . . . . . Length of Emitter Stripe

$d$ . . . . . . . . . . Width of Emitter Stripe

$X_{j_E}$ . . . . . . . . . Depth of Emitter Junction

$\phi$ . . . . . . . . . . Angle Between Two Impurity Distribution Functions at the Junction

$\phi_1$ . . . . . . . . . Angle Between p-Type Distribution Function (Ga, B) and the Constant Background Doping at the Emitter Junction

$\phi_2$ . . . . . . . . . Angle Between n-Type Distribution Function (P) and Constant Background Doping at the Emitter Junction

$N_s$ . . . . . . . . . Surface Concentration

$N_p(x)$ . . . . . . . Acceptor Impurity Distribution

$N_n(x)$ . . . . . . . Donor Impurity Distribution

$N_o$ . . . . . . . . . Constant Donor Background Distribution

$C_{OB}$ . . . . . . . . Collector Barrier Capacitance

$V_{CER}$ . . . . . . . Collector Emitter Voltage (Base and Emitter Connected by 10$\Omega$ Resistor)

DEFINITION OF SYMBOLS (Continued)

$V_{CE_{sat}}$ . . . . . . . Transistor Saturation Voltage

$R_I$ . . . . . . . . . Base Spreading Resistance at High Current Density

$R_{II}$ . . . . . . . . . Part of Base Spreading Resistance Due to Voltage Drop Underneath Emitter

$I_E$ . . . . . . . . . Emitter Current

$I_B$ . . . . . . . . . Base Current

Z . . . . . . . . . . Webster Factor

g(Z) . . . . . . . Webster's "Field Factor"

$\varepsilon$ . . . . . . . . . . 12 for Silicon

$\varepsilon_o$ . . . . . . . . . $8.859 \times 10^{-14}$ A sec./V cm

q . . . . . . . . . . $1.9 \times 10^{-19}$ Coulomb

k . . . . . . . . . . $1.38 \times 10^{-23}$ Watts sec./°C

## PURPOSE

The purpose of this program is to study the problems associated with the design and fabrication of practical transistors which are relatively insensitive to changes of temperature over the temperature range 0 - 75°C. The major emphasis shall be to explore the theoretical design aspects of the problem, select an approach, and substantiate the design by actual construction of twelve devices.

# ABSTRACT

The problem of $h_{FE}$ temperature compensation is studied by examination of the fundamental physical parameters affecting $h_{FE}$. Variable emitter periphery, Fletcher effect, parallel transistor, and diode-transistor effects are considered. Both lumped and distributed device concepts are evolved for design approaches. Preliminary tests of design concepts is achieved by circuit analogues.

## PUBLICATIONS, LECTURES, REPORTS AND CONFERENCES

1. A meeting was held at Signal Corps, Fort Monmouth, June 16, 1961, to discuss program objectives and review progress informally. J. Spanos attended from Hoffman Electronics. K. Fischer, F. Gordon from the Signal Corps.

2. A meeting was held at Hoffman Electronics with K. Fischer of the Signal Corps, July 25, 1961.

## 1.0 INTRODUCTION

The problem of variation of transistor parameters with temperature has been a serious one which has been extensively discussed and has led to extensive circuit manipulations in an attempt to reduce the effects of such variation on systems performance.

It is the intent of this program to investigate the problem of the design of a transistor which meets the specifications given in **Appendix** I.

Since most of the equations which describe transistor performance are quite cumbersome to manipulate, approximate methods must of necessity be considered if a satisfactory design is to be achieved in a reasonable period of time. The validity of these methods can be checked with relative ease by actual device fabrication and measurement and a semiempirical method of achieving a design can be established.

One of the primary parameters to be considered is the $h_{FE}$ of the device, and a convenient starting point is the Webster equation given in Section 2.0.

Since the gain of a transistor can be stated approximately in terms of the basic physical parameters of the device material, in this case silicon, and the temperature dependence of these physical parameters is reasonably well known, the combined effect can be determined and a guide to the actual design of a device can be extracted.

In the sections which follow the explorations made to date are described and the relation to the starting equations is indicated.

The temperature variation of the various terms of the Webster equation gives only the simplest case, and an initial investigation of space charge recombination variation with temperature has been started in an attempt to work this into the gain equation. This effect is of importance at the very low values of emitter current where gain is specified.

The advent of oxide mask devices and the importance of "gettering" as it affects the emitter space charge recombination, surface recombination, as well as the crystal structure of devices, i.e. micro-plasma breakdown, necessitates both the use and extension of these techniques for this work.

At the higher current specification, consideration of the Fletcher effect is necessary since in this region a method of $h_{FE}$ control can be utilized. Again this effect can be considered for incorporation into the gain equation.

Four basic approaches have been established during this period which are described below, and combinations of these are under way as well.

These approaches are based on considerations of the Fletcher effect with an oxide mask technique, distributed dual transistor with temperature compensating resistors, a distributed diode in parallel with the emitter junction, and temperature controlled surface recombination.

Many configurations are possible and are described. Several of these configurations are being seriously considered for actual construction.

Technology required to achieve such designs is under development.

Experimental results to date are included, and an attempt is made to relate those results to the development of the theory to date.

## 2.0 THEORY

### 2.1 Temperature Dependence of the Webster Equation

In this section Webster's approximate equation will be differentiated with respect to temperature in order to determine the relative effects that each term will have on the over-all gain as temperature changes. The device under consideration is an n-p-n silicon transistor. For convenience, initial calculations have been made for a structure with which an extensive background already exists, namely the 2N697 transistor as made at Hoffman Semiconductor Division. This device is typical of the class of transistor to be considered in this program and serves as a useful starting point as a readily available tool.

2.1.1 $$\frac{1}{h_{FE}} = \frac{s\, W\, A_s}{D_n\, A}\, g(Z) + \left[ \frac{\sigma_B\, W}{\sigma_E\, L_E} + \frac{1}{2} \left( \frac{W}{L_B} \right)^2 \right] (1 + Z) \qquad 1.$$

2.1.2 where $$Z = \left[ \frac{W\, \mu_p\, I_E}{D_n\, A\, \sigma_B} \right]$$

or $$Z = \left[ \frac{W\, q\, I_E}{k\, TA\, \sigma_B} \right] \frac{1}{b}, \quad b = \frac{\mu_n}{\mu_p}$$

$$Z = \left( \frac{W\, q\, I_E}{k\, A} \right) \left( \frac{\mu_p}{\mu_n} \right) \left( \frac{1}{T \sigma_B} \right)$$

2.1.3 $$g(Z) = \frac{1 + n_E/N_A}{1 + 2n_E/N_A}$$

$k = 8.6 \times 10^{-5}$ eV/°C

= Boltzmann's Constant

now

$$\text{2.1.4} \qquad \frac{\partial}{\partial T}\left(\frac{1}{h_{FE}}\right) = -\frac{1}{(h_{FE})^2} \frac{\partial (h_{FE})}{\partial T} =$$

$$\frac{\partial}{\partial T}\left[\frac{s\ W\ As}{D_n\ A}\, g(Z)\right] + \frac{\partial}{\partial T}\left[\frac{\sigma_B\ W}{\sigma_E\ L_E} + \frac{1}{2}\left(\frac{W}{L_B}\right)^2\right] \quad (1 + Z)$$

The individual terms of this general equation will now be considered.

## 2.2 Dependency of Base Width W on Temperature. [2.]

The width of the depletion layer is

$$W_d = \left(\frac{3}{2}\frac{V}{K}\right)^{1/3} \qquad K = \frac{q}{\varepsilon\varepsilon_o} \tan\phi \qquad \text{(Appendix V-a)}$$

where $\tan\phi$ is the slope of the erfc impurity distribution due to diffusion at the junction.

or

$$\text{2.2.1} \qquad W_d = \left(\frac{3}{2}\frac{\varepsilon\varepsilon_o}{q}\frac{V}{\tan\phi}\right)^{1/3}$$

$\tan\phi$, , are temperature independent

$$\therefore \frac{\partial W_d}{\partial T} = 0 \quad \text{which causes} \quad \frac{\partial W}{\partial T} = 0 \qquad 1W \approx 1 \times 10^{-4}\ \text{cm}$$

Base width is unaffected by temperature to a first approximation. The $\tan\phi$ term could vary somewhat due to incomplete ionization 95% of impurities at room temperature, but is quite small.

## 2.3 Emitter Region Conductivity $\sigma_E$

2.3.1 $\sigma = q\,(\mu_n \cdot n + \mu_p \cdot p)$

. The drift mobility is given by

$$\mu_n = \mu_{nL} \left[ 1 + M^2 \left\{ C_i M \cos M + S_i \sin M - \frac{\pi}{2} \sin M \right\} \right]$$ [3.]

2.3.2
$$\mu_{n_I} = \frac{8\sqrt{2}\; \varepsilon_0^2\; \varepsilon^2\; (kT)^{3/2}}{\pi^{3/2}\, N_I\, q^3\, m_{eff}^{1/2}\; \ln\left[1 + \left(\frac{3\,\varepsilon_0\,\varepsilon\, kT}{q\, N_I^{1/3}}\right)^2\right]}$$

2.3.3
$$M^2 = \frac{6\,\mu_{nL}}{\mu_{nI}}$$

2.3.4
$$\mu_{nL} = 5 \cdot 5 \cdot 10^6\; T^{-1.5}$$

The evaluation of $\mu_I$ is most conveniently determined from Conwell's paper.[4.] Gärtner, however, has tabulated the curves as a function of temperature[3.] and for the doping level estimated, i.e., $10^{18}/cm^3$ the variation of $\mu_n$ with temperature is negligible.

At doping levels of $10^{18}/cm^3$ the variation of $n = n(T)$ is essentially constant and therefore temperature independent.

$\sigma_E \approx q(\mu_n \cdot n)$ since $\mu_p \cdot p \ll \mu_n \cdot n$. and $\sigma_E$ is essentially independent of temperature.

i.e.

$$\frac{\partial \sigma_E}{\partial T} = 0 \qquad \sigma_E = \frac{1}{\rho_{s_E}\, x_{j_E}} = \frac{2 \cdot 52 \cdot 10^3}{\Omega cm}$$

## 2.4 Ratio of the Mobilities in the Base Region

$\frac{\mu_{pB}}{\mu_{nB}}$ .  $\mu_{pB}$ = mobility of holes in the base region

$\mu_{nB}$ = mobility of electrons in the base region

Since in the base region the impurity concentration $N_a$ is much smaller than in the emitter ($\sim 2 \cdot 10^{15}/cm^3$), the limiting mobility is that due to lattice scattering

$$\mu_I >> \mu_L$$

and $$\mu \approx \mu_L$$

and

$$\frac{\mu_{pB}}{\mu_{nB}} \approx \frac{\mu_{pBL}}{\mu_{nBL}} = \frac{2.3 \cdot 10^9 \cdot T^{-2.7}}{2.1 \cdot 10^9 \cdot T^{-2.5}} \quad \underline{3}.$$

$$\frac{\mu_{pBL}}{\mu_{nBL}} = \frac{1.1}{T^{0.2}}$$

2.4.1 $$\frac{\partial}{\partial T}\left(\frac{\mu_{pBL}}{\mu_{nBL}}\right) = -\frac{0.22}{T^{1.2}}$$

## 2.5 Base Conductivity $\sigma_B$ (P-Type Silicon)

2.5.1 $$\sigma_B = q\,\mu_p\,p \approx q\,p\,\mu_{pL} = q\,p\,2.3 \cdot 10^9 \cdot T^{-2.7}$$

Since p is essentially constant over the temperature range of interest ($\sim 2 \cdot 10^{15}$ see Gärtner Op. Cit. pg. 31)

$$\sigma_B = q\,p\,2.3 \cdot 10^9 \frac{1}{T^{2.7}} = \frac{A}{T^{2.7}}$$

2.5.2 $$\frac{\partial \sigma_B}{\partial T} = A \left(-2.7 \frac{1}{T^{3.7}}\right) \qquad q = 1.6 \cdot 10^{-19} \text{ Coulomb}$$

2.5.3 $$\frac{\partial \sigma_B}{\partial T} = - \frac{0.99 \cdot 10^{-9}}{T^{3.7}} p$$

2.6 Temperature Dependency of Z

From 2.1.2

$$Z = \left(\frac{W\, q\, I_E}{k\, A}\right)\left(\frac{\mu_p}{\mu_n}\right)\left(\frac{1}{T\, \sigma_B}\right) \qquad \underline{12.}$$

($\frac{\mu_{pBL}}{\mu_{nBL}}$ for convenience is here abbreviated to $\frac{\mu_p}{\mu_n}$.)

The first factor is temperature independent, while the second and third factors are temperature dependent.

2.6.1 $$\frac{\partial Z}{\partial T} = \left(\frac{W\, q\, I_E}{k\, A}\right) \cdot \left[\frac{\partial}{\partial T}\left(\frac{1}{\sigma_B\, T}\, \frac{\mu_p}{\mu_n}\right)\right]$$

2.6.2 $$\frac{\partial Z}{\partial T} = \frac{W\, q\, I_E}{k\, A}\left[\frac{\mu_p}{\mu_n} \cdot \frac{\partial}{\partial T}\left(\frac{1}{\sigma_B\, T}\right) + \frac{1}{\sigma_B\, T}\, \frac{\partial}{\partial T}\left(\frac{\mu_p}{\mu_n}\right)\right]$$

now

2.6.3 $$\frac{\partial}{\partial T}\left(\frac{1}{\sigma_B\, T}\right) = \frac{1}{T}\left[\frac{\partial}{\partial T}\left(\frac{1}{\sigma_B}\right)\right] + \frac{1}{\sigma_B}\left[\frac{\partial}{\partial T}\left(\frac{1}{T}\right)\right]$$

$$= \frac{1}{T}\left(-\frac{1}{\sigma_B^2}\, \frac{\partial \sigma_B}{\partial T}\right) + \frac{1}{\sigma_B}\left(-\frac{1}{T^2}\right)$$

and

2.6.4 $$\frac{\partial}{\partial T}\left(\frac{1}{\sigma_B\, T}\right) = -\frac{1}{\sigma_B\, T}\left[\frac{1}{\sigma_B}\, \frac{\partial \sigma_B}{\partial T} + \frac{1}{T}\right]$$

From 2.6.2, 2.6.4, and 2.4.1

2.6.6 $$\frac{\partial Z}{\partial T} = \frac{W\, q\, I_E}{k\, A} \left\{ \left[ -\frac{\mu_p}{\mu_n} \frac{1}{\sigma_B\, T} \left[ \frac{1}{\sigma_B} \frac{\partial \sigma_B}{\partial T} + \frac{1}{T} \right] + \frac{1}{\sigma_B\, T} \left( -\frac{0.22}{T^{1.2}} \right) \right] \right\}$$

From 2.1.2 above

2.6.7 $$\frac{\partial Z}{\partial T} = -Z \left[ \frac{1}{\sigma_B} \frac{\partial \sigma_B}{\partial T} + \frac{1}{T} \right] - \left[ 0.22\, Z\, \frac{\mu_n}{\mu_p} \frac{1}{T}\, 1.2 \right]$$

2.6.8 $$\frac{\partial Z}{\partial T} = -Z \left\{ \frac{1}{\sigma_B} \frac{\partial \sigma_B}{\partial T} + \frac{1}{T} + 0.22 \left( \frac{\mu_n}{\mu_p} \right) \frac{1}{T^{1.2}} \right\}$$

From 2.5.3

2.6.9 $$\frac{\partial Z}{\partial T} = -Z \left\{ \frac{-1}{\sigma_B} \frac{0.99 \cdot 10^{-9}\, p}{T^{3.7}} + \frac{1}{T} + 0.22\, \frac{\mu_n}{\mu_p} \frac{1}{T^{1.2}} \right\}$$

## 2.7 g(Z) Temperature Dependency

2.7.1 $$\frac{\partial g(Z)}{\partial T} = \frac{\partial g(Z)}{\partial Z} \cdot \frac{\partial Z}{\partial T}$$

$\frac{\partial g(Z)}{\partial Z}$ can be determined from a plot of g(Z) vs. Z,

see for example ref. 5, and $\frac{\partial Z}{\partial T}$ is shown in 2.6.9.

## 2.8 Electron Diffusion Coefficient in the Base $D_{nB}$

2.8.1 $$D_n = \frac{kT}{q} \mu_n = D_n(T)$$

Since as mentioned in Section 2.4 $\mu_n \approx \mu_{nL} = 2.1 \cdot 10^9 \cdot T^{-2.5}$

2.8.2 $$D_n \approx 2.1 \cdot 10^9 \frac{k}{q} \cdot T^{-1.5}$$

2.8.3 $$\frac{\partial D_n}{\partial T} = -\, 3.15 \cdot 10^9 \frac{k}{q} \cdot \frac{1}{T^{2.5}}$$

$$k = 8.6 \cdot 10^{-5} \frac{eV}{°C} = 1.38 \cdot 10^{-23} \frac{watt\ sec.}{°C}$$

$$q = 1.6 \cdot 10^{-19} \text{ Coulomb}$$

$$\frac{k}{q} = 8.6 \cdot 10^{-5} \frac{V}{°C}$$

2.8.4

$$\frac{\partial D_n}{\partial T} = - \frac{2.71 \cdot 10^5}{T^{2.5}}$$

## 2.9 Diffusion Length of Holes in Emitter Region $L_{pE}$ Temperature Dependence

$$L_p = \sqrt{D_p \tau_p}$$

$D_p$ decreases with T. $\tau$ increases with T and it is estimated that $\tau$ increases at a more rapid rate than $D_p$ decreases[6].

These results

$$\frac{\Delta L_p}{\Delta T} = + 0.44 \cdot 10^{-5} \frac{cm}{°C} \qquad 25°C \leq T \leq 75°C$$

or this parameter is essentially temperature independent.

## 2.10 Diffusion Length of $L_{nB}$ Electrons in the Base Region

$$L_{nB} = \sqrt{D_{nB} \tau_{nB}}$$

Again due to the varied nature of $\tau_n$, empirical methods have been used to estimate the temperature dependence [6].

| Temp. °C | $L_n$ [cm] | $\Delta L_n$ for 25°C Intervals |
|---|---|---|
| 0 | $1.56 \cdot 10^{-2}$ | |
| 25 | $2.05 \cdot 10^{-2}$ | $0.49 \cdot 10^{-2}$ |
| 50 | $2.55 \cdot 10^{-2}$ | $0.50 \cdot 10^{-2}$ |
| 75 | $3.05 \cdot 10^{-2}$ | $0.50 \cdot 10^{-2}$ |
| 100 | $3.50 \cdot 10^{-2}$ | $0.45 \cdot 10^{-2}$ |

$$\text{Avg. } \frac{\Delta L_n}{\Delta T} = 0.5 \cdot 10^{-2} \frac{\text{cm}}{25°\text{C}} = 2 \cdot 10^{-4} \frac{\text{cm}}{°\text{C}}$$

2.10.1 $\frac{\partial L_n}{\partial T} \approx \frac{\Delta L_n}{\Delta T} = 2 \cdot 10^{-4} \frac{\text{cm}}{°\text{C}}$ or essentially temperature independent.

## 2.11 Diffusion Length of $L_{pB}$ Holes in the Base Region

$$L_{pB} = \sqrt{D_{pB} \tau_{pB}}$$

As in 2.10

| Temp. °C | $L_n$ [cm] | $\Delta L_n$ for 25°C Intervals |
|---|---|---|
| 0 | $8.5 \cdot 10^{-4}$ | |
| 25 | $9.4 \cdot 10^{-4}$ | $0.9 \cdot 10^{-4}$ |
| 50 | $10.5 \cdot 10^{-4}$ | $1.1 \cdot 10^{-4}$ |
| 75 | $11.6 \cdot 10^{-4}$ | $1.1 \cdot 10^{-4}$ |
| 100 | $13.0 \cdot 10^{-4}$ | $1.4 \cdot 10^{-4}$ |

$$\frac{\Delta L_p}{\Delta T} = 1.1 \cdot 10^{-4} \frac{\text{cm}}{25°\text{C}} = 0.44 \cdot 10^{-5} \frac{\text{cm}}{°\text{C}}$$

$$\frac{\partial L_p}{\partial T} \approx \frac{\Delta L_p}{\Delta T} = 0.44 \cdot 10^{-5} \frac{\text{cm}}{°\text{C}}$$

## 2.12 The Term $\frac{\partial}{\partial T}\left[\frac{s\ W\ As}{D_n\ A}\ g(Z)\right]$

Since $\frac{W\ As}{A}$ is temperature independent

2.12.1
$$\frac{W\ As}{A}\ \frac{\partial}{\partial T}\left[\frac{s}{D_n}\ g(Z)\right]$$

2.12.2
$$\frac{\partial}{\partial T}\left[\frac{s}{D_n}\ g(Z)\right] = g(Z)\ \frac{\partial}{\partial T}\left(\frac{s}{D_n}\right) + \frac{s}{D_n}\ \frac{\partial g(Z)}{\partial T}$$

2.12.3 and
$$\frac{\partial}{\partial T}\left(\frac{s}{D_n}\right) = s\frac{\partial}{\partial T}\left(\frac{1}{D_n}\right) + \frac{1}{D_n}\ \frac{\partial s}{\partial T}$$

$$= -\frac{s}{D_n^{2}}\ \frac{\partial}{\partial T}\ D_n + \frac{1}{D_n}\ \frac{\partial s}{\partial T}$$

2.12.4
$$\frac{\partial}{\partial T}\left[\frac{s}{D_n}\ g(Z)\right] = -\frac{g(Z)}{D_n}\left[\frac{s}{D_n}\frac{\partial}{\partial T}\ D_n - \frac{\partial s}{\partial T}\right] + \frac{s}{D_n}\ \frac{\partial g(Z)}{\partial T}$$

From 2.7.1, 2.6.9, 2.8.4, and 2.4.1

$$\frac{\partial}{\partial T}\ D_n = -\ \frac{2.71\cdot 10^{5}}{T^{2.5}} \qquad \frac{\mu_n}{\mu_p} = 0.91\cdot T^{0.2}$$

2.7.1
$$\frac{\partial}{\partial T}\ g(Z) = \frac{\partial g(Z)}{\partial Z}\cdot\frac{\partial Z}{\partial T}$$

2.7.1 and 2.6.9
$$= \frac{\partial g(Z)}{\partial Z}\left[-Z\left\{\frac{-1}{\sigma_B}\ \frac{0.99\cdot 10^{-9}}{T^{3.7}}p + \frac{1}{T} + 0.22\ \frac{\mu_n}{\mu_p}\ \frac{1}{T^{1.2}}\right\}\right]$$

2.12.5
$$\frac{\partial}{\partial T}\ g(Z) = -Z\left[\frac{1.2}{T} - \frac{10^{-9}\ p}{\sigma_B\ T^{3.7}}\right]\frac{\partial g(Z)}{\partial Z}$$

$$\sigma_B \approx q \, \mu_{pL} \, p \qquad \frac{p}{\sigma_B} \approx \frac{1}{q \, \mu_{pL}} = \frac{10^{19}}{1.6 \, \mu_{pL}}$$

$$\mu_{pL} \approx 2.3 \cdot 10^{9} \cdot T^{-2.7}$$

$$\frac{p}{\sigma_B} = 0.27 \cdot 10^{10} \, T^{2.7}$$

$$\frac{10^{-9} \, p}{\sigma_B} \cdot \frac{1}{T^{3.7}} = \frac{2.72}{T}$$

so that

$$\frac{\partial g(Z)}{\partial T} = -Z \left[ \frac{1.2}{T} - \frac{2.72}{T} \right] \frac{\partial g(Z)}{\partial Z}$$

and

2.12.6
$$\frac{\partial g(Z)}{\partial T} = \frac{1.52 \, Z}{T} \frac{\partial g(Z)}{\partial Z}$$

Substituting in 2.12.4

2.12.6
$$\frac{\partial}{\partial T} \left[ \frac{s}{D_n} g(Z) \right] = \frac{-g(Z)}{D_n} \left[ -\frac{s}{D_n} \left( \frac{2.71 \cdot 10^5}{T^{2.5}} \right) - \frac{\partial s}{\partial T} \right] + \frac{s}{D_n} \frac{1.52 \, Z}{T} \frac{\partial g(Z)}{\partial Z}$$

Finally

2.12.7
$$\frac{W \, As}{A} \frac{\partial}{\partial T} \left[ \frac{s}{D_n} g(Z) \right] = \frac{W \, As}{A} \left\{ \frac{g(Z)}{D_n} \left[ \frac{2.71 \cdot 10^5}{D_n \, T^{2.5}} s + \frac{\partial s}{\partial T} \right] + \frac{s}{D_n} \frac{1.52 \, Z}{T} \frac{\partial g(Z)}{\partial Z} \right\}$$

2.13 The term $\left[\frac{\sigma_B}{\sigma_E}\frac{W}{L_E} + \frac{1}{2}\left(\frac{W}{L_B}\right)^2\right](1+z)$

2.1.3.1 $$\frac{\partial}{\partial T}\left[\frac{\sigma_B}{\sigma_E}\frac{W}{L_E} + \frac{1}{2}\left(\frac{W}{L_B}\right)^2\right](1+z)$$

2.13.2 $$\frac{\partial}{\partial T}\left\{\frac{2}{W}\frac{\sigma_B}{\sigma_E L_E} + \frac{1}{L_B^2}\right\}(1+z) = \left\{---\right\}\frac{\partial z}{\partial T} + (1+z)\frac{\partial\{---\}}{\partial T}$$

Now $\sigma_E$ was shown to be temperature independent

2.13.3 $$\frac{\partial}{\partial T}\left\{---\right\} = \left[\frac{2}{W\sigma_E}\left(\frac{1}{L_E}\frac{\partial\sigma_B}{\partial T} - \frac{\sigma_B}{L_E^2}\frac{\partial L_E}{\partial T}\right)\right] - \frac{2}{L_B^3}\frac{\partial L_B}{\partial T}$$

and

2.13.4 $$\frac{2}{W^2}\frac{\partial}{\partial T}\left[\frac{\sigma_B}{\sigma_E}\frac{W}{L_E} + \frac{1}{2}\left(\frac{W}{L_B}\right)^2\right](1+z) = \left\{\frac{2}{W}\frac{\sigma_B}{\sigma_E L_E} + \frac{1}{L_B^2}\right\}\frac{\partial z}{\partial T}$$

$$+ (1+z)\left[\frac{2}{W\sigma_E}\left(\frac{1}{L_E}\cdot\frac{\partial\sigma_B}{\partial T} - \frac{\sigma_B}{L_E^2}\frac{\partial L_E}{\partial T}\right) - \frac{2}{L_B^3}\frac{\partial L_B}{\partial T}\right]$$

From 2.6.9 and 2.5.3 and 2.9 and 2.10

$$\frac{\partial z}{\partial T} = \frac{1.52z}{T} \qquad \frac{\partial\sigma_B}{\partial T} = -\frac{10^9 P}{T^{3.7}} \qquad \frac{\partial L_E}{\partial T} \approx \frac{\Delta L_p}{\Delta T} = 0.44\cdot 10^{-5}$$

$$\frac{\partial L_B}{\partial T} \approx \frac{\Delta L_n}{\Delta T} = 2.0\cdot 10^{-4}$$

2.13.5 $$\frac{\partial}{\partial T}\left\{----\right\}(1+z) = \left\{\frac{2}{W}\frac{\sigma_B}{\sigma_E L_E} + \frac{1}{L_B^2}\right\}\frac{1.52z}{T} +$$

$$\cdot 2(1+z)\left[\frac{1}{W\sigma_E}\left(-\frac{1}{L_E}\frac{10^{-9}P}{T^{3.7}} - \frac{\sigma_B}{L_E^2}\,0.44\cdot 10^{-5}\right) - \frac{1}{L_B^3}\,2\cdot 10^{-4}\right]$$

2.13.6 $$\frac{\partial}{\partial T}\left\{- - -\right\}(1+z) \doteq \frac{1.52z}{T}\left\{\frac{2}{W}\frac{\sigma_B}{\sigma_E L_E} + \frac{1}{L_B^2}\right\} -$$

$$2\cdot 10^{-4}(1+z)\left[\frac{1}{W\sigma_E}\left(\frac{P\cdot 10^{-5}}{L_E T^{3.7}} + \frac{0.044\,\sigma_B}{L_E^2}\right) + \frac{2}{L_B^3}\right]$$

## 2.14 Temperature Dependence of Z.

2.14.1
$$Z = \frac{W q}{k \sigma_B A} \frac{\mu_p}{\mu_n} \frac{I C}{T}$$

and from previous evaluations

2.14.2
$$Z = \frac{0{\cdot}478{\cdot}10^{-9} \; W I_E}{k \; p{\cdot}A} \; T^{1.5}$$

## 2.15 $\frac{\partial}{\partial T}\left(\frac{1}{h_{FE}}\right)$

From 2.1.4
$$\frac{\partial}{\partial T}\left(\frac{1}{h_{FE}}\right) = \frac{\partial}{\partial T}\left[\frac{S \; W \; As}{D_n \; A} \; g(Z)\right] + \frac{\partial}{\partial T}\left[\frac{\sigma_B \; W}{\sigma_E L_E} + \frac{1}{2}\left(\frac{W}{L_B}\right)^2\right](1 + Z)$$

Substituting from 2.12.7 and 2.13.6

2.15.1
$$\frac{\partial}{\partial T}\left(\frac{1}{h_{FE}}\right) = \frac{WAs}{A}\left\{\frac{g(Z)}{D_n}\left[\frac{2.71 \cdot 10^5}{T^{2.5}} \frac{S}{D_n} + \frac{\partial S}{\partial T}\right] + \frac{S}{D_n} \frac{1.52Z}{T} \frac{\partial g(Z)}{\partial Z}\right\} +$$
$$\frac{W^2}{2}\left\{\frac{1.52 \; Z}{T}\left\{\frac{2}{W} \frac{\sigma_B}{\sigma_E L_E} + \frac{1}{L_B{}^2}\right\} - 2{:}10^{-4}(1+Z)\left[\frac{1}{W\sigma_E}\left(\frac{P \cdot 10^{-5}}{L_E \; T^{3.7}} + \frac{0.044\sigma_B}{L_E{}^2}\right) + \frac{2}{L_B{}^3}\right]\right\}$$

## 2.16 Discussion of the Webster Expression for Gain

The intent of the foregoing sections was to examine the various physical parameters which affect the gain of a transistor, and how a temperature change in the range of interest affects them.

From a consideration of the various terms, several approaches have been evolved which have been influenced by the behavior of the individual terms.

It must be realized that this first derivation is approximate only and was undertaken to develop an approach and to get a feel for the problem. As a geometry is evolved for a practical device, a re-examination of the gain equation will be required which incorporates the influence of space charge recombination in the emitter transition region as well as the transverse fields from the so-called Fletcher effect.

Since one of the most difficult variables to treat is the $\frac{\partial S}{\partial T}$ term, the use of oxide mask or so-called "planar" diffusions may provide an approach to gaining control and possibly a quantitative grasp of this variable.

2.17 Fletcher Effect

Since the emitter efficiency increases with temperature, the Fletcher effect can be utilized to control this term if the current density is sufficiently high.

The voltage drop underneath the emitter due to the base current causes a change of the emitter forward bias voltage. Therefore, the emitter current density is location dependent.

N. H. Fletcher [7,8] calculated this current density for a bar emitter/base geometry.

For a low injection level, the current density is

2.17.1 $$j(x) = j(0)\left[1 + x\sqrt{\frac{1}{2W\sigma_B}\left(\frac{\sigma_B W}{\sigma_E L_{pE}} + \frac{1}{2}\frac{W^2}{L_{nB}^2}\right)\frac{q}{kT}\, j(0)}\,\right]^{-2}$$

(for n-p-n transistor)

and for a high injection level, greater than 20 amperes per square centimeter

2.17.2 $$j(x) = j(0)\left[1 + x\sqrt{\frac{1}{6W\sigma_B}\left(\frac{\sigma_B W}{\sigma_E L_{pE}} + \frac{1}{2}\frac{W^2}{L_{nB}^2}\right)\frac{q}{kT}\, j(0)}\,\right]^{-2}$$

(for n-p-n transistor)

$j(0)$ = current density on emitter edge ($x=0$)

$W$ = base width

$\sigma_B$ = conductivity of the base

$\sigma_E$ = conductivity of the emitter

$L_{pE}$ = diffusion length of holes in emitter

$L_{nB}$ = diffusion length of electrons in base region

A typical design has the following parameters:

$W$ = $1 \times 10^{-4}$ cm

$\sigma_B$ = $1.63\ [\Omega\text{cm}]^{-1}$

$\sigma_E$ = $2.5 \times 10^3\ [\Omega\text{cm}]^{-1}$

$L_{pE}$ = $0.94 \times 10^{-3}$ [cm] at 25°C [6]

$L_{nB}$ = $2 \times 10^{-2}$ [cm] at 25°C [6]

With this data we get a low injection level distribution

2.17.3 $$j(x) = j(0) \left[1 + 3.13\, j(0)^{1/2}\, x\right]^{-2}$$

and a high injection level distribution

2.17.4 $$j(x) = j(0) \left[1 + 1.807\, j(0)^{1/2}\, x\right]^{-2}$$

To determine j(0), we have to integrate over the whole emitter surface.

The total emitter current $I_E$ is

2.17.5 $$I_E = \ell_E \int_0^W j(x)\, dx$$ , $\ell_E$ = effective emitter length

If we substitute j (x) in 2.17.5 from 2.17.3 and 2.17.4, we get equations to calculate j(0).

2.17.6 $$I_E = j(0)\, \ell_E\, W \left[1 + 3.13\, j(0)^{1/2}\, W\right] \text{ or } j(0) \left[\ell_E W\right] - 3.13W\, j(0)^{1/2}\, I_E - I_E = 0$$ (low injection level)

2.17.7 $$I_E = j(0)\, l_E\, W \left[1 + 1.807\, j(0)^{1/2}\, W\right] \text{ or } j(0) \left[\ell_E W\right] - 1.807W\, j(0)^{1/2}\, I_E - I_E = 0$$ (high injection level)

To evaluate 2.17.6 and 2.17.7 we use the data of our design.

A) <u>Single bar geometry</u>: $\ell_E$ = 10 [mils]

= $2.5 \times 10^{-2}$ cm

d = 3 [mils]

= $0.75 \times 10^{-2}$ cm

$\ell_E$ = length of emitter

d = width of emitter

B) Double bar geometry: $\ell_E = 20$ [mils]

$= 5 \times 10^{-2}$ cm

$d = 1.5$ [mils]

$= 0.75 \times 10^{-2}$ cm

With this data substituted in (6) and (7) we get for the low injection level:

2.17.8 $$1.875 \times 10^{-4}\, j(0) - 2.35 \times 10^{-2}\, j(0)^{1/2}\, I_E - I_E = 0$$

for single bar geometry

2.17.9 $$1.875 \times 10^{-4}\, j(0) - 1.173 \times 10^{-2}\, j(0)^{1/2}\, I_E - I_E = 0$$

for double bar geometry

and for the high injection level:

2.17.10 $$1.875 \times 10^{-4}\, j(0) - 1.357 \times 10^{-2}\, j(0)^{1/2}\, I_E - I_E = 0$$

for single bar geometry

2.17.11 $$1.875 \times 10^{-4}\, j(0) - 0.677 \times 10^{-2}\, j(0)^{1/2}\, I_E - I_E = 0$$

for double bar geometry

Figures 2.17.1, 2.17.2, and 2.17.3 show the results for emitter current of $I_E = .5$ ma and 100 ma.

Discussion:

There is almost no Fletcher effect at current level $I_E = 50$ ma, and at $I_E = 20$ ma there is only a small Fletcher effect. At 100 ma the Fletcher effect has quite an influence, so that the Fletcher effect becomes important at the high current level in our attempt to control the gain.

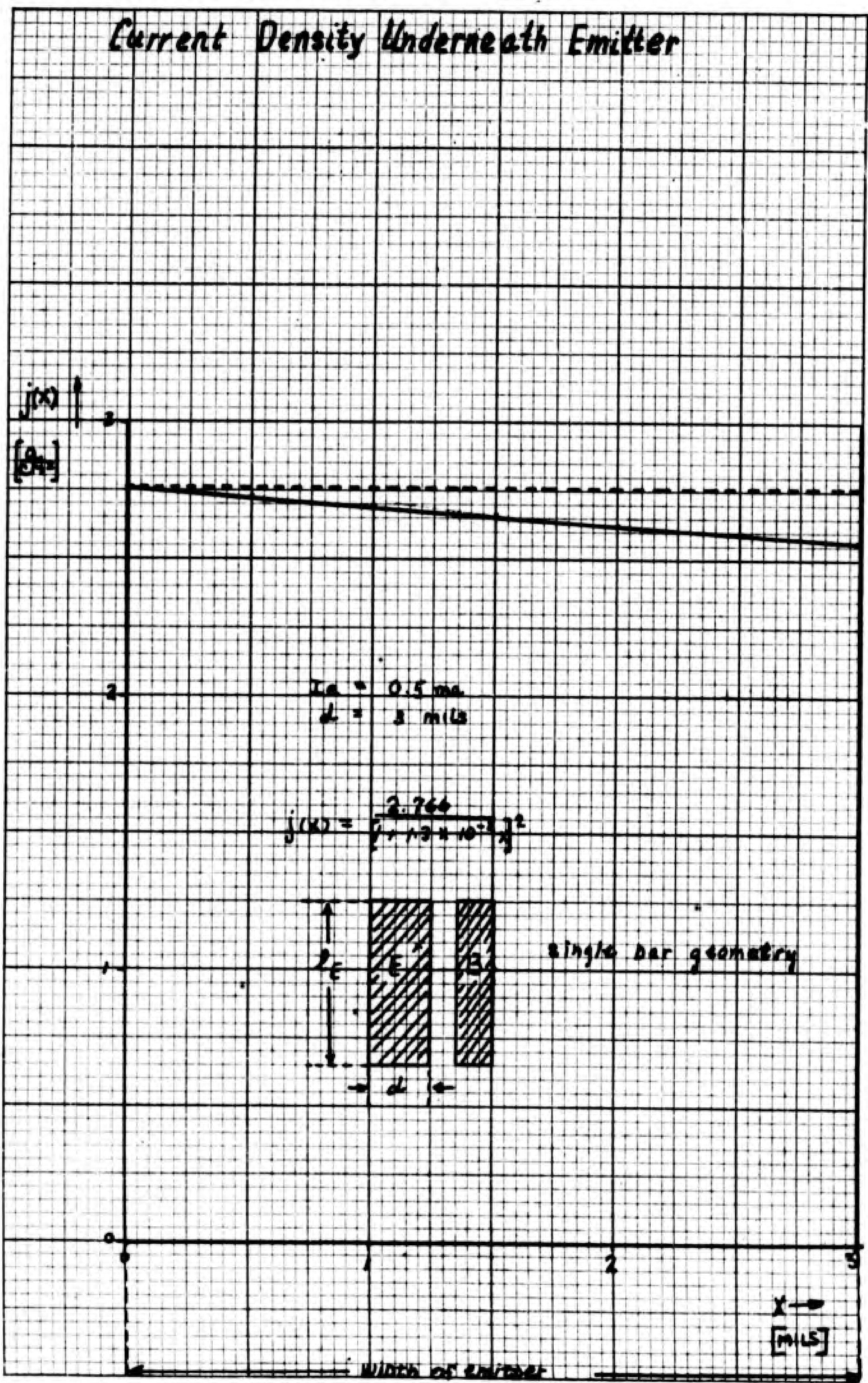


FIG. 2.17.1

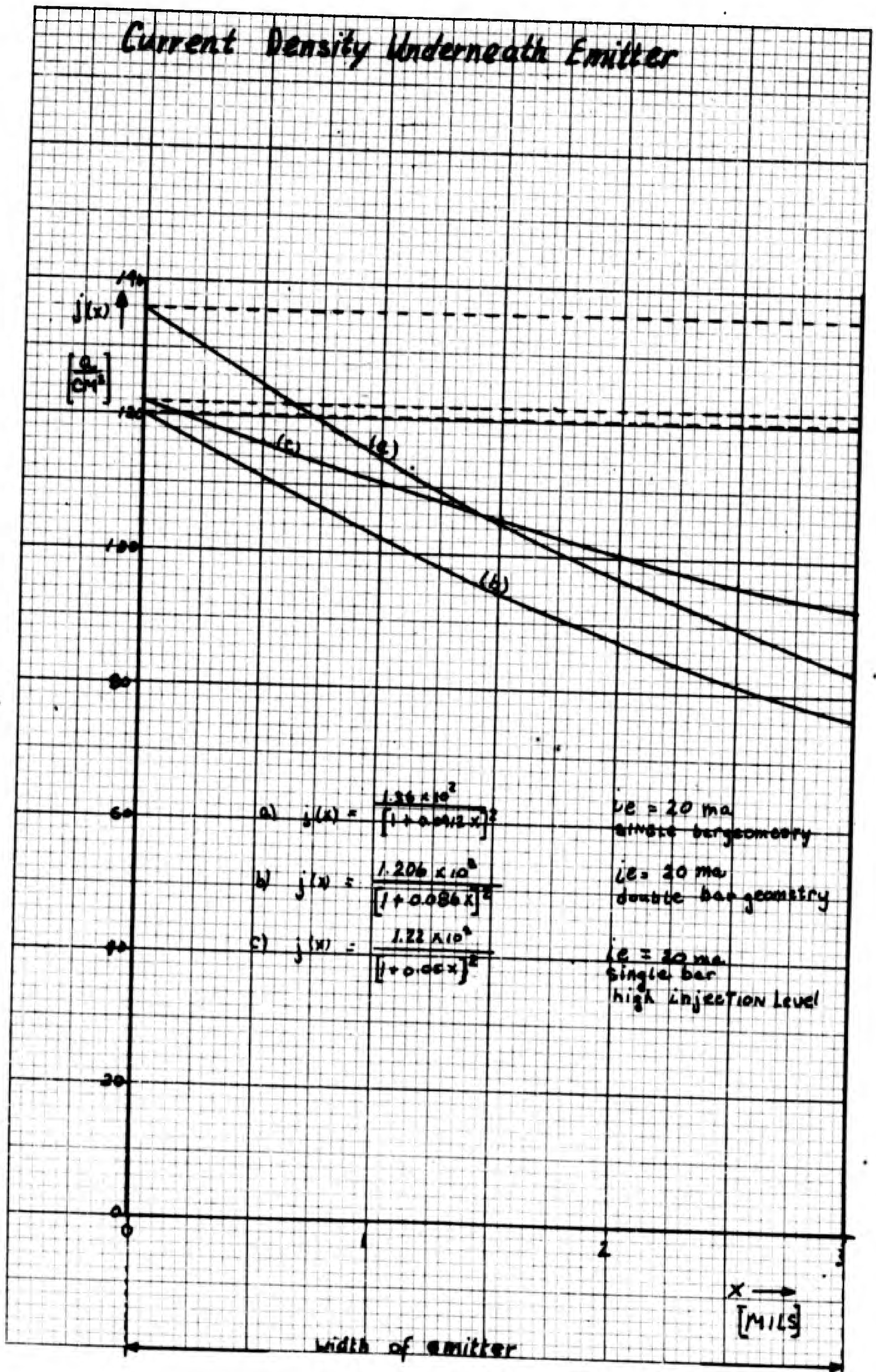


FIG. 2.17.2

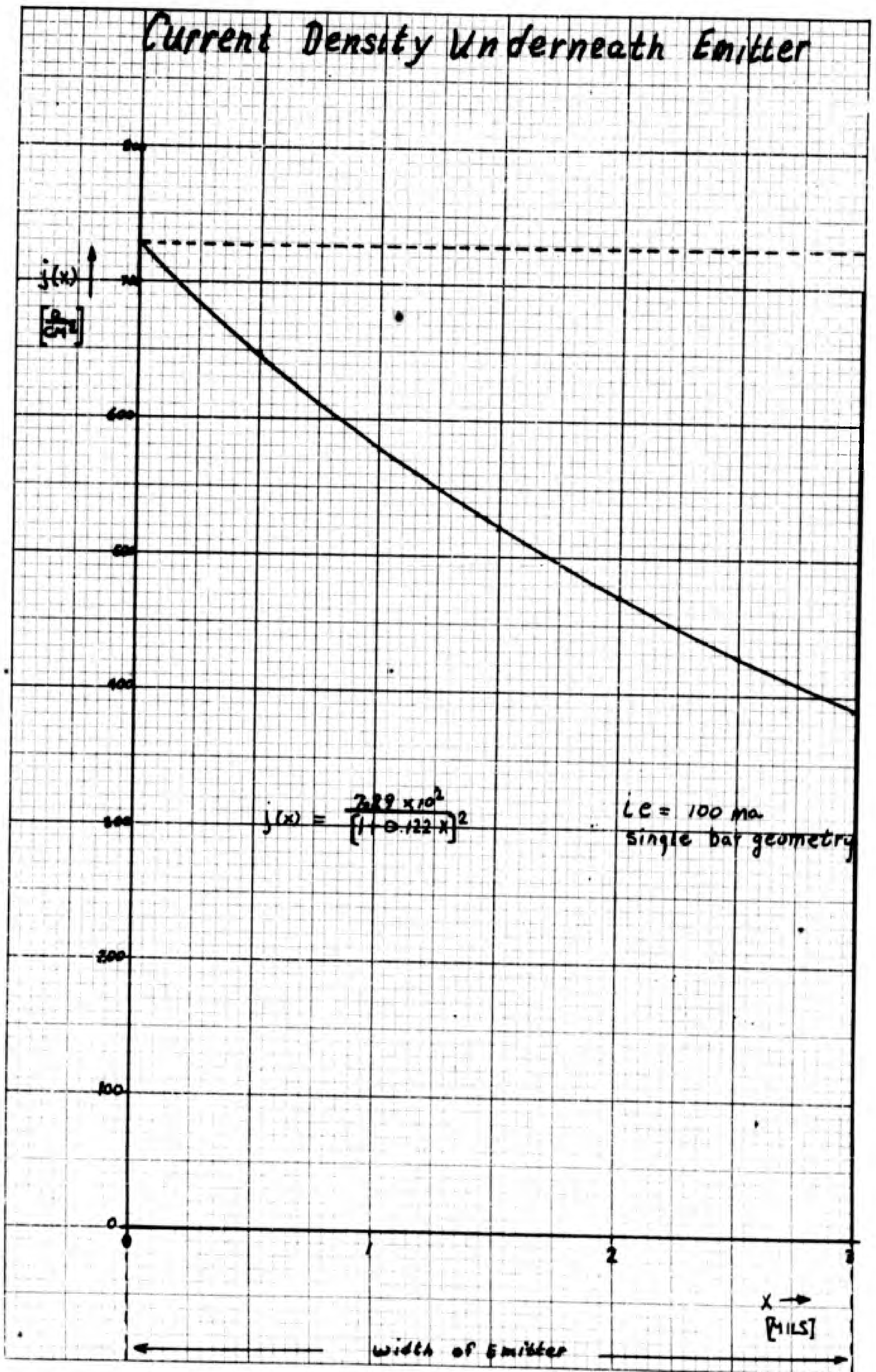


FIG. 2.17.3

## 2.18 $h_{FE}$ at Low Current Levels - Consideration of Space Charge Recombination

In the following section the junction current equations are considered with and without space charge recombination and generation.

This work is in an early state and will be extended during the next quarter.

The expression for the grounded base gain is considered and the effect on $\alpha$ is shown due to recombination.

A) $I_C$ and $I_E$ Neglecting Space Charge Recombinations[9]

p-n-p Transistor:

2.18.1 $$I_C = \text{Csch}\,\frac{2W'}{L_p}\,I_{po}\,(\phi_E) + \text{Coth}\,\frac{2W'}{L_p}\,I_{po}(\phi_C) + I_{no}(\phi_C)$$

2.18.2 $$I_E = \text{Coth}\,\frac{2W'}{L_p}\,I_{po}(\phi_E) + -\text{Csch}\,\frac{2W'}{L_p}\,I_{po}(\phi_C) + I_{no}(\phi_E)$$

n-p-n Transistor:

2.18.3 $$I_C = -\text{Csch}\,\frac{W}{L_n}\cdot I_{no}(\phi_E) + \text{Coth}\,\frac{W}{L_n}\,I_{no}(\phi_C) + I_{po}(\phi_C)$$

2.18.4 $$I_E = \text{Coth}\,\frac{W}{L_n}\cdot I_{no}(\phi_E) - \text{Csch}\,\frac{W}{L_n}\,I_{no}(\phi_C) + I_{po}(\phi_E)$$

2.18.5 $W = 2W'$ , $I_{no}(\phi_E) = \frac{n_p q D}{Ln} \left( e^{\frac{q\phi_E}{kT}} - 1 \right)$

$$I_{no}(\phi_C) = \frac{n_p q D}{Ln} \left( e^{\frac{q\phi_C}{kT}} - 1 \right)$$

B) Consideration of Space Charge Recombinations [10]

2.18.6 $I_C = \text{Csch} \frac{W}{L_n} I_{no}(\phi_E) + \text{Coth} \frac{W}{L_n} I_{no}(\phi_C) \; + I_{po}(\phi_C) + I_{rg}$

2.18.6a $I_{rg} = \frac{-q W n_i}{2\tau_o}$ $W$ = width of space charge

2.18.7 $I_E = \text{Coth} \frac{W}{L_n} I_{no}(\phi_E) - \text{Csch} \frac{W}{L_n} I_{no}(\phi_C) \; + I_{po}(\phi_E) + I_{rg}$

2.18.7a $I_{rg} = \frac{2q\, n_i}{2\tau_o} \frac{kT}{q(\psi_D - V)} e^{\frac{qV}{2kT}}$

2.18.7b $I_{po}(\phi_E) = \frac{-2q\, P_n\, L_o}{\tau_o}$

C) D.C. Current Gain

No Consideration of Space Charge Recombination:

2.18.8 $\alpha_o = -\frac{\partial I_C}{\partial I_E} = \frac{\text{Csch} \frac{W}{L_n} I_{no}(\phi_E) - \text{Coth} \frac{W}{L_n} I_{no}(\phi_C) - I_{po}(\phi_C)}{\text{Coth} \frac{W}{L_n} I_{no}(\phi_E) - \text{Csch} \frac{W}{L_n} I_{no}(\phi_C) + I_{po}(\phi_E)}$

2.18.9 $\alpha_o \approx \frac{\text{Csch} \frac{W}{L_n} I_{no}(\phi_E)}{\text{Coth} \frac{W}{L_n} I_{no}(\phi_E)} = \frac{\text{Csch} \frac{W}{L_n}}{\text{Coth} \frac{W}{L_n}} = \frac{\text{Tanh} \frac{W}{L_n}}{\text{Sinh} \frac{W}{L_n}}$

2.18.10 $\alpha_o \approx \frac{1}{\text{Cosh} \frac{W}{L_n}} = \text{Sech} \frac{W}{L_n}$

2.18.11 $$\alpha_o = \text{Sech}\left(\frac{W}{L_n}\right)$$

Considering of Space Charge Recombination:

2.18.12 $$I_C = -\text{Csch}\,\frac{W}{L_n}\,I_{no}(\phi_E) + \text{Coth}\,\frac{W}{L_n}\,I_{no}(\phi_C) + I_{po}(\phi_C)$$

2.18.13 $$I_E = \left\{\text{Coth}\,\frac{W}{L_n}\,I_{no}(\phi_E) - \text{Csch}\,\frac{W}{L_n}\,I_{no}(\phi_C)\right\} + I_{po}(\phi_E) + I_{rg}$$

2.18.14 $$\alpha = \frac{-\partial I_C}{\partial I_E} = \alpha_o \frac{1}{\left[1 + \dfrac{I_{po}(\phi_E) + I_{rg}}{\text{Coth}\,\frac{W}{L_n}\,I_{no}(\phi_E) - \text{Csch}\,\frac{W}{L_n}\,I_{no}(\phi_C)}\right]}$$

2.18.15 $$\alpha = \alpha_o \frac{1}{1 + \dfrac{(I_{rg} + I_{po}(\phi_E))}{\text{Coth}\,\frac{W}{L_n} \cdot I_{no}(\phi_E)}} = \frac{\alpha_o}{1 + \text{Tanh}\,\frac{W}{L_n}\,\dfrac{(I_{rg} + I_{po}(\phi_E))}{I_{no}(\phi_E)}}$$

2.18.16 $$\alpha = \frac{\alpha_o}{1 + \dfrac{I_{rg} + I_{po}(\phi_E)}{I_{no}(\phi_E)} \cdot \text{Tanh}\left(\frac{W}{L_n}\right)}$$

## 3.0 DESIGN APPROACHES

### 3.1 Use of the Fletcher Effect to Control $h_{FE}$ Variation

From the Webster Expression

2.1.1 $$\frac{1}{h_{FE}} \approx \frac{s\,W\,A_s}{D_n\,A}\,g(Z) + \left[\frac{\sigma_B\,W}{\sigma_E\,L_E} + \frac{1}{2}\left(\frac{W}{L_B}\right)^2\right](1 + Z)$$

and Z the Webster Factor.

2.1.2 $$Z = \frac{W\,q\,I_E}{k\,TA}\left(\frac{\mu_p}{\mu_n}\right)$$ for an n-p-n transistor

A is the cross sectional area of the conduction path and $A_s$ is the effective surface area for recombination. The term A is temperature independent, and, if a method can be found to control A as a function of temperature, the possibility of utilizing the Fletcher effect to control $h_{FE}$ exists.

At low injection levels A is about equal to the geometrical emitter area. At high injection levels A can be much smaller than the geometrical emitter area where the geometrical emitter area is defined as the diffused region which forms an n-p junction due to the Fletcher effect.[11]

As indicated (Section 2.18), space charge recombination must be considered at low injection levels, since this effect is more important than the bulk recombination factor, and the

Webster equation must be modified to account for $h_{FE}$ under these conditions.

The foregoing considerations suggest that the Fletcher effect will not be important in attempting to control $h_{FE}$ at low injection levels, but can provide a definite approach at high injection levels.

Decreasing the effective current path A, if done in such a way that the increase of $h_{FE}$ due to the various factors noted in Eq. 2.15.1 can be offset, the $h_{FE}$ can be controlled over the temperature range of interest. Figure 3.1.1 depicts a scheme for achieving a variable A.

Two base stripes are connected by a resistor R with a positive temperature coefficient. R can be a separate resistor or be "built-in" to the base surface.

The resistivity of silicon increases over the temperature range of interest.[6] Since the base region would be p-type with an acceptor concentration of $\sim 5 \cdot 10^{17}$ cm$^{-3}$, a 70% positive change could be expected from 0°C to 100°C.

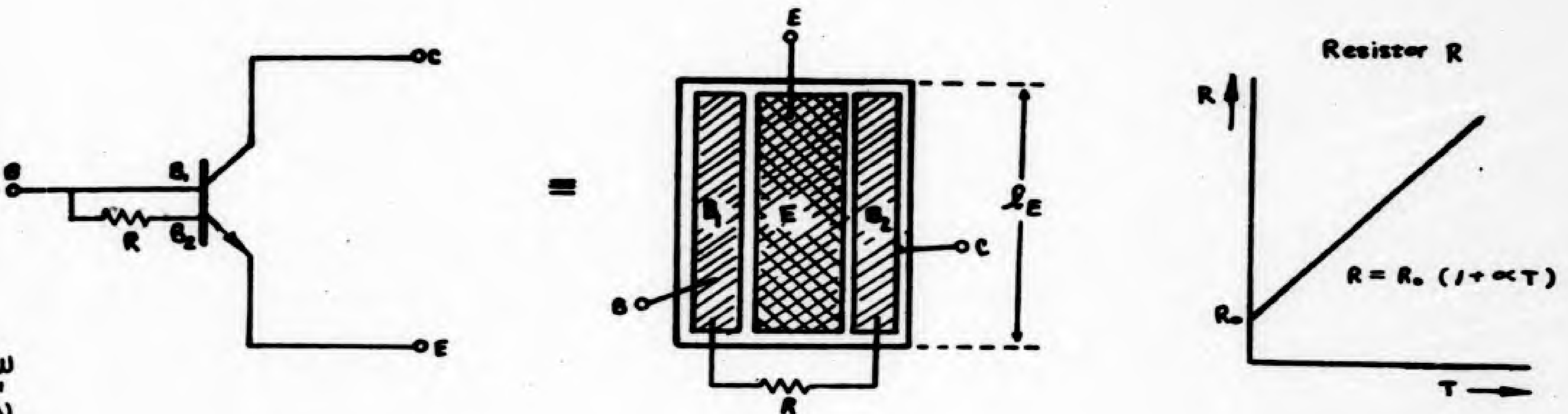


Fig. 3.1.1

3-2-A

### 3.2 High Injection Level Case - Fletcher Effect

At high injection levels a base fringing effect occurs and with this a corresponding decrease of the "effective" cross sectional area of the conduction path A. This is shown for a special case in Section 2.17, Figures 2.17.1, 2, and 3.

At a high current density practically the entire emitter current is concentrated on the emitter perimeter (or depending on base-emitter configuration, emitter edge). At very high injection levels the effective conduction path width is

$$Y_1 = W\sqrt{2\frac{I_E}{I_B}} \qquad \underline{11}.$$

where

$W$ = base width

$I_E$ = emitter current

$I_B$ = base current.

Figure 3.2.1 depicts this situation for $h_{FE}$ compensation. At room temperature $R = R_O$ is low and almost shorts the two base stripes. The cross sectional area is A where

3.2.1 $$A = 2\,\ell_E\,Y_1$$

3.2.2 $$A = 2\,\ell_E\,W\sqrt{2\frac{I_E}{I_B}}$$

As the temperature increases, R increases. The base current flowing to the base stripe $B_2$ gets smaller and smaller due to the voltage drop in R which decreases the forward bias of the emitter junction facing $B_2$. In the limit, A becomes

3.2.3 $$A = \ell_E Y_1 = \ell_E W \sqrt{\frac{2 I_E}{I_B}}$$

As A changes, $A_s$ also changes since the concentration of the emitter current injection on the perimeter of the emitter A is proportioned to $A_s$. The ratio of $\frac{A_s}{A}$ is essentially temperature independent particularly if the spacing between emitter and base is less than the diffusion length of carriers on the surface so that the effective diffusion length is not changed with increasing temperature. In the present discussion, the spacing is considered to be much less than the diffusion length.

A decrease of A causes an increase of the Webster factor Z which decreased $h_{FE}$. However, g(Z) decreases as Z increases and causes a corresponding rise in $h_{FE}$ by means of the surface recombination factor.

If $Z > 5$ the change of g(Z) with Z can be neglected. From the foregoing the conclusion is that the effect of the g(Z) term

must be kept small so that the increase of $h_{FE}$ with temperature can be avoided. This can be achieved by keeping s, the surface recombination term, as small as possible (note Eq. 2.15.1). An oxide masked or so-called "planar" structure is indicated to achieve a small s.

### 3.3 Low Injection Level - Fletcher Effect

In Section 2.17 it was shown that at emitter currents of 2 mA and less, the Fletcher effect is negligible. In order to change the emitter area A, a structure of the sort shown in figure 3.3.2 can be considered. In this case the emitter split as well and a resistive path between the emitters such that base current flow from $E_1$ to $B_2$ and $E_2$ to B, can be prevented at a desired temperature and the base controlled as before.

R again must have a positive temperature coefficient so that at room temperature $R = R_0$ essentially shorts $B_1$ and $B_2$ and both emitters are working equally.

The area of the emitter path is

3.3.1 $$A = 2 \ell_E d$$

As the temperature increases, R increases and the mechanism explained above again gives

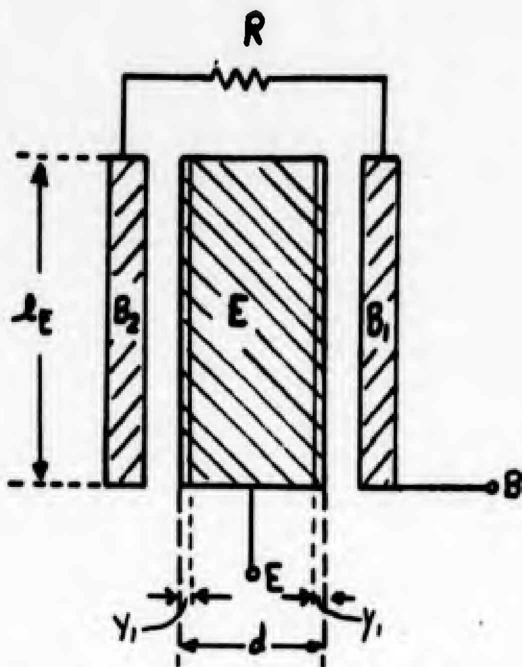


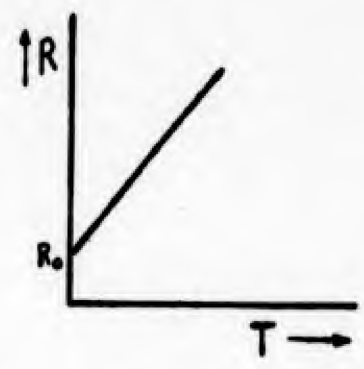


Fig. 3.2.1

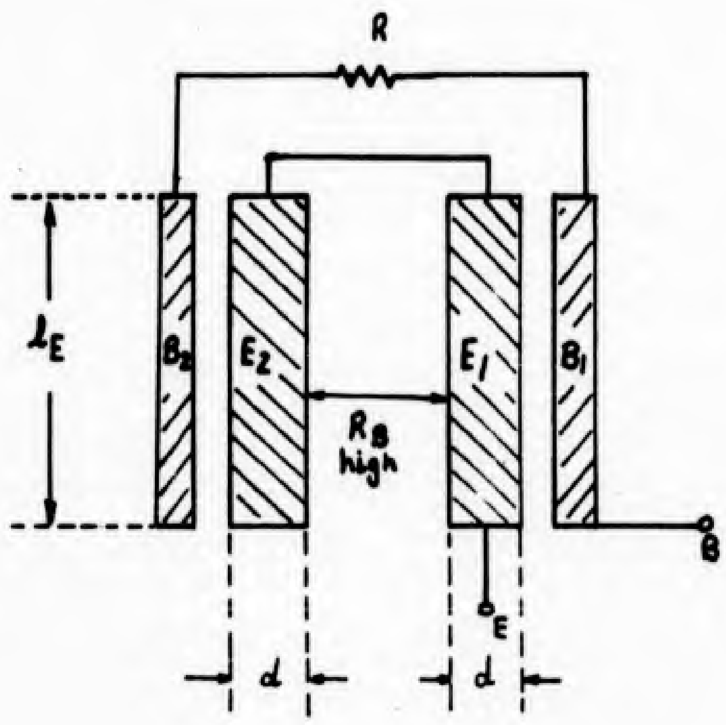


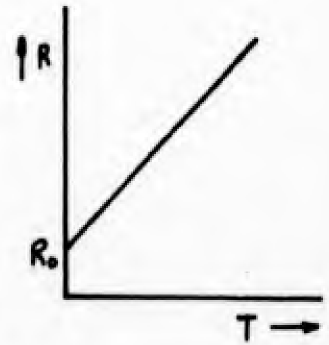


Fig. 3.3.2

3.3.2 $$A = \ell_E d$$

3.4 Two Transistors in Parallel

From the preceding section it can be seen that the design geometry evolved to two transistors in parallel.

If two separate transistors are connected in parallel it can be shown that the gain of the combination will lie between the gains of the individual transistors. This calculation is shown in appendix two and the result is given as.

3.4.1 $$\beta = \beta_2 \left[ \frac{1 + C}{\beta_2/\beta_1 + C} \right] \quad \text{or if } C = 1$$

3.4.2 $$\beta = 2 \left[ \frac{\beta_1 \beta_2}{\beta_1 + \beta_2} \right]$$

where C = constant $\beta = h_{FE}$ of the parallel circuit

$\beta_1 = h_{FE_1}$ current gain of transistor #1

$\beta_2 = h_{FE_2}$ current gain of transistor #2

In order to achieve a variation of $h_{FE}$ with temperature, a resistor or thermistor must be connected as shown in Figure 3.4.1 and Figure 3.4.2.

In the case of the resistor, a positive temperature coefficient is required while in the case of a thermistor a negative temperature coefficient is required. As indicated in the

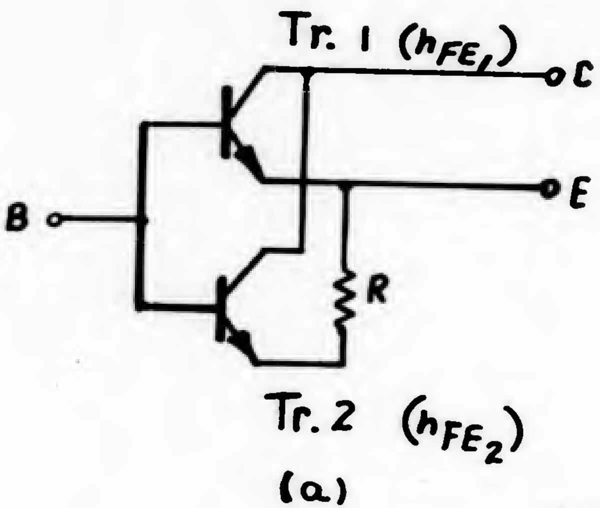


(a)

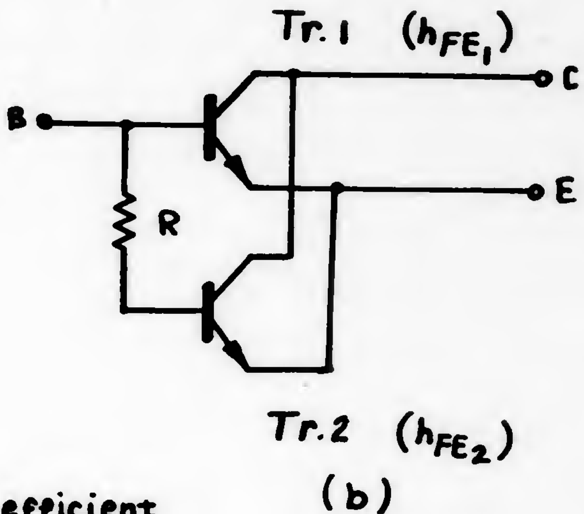


(b)

R = Resistor
positive temperature coefficient

$h_{FE_1} < h_{FE_2}$

Fig. 3.4.1

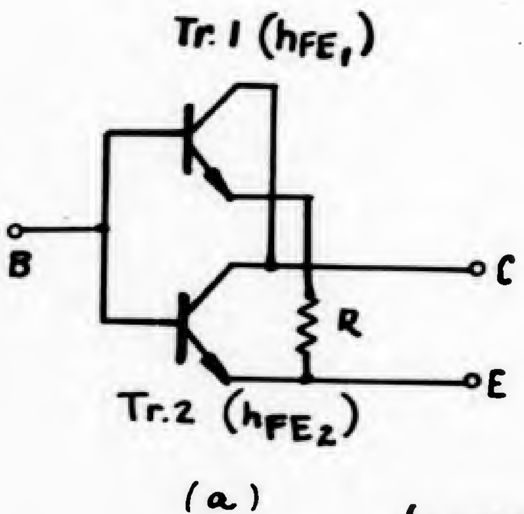


(a)

Tr. 1 ($h_{FE_1}$)
R
C
B
E
Tr. 2 ($h_{FE2}$)

(b)

R = Thermistor
(negative temperature coefficient)

$h_{FE_2} > h_{FE_1}$

Fig. 3.4.2

figures the connection can be made to either the emitter or the bases, the effect is the same. When R becomes very large the bias of one of the devices drops and the circuit behaves essentially as one transistor.

If a <u>resistor</u> is used, the direct connected transistor $\beta$ must be less than the parallel connected transistor $\beta$ (Fig. 3.3.1). If the <u>thermistor</u> is used, the direct connected transistor $\beta$ must be greater than the parallel connected transistor $\beta$.

The parallel circuit of two transistors and a resistor or thermistor can be realized by mounting separate components on a header as an integrated circuit with each component separated.

Two transistors can also be fabricated on the same die with a step collector to give a differential $h_{FE}$ between the two devices. For this case a built in resistor can be considered as a portion of the base region.

## 3.5 Diode in Parallel to the Emitter Junction

If the temperature behavior of an inverted transistor (collector used as an emitter and emitter used as a collector) is investigated, it will be found that the $h_{FE}$ in the temperature range 0°C to 80°C will be unaffected.

The magnitude of $h_{FE}$ will be very low, however. This can be explained by the poor inverse collector efficiency as shown in Fig. 3.5.1b.

Although the emitter efficiency of the collector junction is poor, it does not explain an observed $h_{FE}$ of the order of one. In Appendix IV the emitter efficiency of the collector junction is considered and its influence on the inverse $h_{FE}$ is determined. The conclusion is drawn that the low $h_{FE}$ is due to the geometry of the structure.

The current flow map in Fig. 3.5.1b can also be interpreted as a regular transistor with a forward biased diode in parallel to the emitter junction.

Appendix III contains a description of the effect on gain of a diode in parallel with the emitter of a transistor as a function of temperature. If properly designed, such a circuit can provide temperature compensation.

Fig. 3.5.2 depicts the circuit discussed above for the transistor diode combination. To control the diode effect, a resistor R is included in series with the diode. In Fig. 3.5.2a, an external diode is shown. In Fig. 3.5.2b a portion of the emitter is used as a diode.

MINORITY CARRIER FLOW MAP

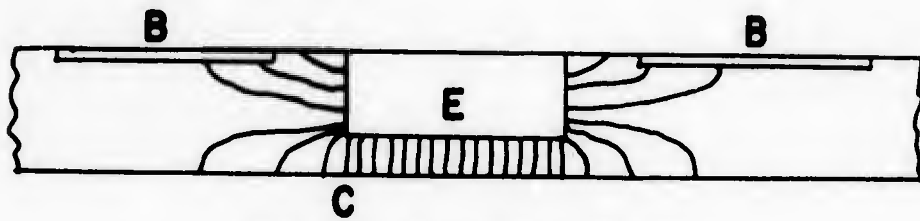


a.
REGULAR
TRANSISTOR

REGULAR TRANSISTOR

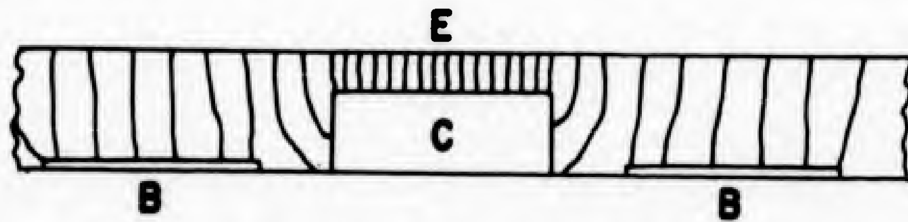


b.
INVERTED
TRANSISTOR

INVERTED TRANSISTOR

FIG. 3.51

B
C
E
R

a)

B
C
E
R

b)

E = EMITTER
C = COLLECTOR
B = BASE

Fig. 3.5.2

(INTEGRATED CIRCUIT)



Fig. 3.5.3

Separate components can be mounted on the same header to build the configuration shown in Fig. 3.5.3.

Placing both elements on a single die can be accomplished as shown in Fig. 3.5.4 where the diode on the left is fabricated in a separate p region for "effective" electrical isloation from the transistor on the right.

Incorporating the resistor as in Section 3.5.5 can be accomplished by forming a connecting p region to the base. A planar technique would be most convenient for the fabrication of such a device.

### 3.6 Controlled Surface Recombination

A recent paper by Sah[13.] suggests still another approach to $h_{FE}$ control with temperature. If the $A_s$ (surface recombination) term could be controlled independently of A with temperature; for example, by increasing $A_s$ as temperature increases, the normal increase of $h_{FE}$ could be controlled.

The device reported by Sah is a surface recombination controlled tetrode. **Fig. 3.6.1 depicts Sah's configuration** in which a grid electrode is placed on an oxide film directly over the emitter periphery by applying a potential from grid to base. The surface potential is controlled as well as the

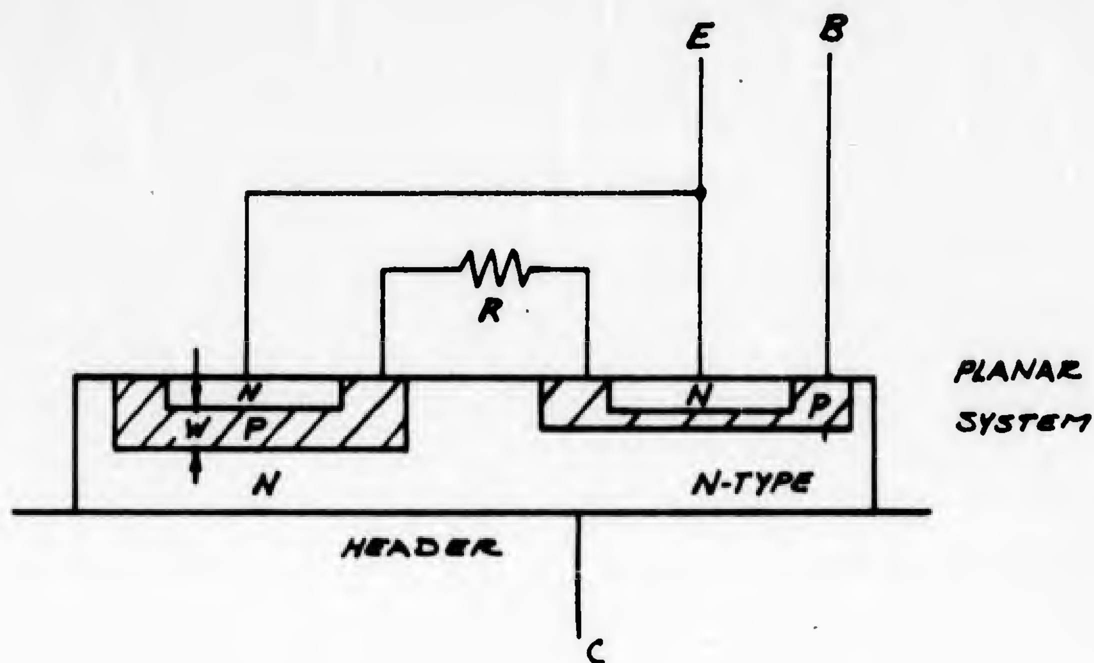


FIG. 3.5.4

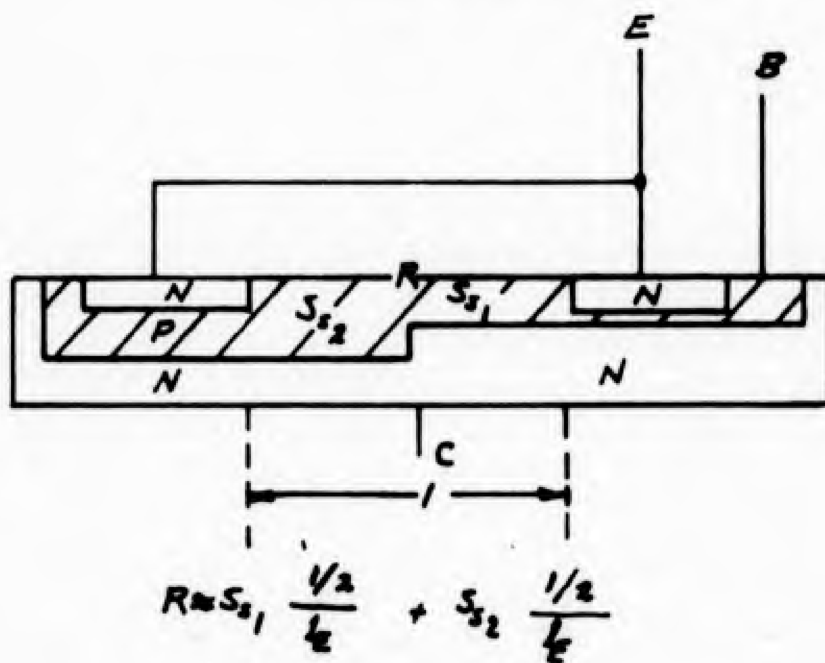


$$R \approx S_{s_1} \frac{l/2}{l_E} + S_{s_2} \frac{l/2}{l_E}$$

FIG. 3.5.5

recombination rate s and an inversion layer is induced under the oxide. With control of these factors, the gain can be affected.

Figure 3.6.2 taken from Sah's paper shows the influence of the grid voltage on gain as a function of collector current.

Utilizing a temperature sensitive resistor as shown above and the voltage divider indicated in Fig. 3.6.3, a feedback network could be constructed to compensate for $h_{FE}$.

Here the grid-emitter voltage is given by

3.6.1 $$V_{GE} = V_o \frac{R_2}{R_1 + R_2}$$

If $R_1 >> R_2$

3.6.2 $$V_{GE} = V_o \frac{R_2}{R_1}$$

If $R_2$ is a resistor and $R_1$ is a thermistor, $V_{GE}$ increases with temperature and therefore decreases the d.c. current gain.

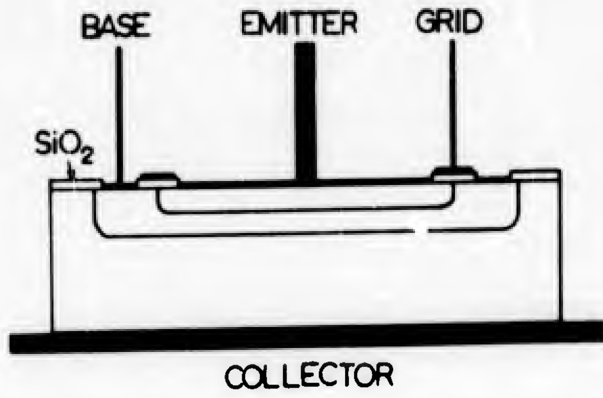


Fig. 3.6.1

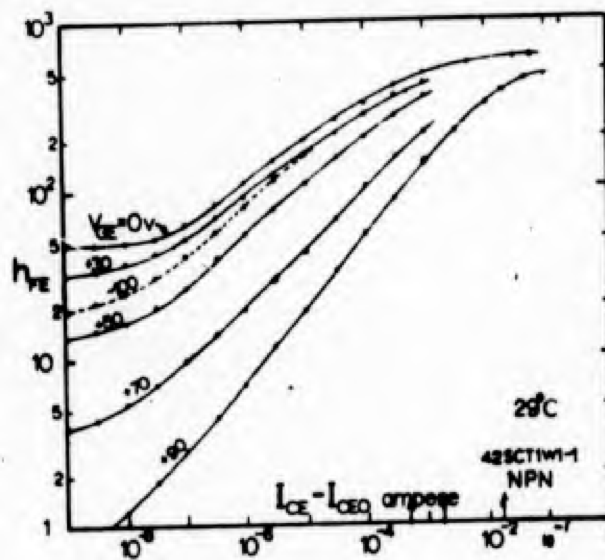


Fig. 3.6.2

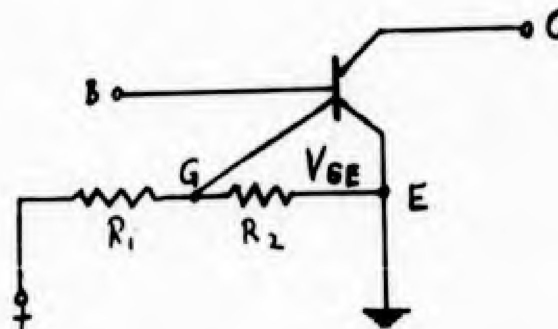


Fig. 3.6.3

## 4.0 PRELIMINARY DESIGN CONSIDERATIONS

### 4.1 Determination of Background (Base Region) Resistivity

The resistivity of the starting Si-material is bounded by two limits. The upper limit is given by the $V_{CE}$ sat specification and the lower limit by the $V_{CER}$.

By determining first the lower limit of the resistivity $\rho$, required for meeting $V_{CER}$, a resistivity range is chosen from $\rho_{min.}$ up, which depends upon the variation of slice resistivity inherent in the crystal growing procedure used. Then $V_{CE\ sat}$ is calculated to determine the upper limit of the resistivity range. Fig. 4.1.1 was obtained by measuring $V_{CER}$ on units with different background resistivity $\rho$. All units had about the same collector and emitter junction depth, the same base width and about the same Ga and P surface concentration. Although $h_{FE}$ will have an effect on $V_{CER}$, it was not felt to be a significant variable in these measurements. Since the resistivity $\rho$ was not measured on the individual units, but in the center of the slice of the starting material, the $V_{CER}$ vs $\rho$ curve in Fig. 4.1.1 is of limited accuracy.

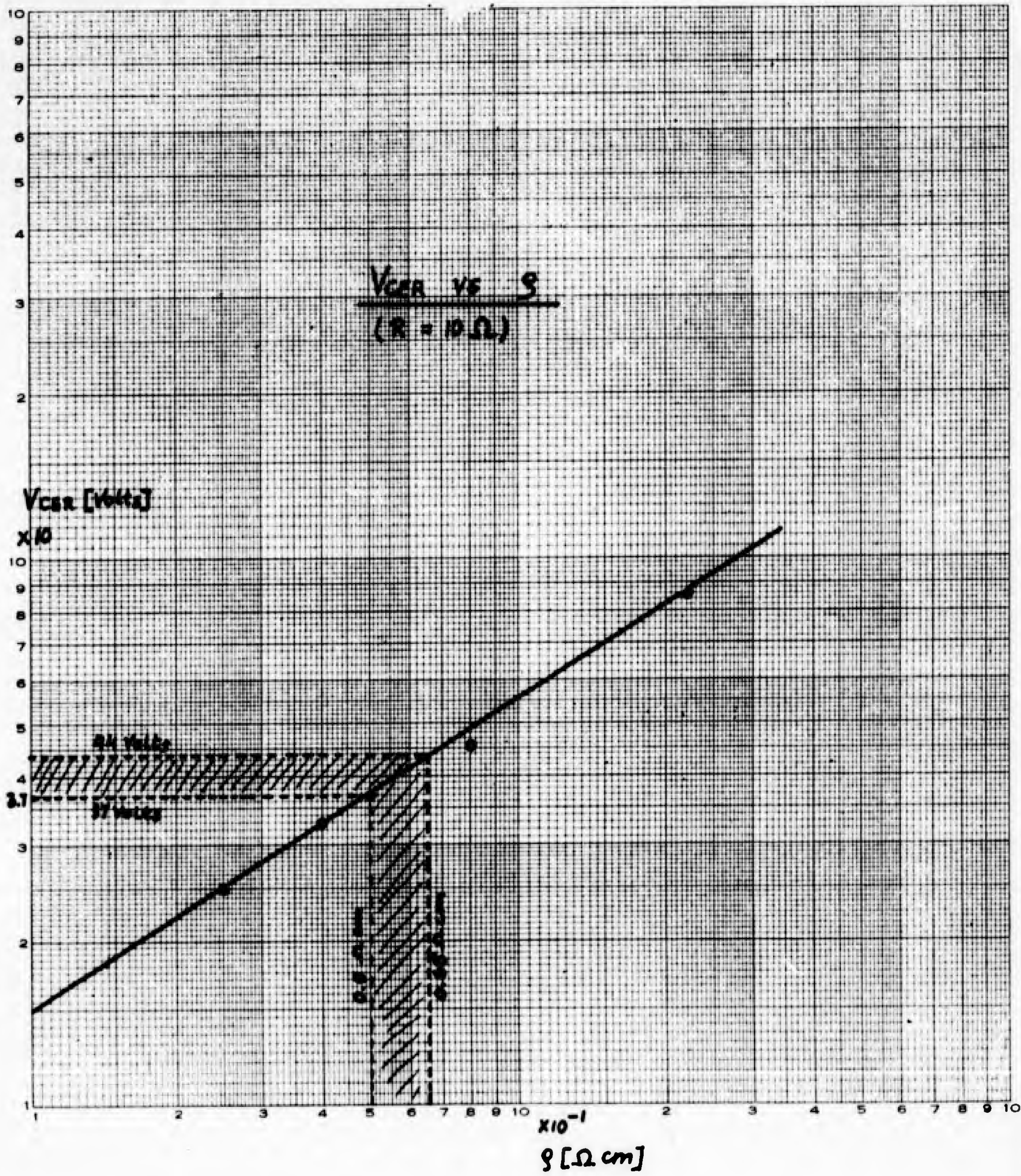


FIG. 4.1.1

Measurements of resistivity on individual slices show a variation of $\rho$ across the slices in spite of efforts to keep this change as low as possible.

In order to determine the significance of the $V_{CER}$ vs $\rho$ curve, the correlation between $V_{CER}$ and $C_{OB}$ was examined.

$C_{OB}$ here is the collector barrier capacitance which is readily measured and depends on $\rho$ in the following way.

4.1.1 $$C_{OB} = \frac{A\kappa\varepsilon_o}{2} \left[\frac{2q\,|a|}{3\kappa\,\varepsilon_o\,V'}\right]^{1/3}$$ 14.

4.1.2 $$|a| = \tan\phi = \frac{N_s}{(\pi D t)^{1/2}}\, e^{-\frac{x_j^2}{4Dt}}$$

4.1.3 $$\frac{1}{\rho} = \mu q\, N_s \operatorname{erfc} \frac{x_j}{2\sqrt{Dt}}$$

Equation 4.1.1 shows how $C_{OB}$ depends on $|a| = \tan\phi$. (See appendix V for a discussion of $\tan\phi$). Equation 4.1.2 is a function relating $\tan\phi$ and the diffusion time t, and equation 4.1.3 finally shows the correlation of $\rho$ and diffusion time t.

A large number of units have been tested and the results are shown in Fig. 4.1.2.

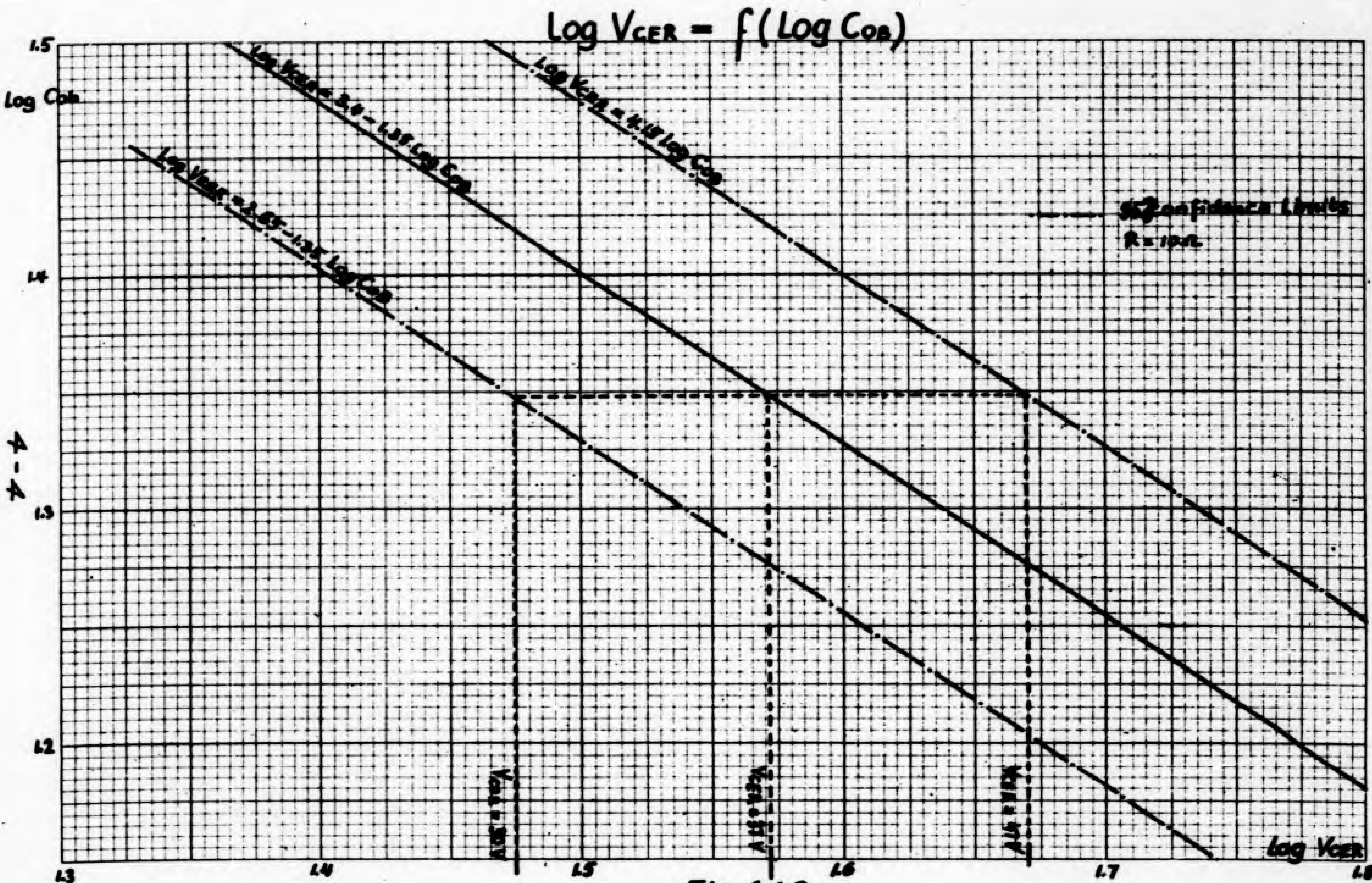

Fig. 4.1.2

To determine the best curve fit and the 95% confidence limits, the equations given in "Facts and Figures" by M. J. Moroney were used.

In order to be sure that 95% of transistors with the same $C_{OB}$, and therefore the same $\rho$, have $V_{CER} > 30$ volts, the average $V_{CER}$ must be 37 volts (Fig. 4.1.2). This means that in Fig. 4.1.1 the lower $V_{CER}$ limit is not 30 volts but 37 volts. To obtain $V_{CER} = 37$ volts, the collector body resistivity must be 0.5 $\Omega$cm. This is the minimum resistivity.

The upper practical limit for the resistivity which depends upon the crystal pulling variation on 0.5 $\Omega$cm resistivity Si becomes the resistivity range $0.5 \leqslant \rho \leqslant 0.65$ $\Omega$cm, since $V_{CE\ sat}$ is always made as low as possible rather than specifically calculated for an upper range. (Production economics may require a wider range.)

## 4.2 Device Geometry

The lower limit of the device size, i. e., collector geometry, is given by $V_{CE\ sat}$ and the base spreading resistance and the upper limit by the collector capacitance and the switching conditions.

The smallest dimensions which the device may have and still pass the $V_{CE\ sat}$ condition is calculated first and then the base spreading resistance.

For emitter and base, a bar geometry is chosen (Fig. 4.2.1 and 4.2.2).

<u>One Emitter and One Base Stripe</u> (Fig. 4.2.1)

The following non-linear effects must be considered to calculate $V_{CE}$ sat. [15.], [8.]

1. "Fringing of effective area of the collector due to the 'Fletcher' effect."

2. Decreasing of collector body resistivity by injection of minority carriers.

3. Mobility limiting at high current levels and therefore high electric fields.

At the current level we are interested in, we can neglect 2. and 3. The maximum current is limited by the carrier velocity:

4.2.1 $$I_{c_{max}} = qN_C v_{\ell} A_{Eff}$$

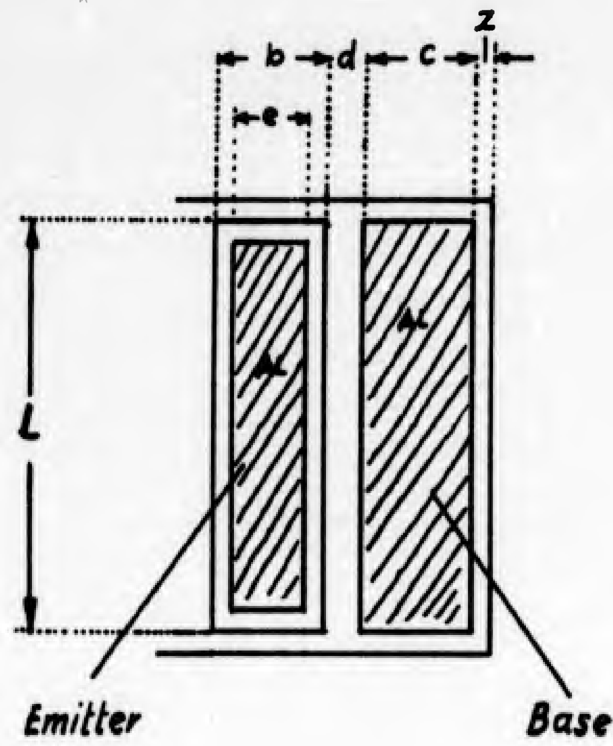


Fig. 4.2.1

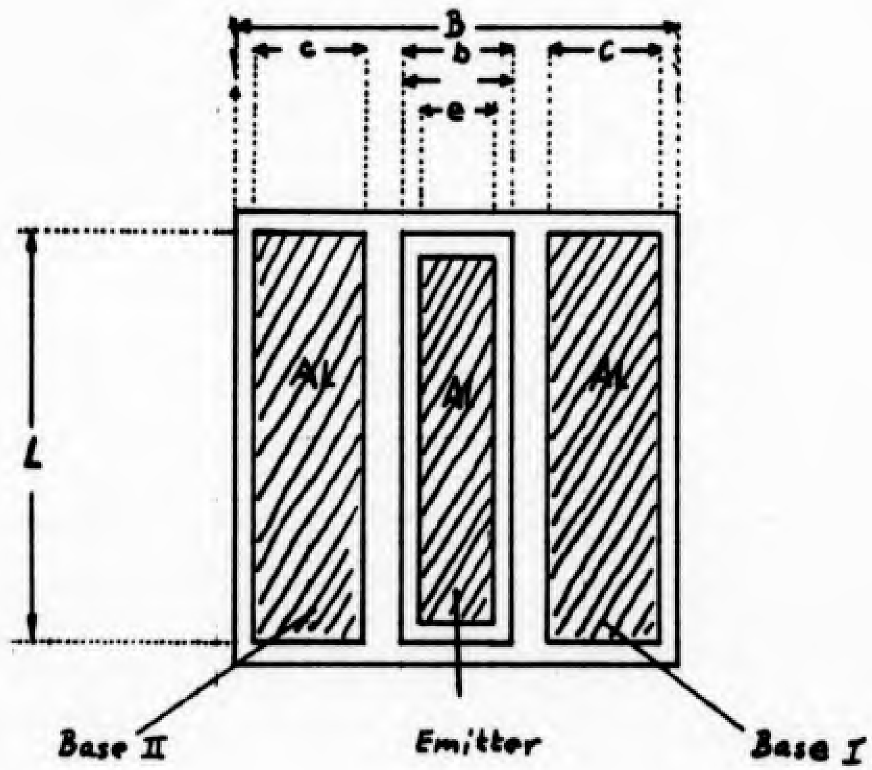


Fig.4.2.2

$N_C$ is the doping concentration in the collector.

$v_\ell$ carrier velocity.

$A_{Eff}$ effective collector area

4.2.2 $$A_{Eff} = \Delta Y_1 L$$

$\Delta Y_1$ = collector current path width due to the fringing effect.

$L$ = length of the active emitter base junction periphery.

The voltage drop across the collector junction is

4.2.3 $$V_{CS} = E_C \Delta Y_1$$

4.2.4 $$\Delta Y_1 \approx W_{C_{Eff}}$$

$E_C$ = electric field in the collector body

$\Delta Y_1$ = collector current path width

$W_{C_{Eff}}$ = effective thickness of the collector body

The collector current path width depends on the base width $W_b$ and the ratio of emitter to base current in the following way.

4.2.5 $$\Delta Y_1 \approx Y_1 = W_b \cdot \sqrt{2 \frac{I_e}{I_b}}$$

for a conventional collector geometry.

If we consider

$$4.2.6 \qquad E_C = \frac{v}{\mu}$$

we get

$$4.2.7 \qquad V_{CS} = \frac{I_C}{q\, N_C\, \mu L}$$

4.2.7 considers the voltage drop due to the fringing effect. In addition to this, a voltage drop exists in the collector body, which is proportional to its thickness $L_{CB}$ and its resistivity $\rho_{CB}$. This voltage drop can be aided considerably by use of an epitaxial layer.

$$4.2.8 \qquad V_{CBS} = \frac{I_C\, \rho_{CB}\, L_{CB}}{A}$$

A is the effective current path in the collector body. The over-all saturation voltage is

$$4.2.9 \qquad V_{CE\ sat} = V_{CS} + V_{CBS} = \rho_{CB}\, I_C \left[\frac{1}{L} + \frac{L_{CB}}{A}\right]$$

$$A = 2\left[\frac{b}{2} + c + d + z\right] \emptyset \quad L = B \times L$$

$$B = 2\left[\frac{b}{2} + c + d + z\right]$$

Equation 4.2.9 allows to calculate the emitter-base dimension L.

$$\boxed{L = \frac{\rho_{CB}\, I_C}{V_{CE\ sat}} \left[1 + \frac{L_{CB}}{B}\right]}$$

| | | |
|---|---|---|
| $V_{CE\ sat} = 0.7$ volts, | $b = 3$ mils | $B = 12$ mils |
| $I_C = 20 \times 10^{-3}$ amperes | $c = 3$ mils | |
| $\rho_{CB} = 0.6\ \Omega cm$ | $e = 2$ mils | |
| $L_{CB} = 5$ mils | $z = 1/2$ mil | |

$$L = 10 \text{ mils}$$

The other dimensions beside L are determined by the base spreading resistance (d) and the different bonding operation requirements (c, e).

<u>One Emitter and Two Base Stripes</u>

We have to substitute L in equation (2.9) by 2L. This leads to L = 5 mils. If we use L = 10 mil, the $V_{CE}$ sat is half of the value at a).

## 4.3 Base Spreading Resistance

The base spreading resistance R consists of two parts, $R_I$ and $R_{II}$ (see Fig. 4.3.1). $R_I$ is the resistance between emitter and base stripe and $R_{II}$ the resistance under the emitter.

At high current density the effective emitter area is limited to a small area along the emitter perimeter due to the "Fletcher Effect". This means R is almost identical with $R_I$.

However, at low current density the effective emitter area is the geometric emitter area.

If $R_{II}$ is not too large and if the emitter current is very small, we can assume an equal current density over the whole emitter area. The base spreading resistance is calculated for this case.

As mentioned above, the base spreading resistance consists of two parts, $R_I$ and $R_{II}$.

A. Resistance Between Emitter and Base Stripe $R_I$ (Fig. 4.3.1)

4.3.1 $$R_I = \rho_s \cdot \frac{d}{\ell}$$

$\rho_s$ = surface concentration on the base area

$d, \ell$ = dimensions shown in Fig. 4.3.1

$R_I$ is the base spreading resistance at high current density.

B. <u>Resistance Under the Emitter Area $R_{II}$ (Fig. 4.3.1)</u>

$J_E$ is the emitter current density.

4.3.2 $$J_E = \frac{I_E}{A_E} \qquad A_E = \ell \cdot a$$

where $I_E$ = emitter current

$A_E$ = emitter area.

The relationship between base current and emitter current density is (Fig. 4.3.2)

4.3.3 $$I_B(x) = \ell \int_0^x (1 - \alpha)\, J_E\, dx$$

$\alpha$, $J_E$ = constant.

4.3.4 $$I_B(x) = \ell(1 - \alpha)\, J_E\, x$$

This current causes a voltage drop along dx of

4.3.5 $$dV = dR_{II}\, I_B\,(x)$$

4.3.6 $$dR_{II} = \rho_s^* \frac{dx}{\ell}$$ $\rho_s^*$ = sheet resistance below the emitter.

By integrating 4.3.5

4.3.7 $$V = (1 - \alpha)\, \rho_s^*\, J_E \int_0^a x dx$$

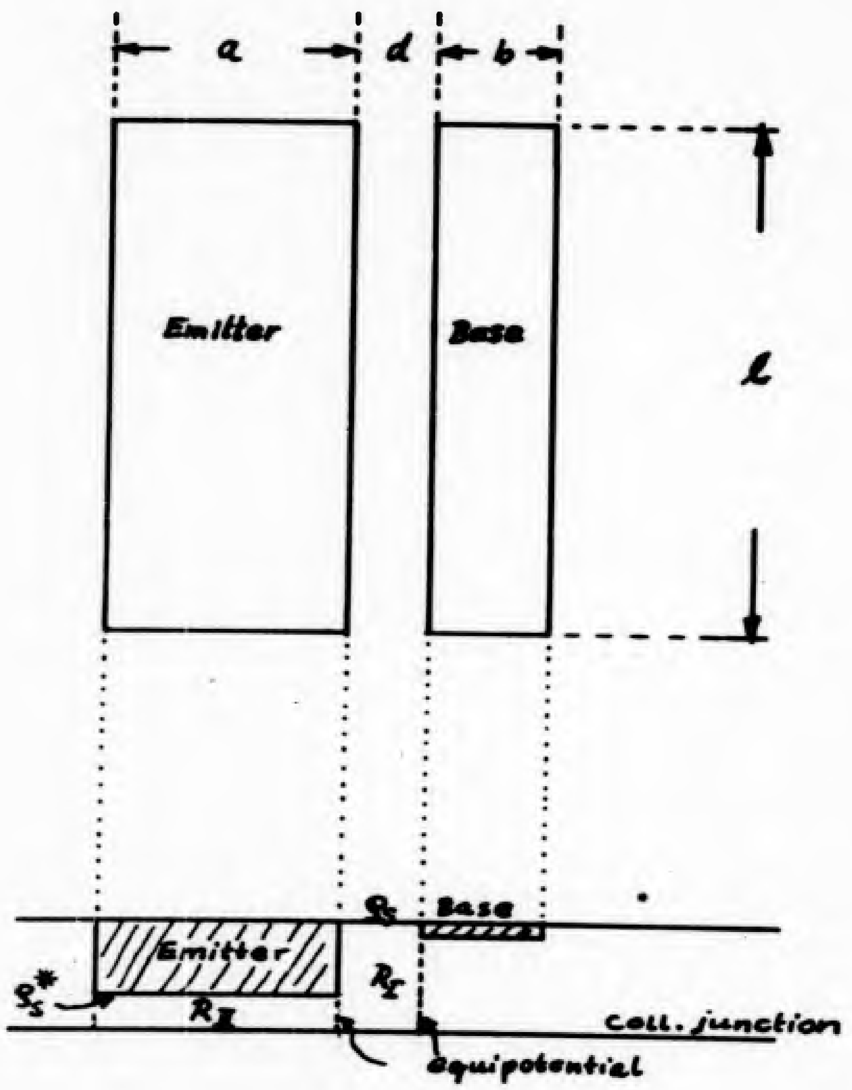


Fig. 4.3.1

$$R_I = \rho_s \frac{d}{\ell}$$

$$R_{II} = \frac{1}{2} \rho_s^* \frac{a}{\ell}$$

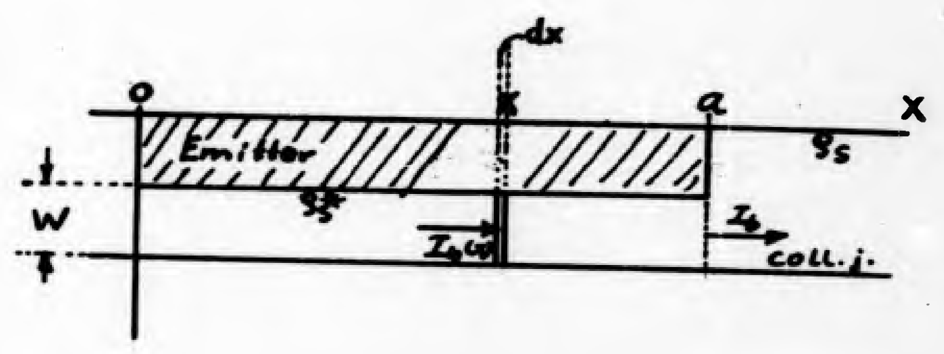


Fig. 4.3.2

4.3.8 $$V = \rho_s^* \, (1 - \alpha) \, J_E \, \frac{a^2}{2}$$

An alternative way of calculating V is

4.3.9 $$V = R_{II} \, I_B = R_{II} \, \ell (1 - \alpha) \, I_E \, a.$$

From 4.3.7 and 4.3.9 $R_{II}$ can be determined, or

4.3.10 $$R_{II} = \frac{1}{2} \rho_s^* \frac{a}{\ell}$$

This is half the resistance if the entire emitter current enters at $x = 0$.

Now the base spreading resistance R is

4.3.11 $$R = R_I + R_{II} = \rho_s \frac{d}{\ell} + \frac{1}{2} \rho_s^* \frac{a}{\ell}$$

Because $\rho_s^* >> \rho_s$ the second term is very important.

Equation 4.3.11 is valid for the case of one emitter and one base stripe.

In order to calculate the base spreading resistance, we have to know the surface concentration $\rho_s^*$ underneath the emitter.

4.3.12 $$\frac{1}{\rho_s^*} = q \int_{x_j \text{ (emitter)}}^{x_j \text{ (collector)}} \mu_p(N) \left[ N_p(x) - N_n(x) - N_o \right] dx$$ 16.

$\mu_p(N)$ is the hole mobility which is concentration dependent.

$N_p(x)$ is the p-type impurity distribution (boron), $N_n(x)$ is the n-type impurity distribution due to the phosphorus diffusion, and $N_o$ is the constant n-type background doping.

The integral 4.3.12 is evaluated by a graphical method in Figure 4.3.3 and Figure 4.3.4 under the assumption of a boron sheet resistance of $\rho_s$ 250 $\Omega/\square$. The result is

4.3.13 $$\rho_s^* = 6.1 \times 10^3 \ \Omega/\square .$$

With $\rho_s^*$ and the earlier calculated emitter-base dimensions, we can now calculate the base spreading resistance

$$\ell = 10 \text{ mils}$$

$$a = 3 \text{ mils}$$

$$b = 3 \text{ mils}$$

$$d = 1 \text{ mil}$$

$$\rho_s = 250 \ \Omega/\square , \quad \rho_s^* = 6.1 \times 10^3 \ \Omega/\square$$

Single Emitter-Base Bar Geometry

$$R_I = 75 \ \Omega \quad , \quad R = 985 \ \Omega$$

$$R_{II} = 910 \ \Omega$$

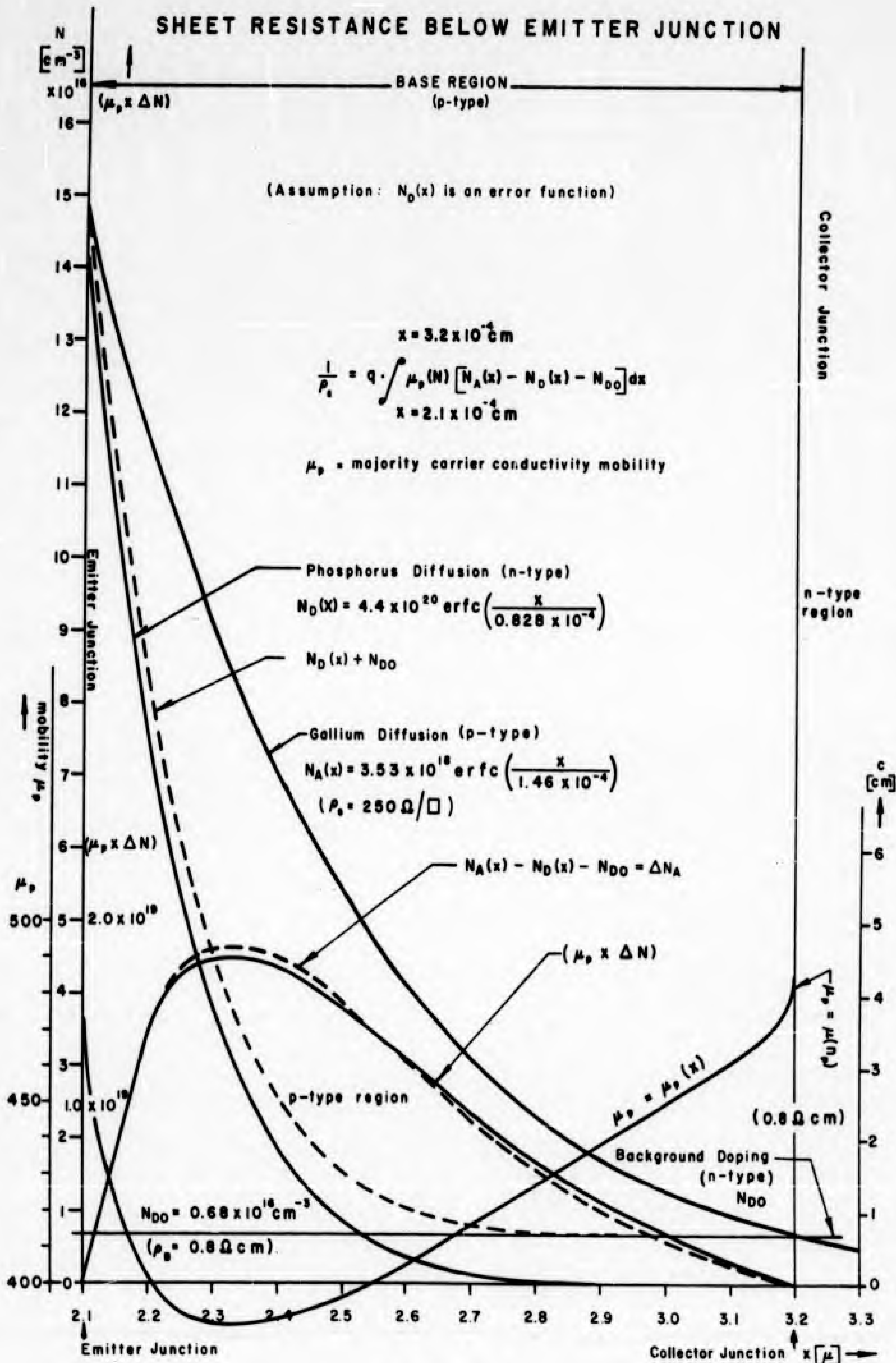


FIGURE 4.3.3

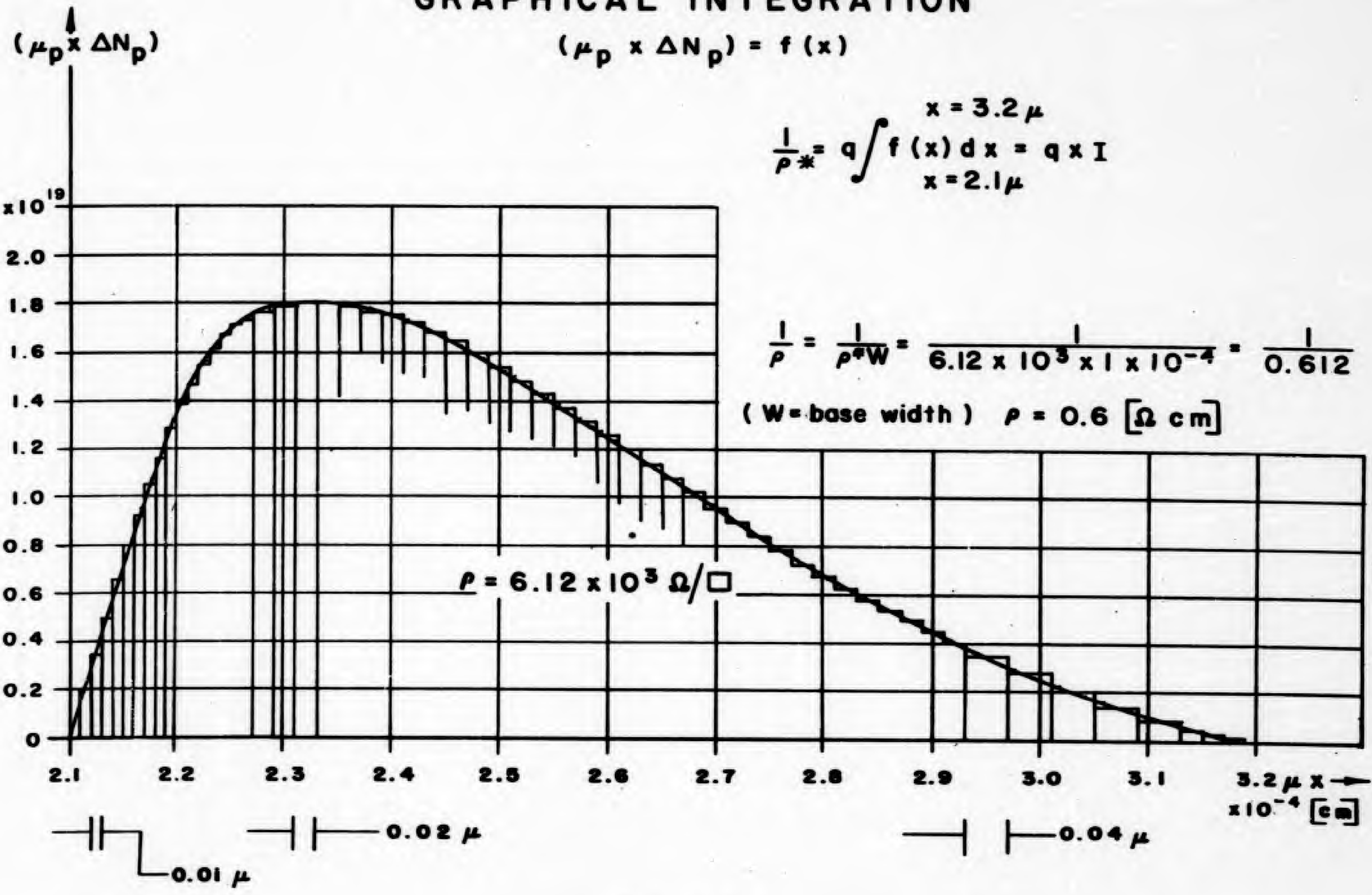


Fig. 4.3.4

## 4.4 Boron Diffusion

In this section consideration is given to the problem of calculating the boron diffusion parameters. The boron diffusion is compared with the gallium diffusion. The diffusion constant of both in silicon is not too different, therefore, Hoffman experience with Ga diffusion can be used as a starting point.

The first concern is the time schedule of boron diffusion into silicon for $0.55 \leqslant \rho \leqslant 0.65$ $\Omega$cm. The second question concerns any changes in the P diffusion time to obtain the same base width for an increase in the B surface concentration over present surface concentrations with Ga.

A diffusion temperature of T = 1180°C for the Ga and B diffusion will be used.

The collector junction depth is taken as $x_{j_2} = 3.3 \times 10^{-4}$ cm.

The emitter junction depth is taken as $x_{j_1} = 2.3 \times 10^{-4}$ cm.

The base width is then $x_{j_2} - x_{j_1} = 1 \times 10^{-4}$ cm.

Error functions are assumed for the B and Ga diffusions as well as for the P diffusion. Taunenbaum[17] showed that this is not correct for the P diffusion. In spite of this,

reasonable estimates can be made.

A. B Diffusion in Si of the Resistivity $0.55 \leq \rho \leq 0.65\ \Omega cm$ at $T = 1180°C$

4.4.1
$$N(x)_B = N_{S_B} \operatorname{erfc} \frac{x}{2(D_B \cdot t)^{1/2}}$$

4.4.2
$$N_B = N_{S_B} \operatorname{erfc} \frac{x_{j_2}}{2(D_B \cdot t_B)^{1/2}}$$ at the collector junction.

$N_B$ = Background concentration

$N_{S_B}$ = Boron surface concentration ($\rho_S = 150\ \Omega$'s/□)

$D_B$ = Boron diffusion constant in Si at $T = 1180°C$

$t_B$ = Boron diffusion time to get the collector junction at $x_{j_2} = 3.3\mu$

B. Ga Diffusion in Si of the Resistivity $0.75 \leq \rho \leq 0.85\ \Omega cm$ at $T = 1180°C$

4.4.3
$$N(x)_{Ga} = N_{S_{Ga}} \operatorname{erfc} \frac{x}{2(D_{Ga} \cdot t)^{1/2}}$$

4.4.4
$$N_B = N_{S_{Ga}} \operatorname{erfc} \frac{x_{j_2}}{2(D_{Ga} \cdot t_{Ga})^{1/2}}$$ at the collector junction.

$N_B$ = Background concentration

$N_{S_{Ga}}$ = Gallium surface concentration ($\rho_S = 250\ \Omega$'s/□)

$D_{Ga}$ = Gallium diffusion constant in Si at $T = 1180°C$

$t_{Ga}$ = Gallium diffusion time to get the collector junction at $x_{j_2} = 3.3\mu$

Evaluation after Backenstoss [16].

4.4.5 Boron: $N_{S_B} = 5 \times 10^{18}\ \text{cm}^{-3}$ for $\rho_S = 150\ \Omega/\square$ (p-type layer)

$N_B = 0.947 \times 10^{16}\ \text{cm}^{-3}$ for $\rho_B = 0.6\ \Omega\text{cm}$

4.4.6 Gallium: $N_{S_{Ga}} = 3.53 \times 10^{18}\ \text{cm}^{-3}$ for $\rho_S = 250\ \Omega/\square$ (p-type layer)

$N_B = 0.68 \times 10^{16}\ \text{cm}^{-3}$ for $\rho_B = 0.8\ \Omega\text{cm}$

4.4.7 $$\frac{N_B}{N_{S_B}} = \frac{0.947 \times 10^{16}}{5 \times 10^{18}} = 1.9 \times 10^{-3}$$

4.4.8 $$\frac{N_B}{N_{S_{Ga}}} = \frac{0.68 \times 10^{16}}{3.53 \times 10^{18}} = 1.925 \times 10^{-3}$$

4.4.7 and 4.4.8 show that both error functions are about the same. Therefore, the error function arguments are about the same.

4.4.9 $$\frac{x_{j_2}}{2(D_B \cdot t_B)^{1/2}} = \frac{x_{j_2}}{2(D_{Ga} \cdot t_{Ga})^{1/2}}$$

4.4.10 $$D_B \cdot t_B = D_{Ga} \cdot t_{Ga} \qquad \text{or,}$$

4.4.11 $$\boxed{t_B = \left(\frac{D_{Ga}}{D_B}\right) t_{Ga}}$$

After Fuller [18] $D_{Ga}$ and $D_B$ for T = 1180°C.

4.4.12 $$D_B = 1.83 \times 10^{-12}\ \text{cm}^2/\text{sec}.$$

4.4.13 $$D_{Ga} = 2.76 \times 10^{-12} \ cm^2/sec.$$

4.4.14 $$\left[ D_{Ga}/D_B \right]_{1180°C} = 1.51$$

4.4.15 $$t_B = 1.51 \cdot t_{Ga}$$

Ga diffusion experiments have shown that $t_{Ga}$ is about 60 minutes. This gives

4.4.16 $$\underline{t_B = 90 \ min.}$$

If the diffusion data published at the TI lecture series given at Texas A & M, Spring 1960, is used, the ratio of the diffusion constant is different.

At a diffusion temperature of 1180°C,

4.4.17 $$D_B = 1.7 \times 10^{12} \ cm^2/sec.$$

4.4.18 $$D_{Ga} = 3.4 \times 10^{-12} \ cm^2/sec.$$

4.4.19 $$\left[ D_{Ga}/D_B \right] = 2$$

and therefore

4.4.20 $$t_B = 2 \ t_{Ga}$$

If $t_{Ga}$ is 60 minutes, $t_B$ is then

4.4.21 $$t_B = 120 \ min.$$

The diffusion data published at the TI lecture series is probably the more reliable. Further diffusion data is given by F. M. Smits [19].

With this data the diffusion constant for Ga and B in Si becomes

A. $D_{Ga}$ in Si at 1180°C

4.4.22 $$D_{Ga} = D_o e^{-\frac{\Delta Q}{kT}}$$

$$D_o = 4.0 \text{ cm}^2/\text{sec.}$$

$$\Delta Q = 3.5 \text{ eV}$$

$$D_{Ga} = 4.0 e^{-28.0}$$

4.4.23 $$D_{Ga} = 3.33 \times 10^{-12} \text{ cm}^2/\text{sec.}$$

B. $D_B$ in Si at 1180°C

4.4.24 $$D_B = D_o e^{-\frac{\Delta Q}{kT}}$$

$$D_o = 14 \text{ cm}^2/\text{sec.}$$

$$\Delta Q = 3.7 \text{ eV}$$

$$D_B = 14 e^{-29.6}$$

4.4.25 $$D_B = 1.95 \times 10^{-12} \text{ cm}^2/\text{sec.}$$

C. Influence of Change in Boron-Surface Concentration on Base Width

By inspection of Figure 4.4.1

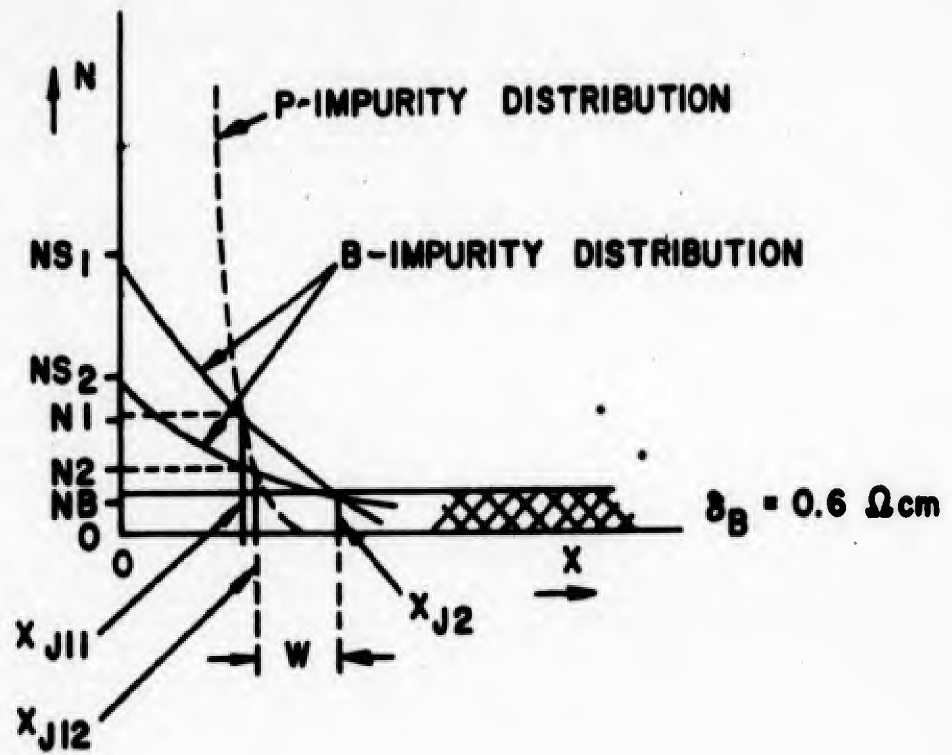


FIG. 4.4.1

4.4.26 $N(x) = N_{S_2} \operatorname{erfc} \frac{x}{K\sqrt{t_2}}$ is the B-impurity distribution

for a sheet resistance of $\rho_{S_2} = 250\ \Omega/\square$ .

4.4.27 $N(x) = N_{S_1} \operatorname{erfc} \frac{x}{K\sqrt{t_1}}$ is the B-impurity distribution

for a sheet resistance of $\rho_{S_1} = 150\ \Omega/\square$ .

Both distributions should have the collector junction at the same position $x_{j_2}$.

4.4.28 $N_B = N_{S_2} \operatorname{erfc} \frac{x_{j_2}}{K\sqrt{t_2}}$ , $N_{S_2} = 3.52 \times 10^{18}\ cm^{-3}$

$N_B = 0.95 \times 10^{16}\ cm^{-3}$

4.4.29 $N_B = N_{S_1} \operatorname{erfc} \frac{x_{j_2}}{K\sqrt{t_1}}$ , $N_{S_1} = 5.0 \times 10^{18}\ cm^{-3}$

4.4.30 $\frac{N_B}{N_{S_1}} = 1.9 \times 10^{-3}$ , $\frac{N_B}{N_{S_2}} = 2.7 \times 10^{-3}$

4.4.31 $K\sqrt{t_1} = \frac{x_{j_2}}{2.196}$

4.4.32 $K\sqrt{t_2} = \frac{x_{j_2}}{2.12}$

$(x_{j_{11}} - x_{j_{12}}) = \Delta x_{j_1}$ is due to the change of x of the P-impurity distribution by changing from $N = N_1$ to $N = N_2$.

4.4.26, 4.4.27, 4.4.31, and 4.4.32 are used to calculate $N_1$ and $N_2$.

4.4.33 $$N_2 = N_{S_2} \text{ erfc } 2.12 \left(\frac{x_{j_{12}}}{x_{j_2}}\right)$$

4.4.34 $$N_1 = N_{S_1} \text{ erfc } 2.196 \left(\frac{x_{j_{11}}}{x_{j_2}}\right)$$

$$x_{j_{11}} \approx x_{j_{12}} = 2.3 \times 10^{-4} \text{ cm}$$

$$x_{j_2} = 3.3 \times 10^{-4} \text{ cm} \quad , \quad \frac{x_{j_{11}}}{x_{j_2}} \approx \frac{x_{j_{12}}}{x_{j_2}} = 0.697$$

$$N_2 = N_{S_2} \text{ erfc } 1.477 \quad , \quad N_2 = 3.66 \times 10^{-2} N_{S_2}$$

$$N_1 = N_{S_1} \text{ erfc } 1.53 \quad , \quad N_1 = 3.05 \times 10^{-2} N_{S_1}$$

$$N_1 = 1.525 \times 10^{17} \text{ cm}^{-3}$$

$$N_2 = 1.288 \times 10^{17} \text{ cm}^{-3}$$

Assume now a phosphorus error function distribution

4.4.35 $$N(x) = 4.4 \times 10^{20} \text{ erfc } \frac{x}{0.828 \times 10^{-4}}$$

(standard transistor P-diffusion, $\rho_S = 1.5\ \Omega/\square$)

4.4.36 $$N_1 = 4.4 \times 10^{20} \text{ erfc } \frac{x_{j_{11}}}{0.828 \times 10^{-4}}$$

4.4.37 $$N_2 = 4.4 \times 10^{20} = 4.4 \times 10^{20} \text{ erfc } \frac{x_{j_{12}}}{0.828 \times 10^{-4}}$$

Substitute $N_1$ and $N_2$ in 4.4.36 and 4.4.37 and

$$x_{j_{11}} = 2.095\mu$$

$$x_{j_{12}} = 2.12\ \mu$$

or

$$\Delta x_{j_1} = (x_{j_{11}} - x_{j_{12}}) = \underline{0.025\mu}.$$

This shows that a change in phosphorus diffusion time should not be necessary. By decreasing the B-sheet resistance from $\rho_S = 250\ \Omega/\square$ to $150\ \Omega/\square$ there is no appreciable change in base width W.

## 5.0 EXPERIMENTAL

### 5.1 Test of Fletcher Effect

A group of devices was built with the special geometry shown in Figure 5.1.1 from existing masks. The resistor R was external, and the conditions R = 0 to $R \approx \infty$ could be checked and the effect of the variation of emitter periphery on $h_{FE}$ determined. The results are shown in Figures 5.1.2, 5.1.3, 5.1.4, 5.1.5, 5.1.6, and 5.1.7. These measurements were made on a Tektronix 545 curve tracer, and the individual units were heated with Kennedy thermo probes to test individual combinations. The graphs of Figures 5.1.8, 5.1.9, and 5.1.10 were abstracted from the curves mentioned above. In general, very little compensation is discernable at low current levels, but approximately a factor of two (Fig. 5.1.11) change takes place at high current levels. This observation bears out the argument of Sections 3.1, 3.2, and 3.3, since the insertion of a resistor with the device hot is comparable to a transistor with base connected with a resistor of positive temperature coefficient. A limit of the effect of external resistance applied was caused by the resistance of the area marked R* in Figure 5.1.1, and the actual limit of change was due to this resistance, rather than the external resistance. R* must be much larger in magnitude if appreciable

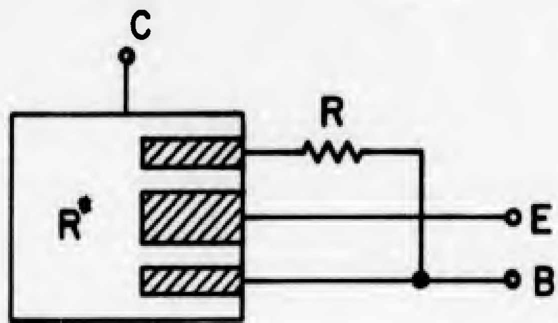


a. $R = \infty$

b. $R = 0$

Fig. 5.1.1

UNIT #1

25°C

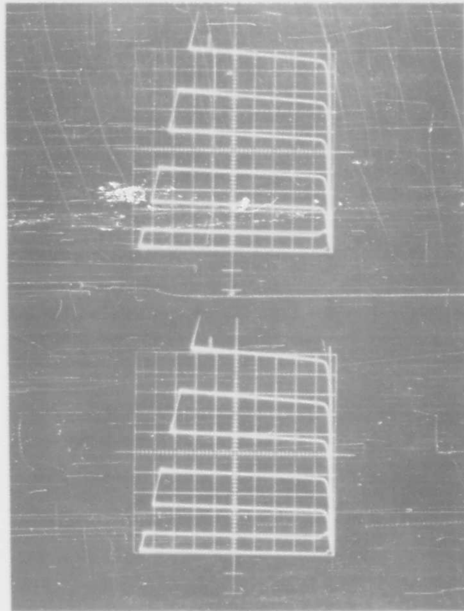

75°C

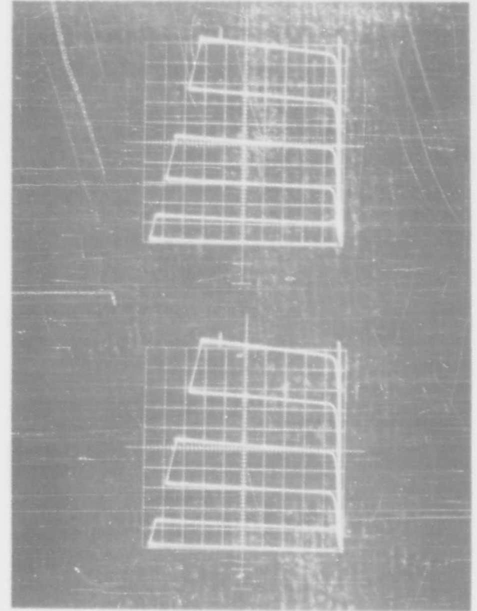

$i_c$ ↑ $\frac{0.2 \text{ ma}}{\text{div}}$

R=∞ R=0

$i_b$ ↑ $\frac{0.01 \text{ ma}}{\text{step}}$

R=∞ R=0

$V_{CB}$ ← 0.5 V/div

a

$V_{CB}$ ← 0.5 V/div

b

25°C

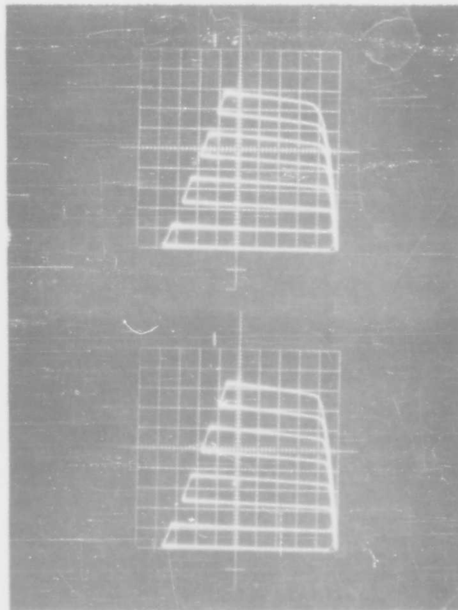

75°C

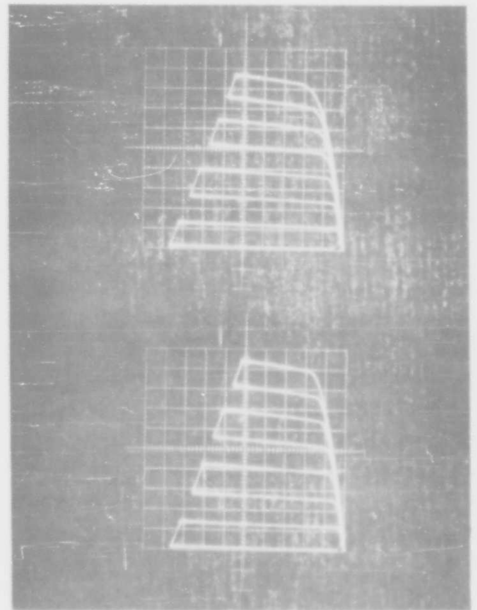

$i_c$ ↑ $\frac{5 \text{ ma}}{\text{div}}$

R=∞ R=0

$i_b$ ↑ $\frac{0.1 \text{ ma}}{\text{step}}$

R=∞ R=0

$V_{CB}$ ← 1.0 V/div

c

$V_{CB}$ ← 1.0 V/div

d

Fig. 5.1.2

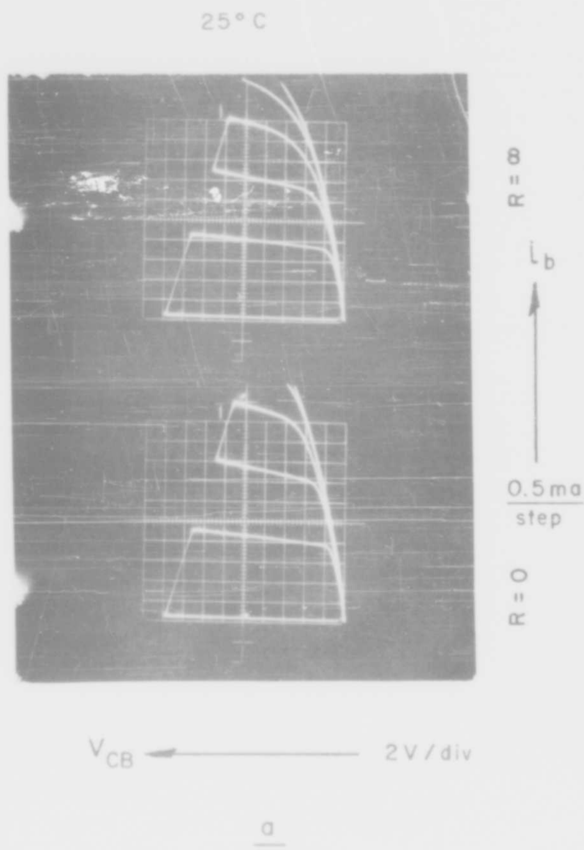


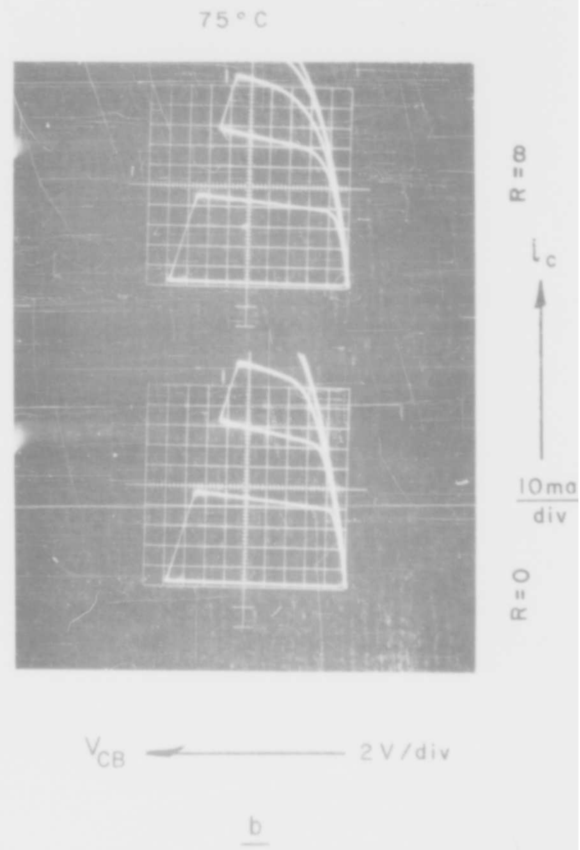


Fig 5.1.3

UNIT #2

25 °C

75 °C

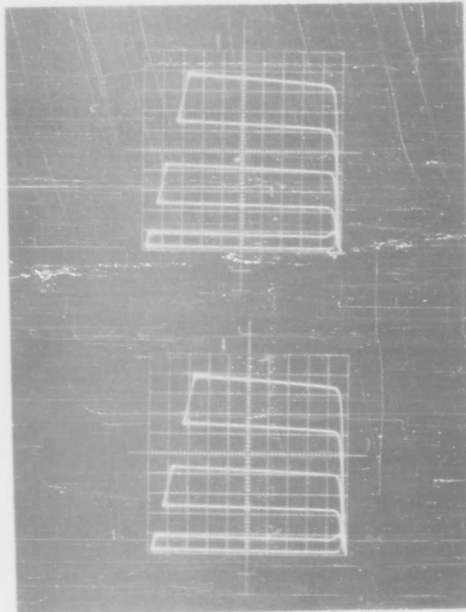

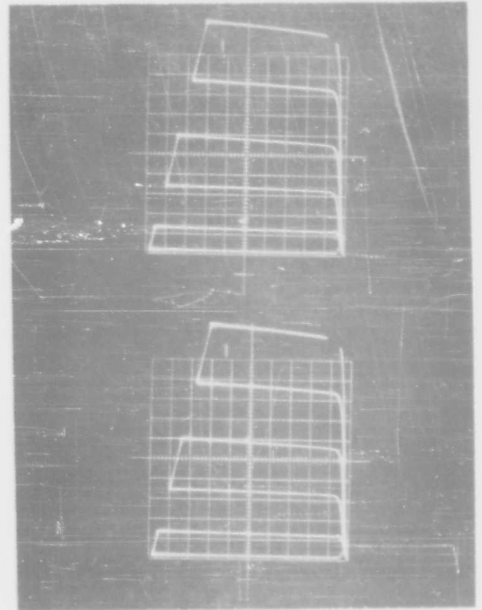



a

b

25 °C

75 °C

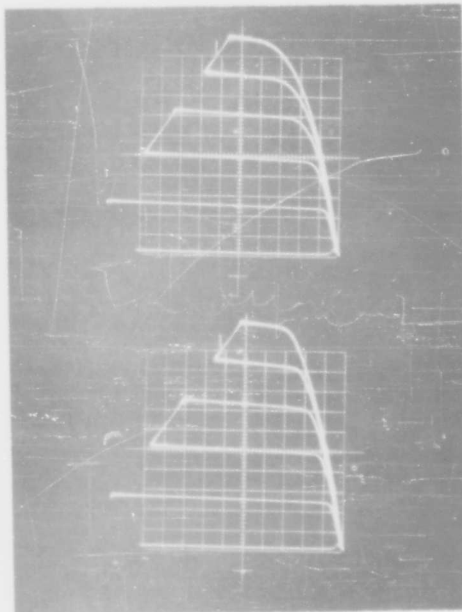

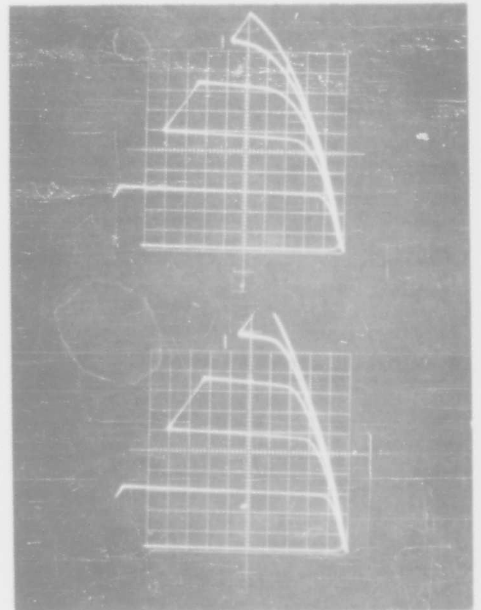



c

d

Fig 5.1.4

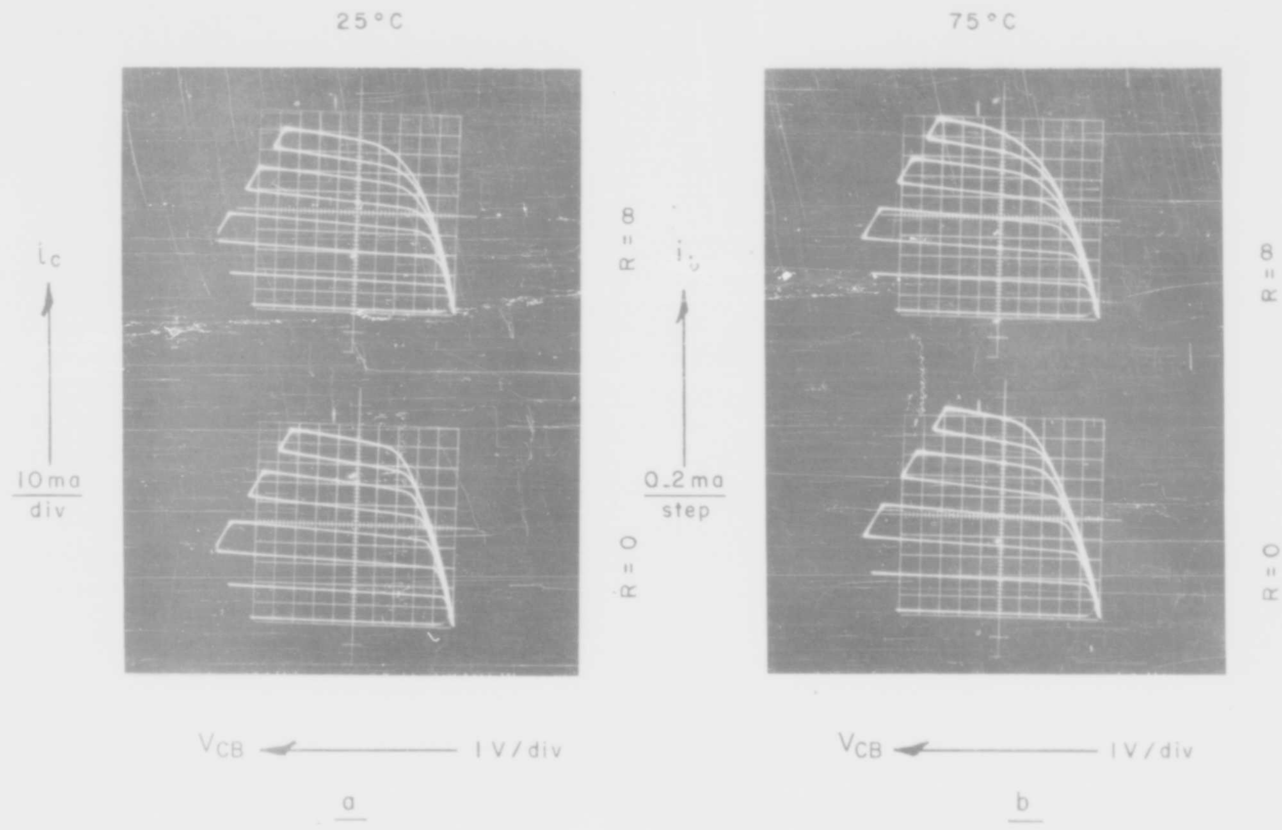


Fig. 5.1.5.

UNIT #3

25 °C | 75 °C

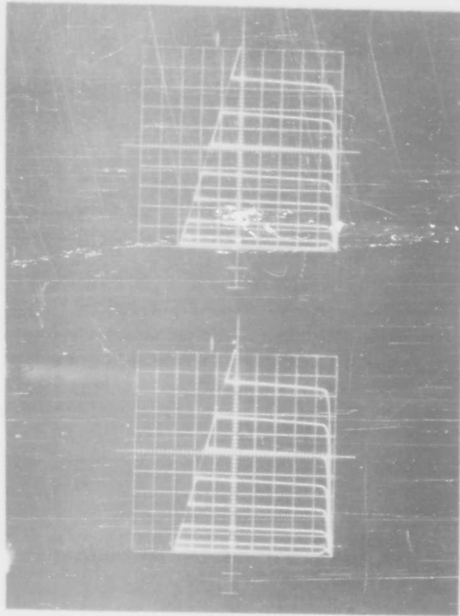

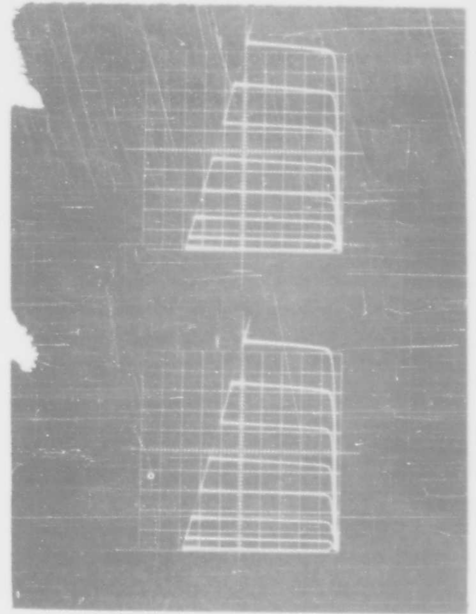



25 °C | 75 °C

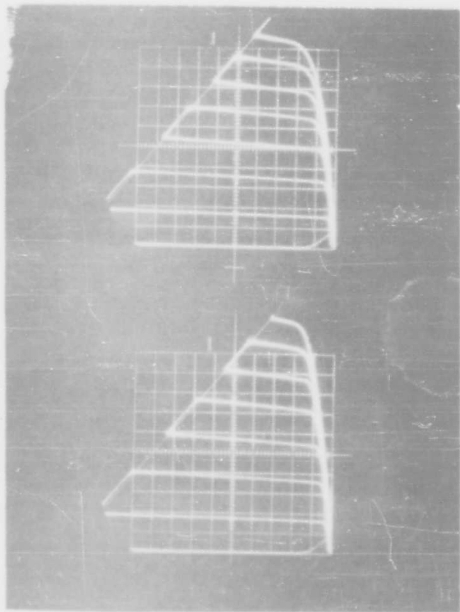

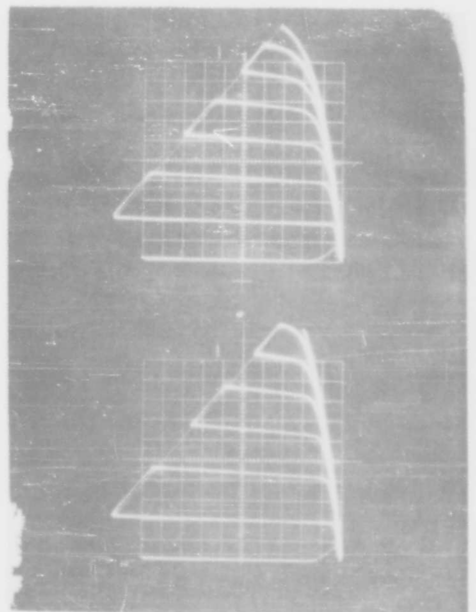



Fig. 5.1.6

25 °C

75 °C

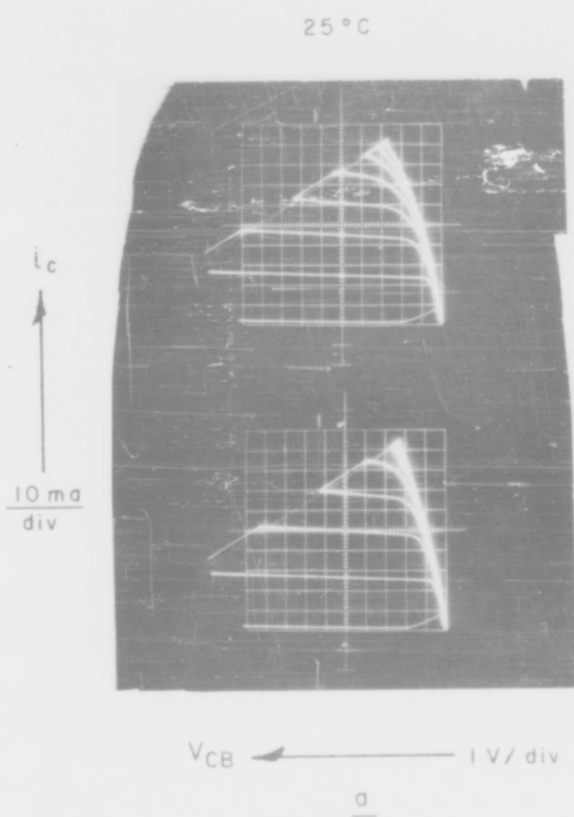


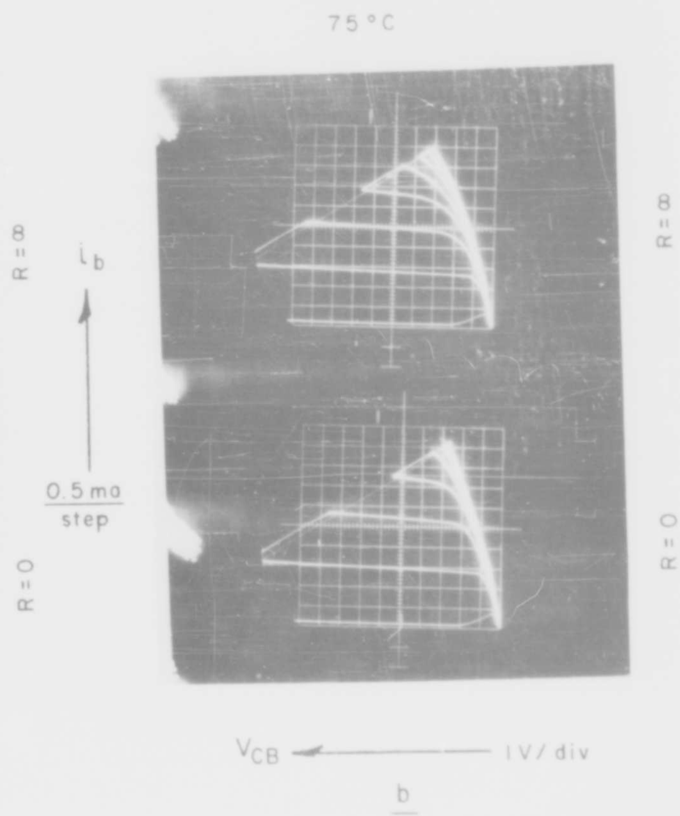


Fig. 5.1.7

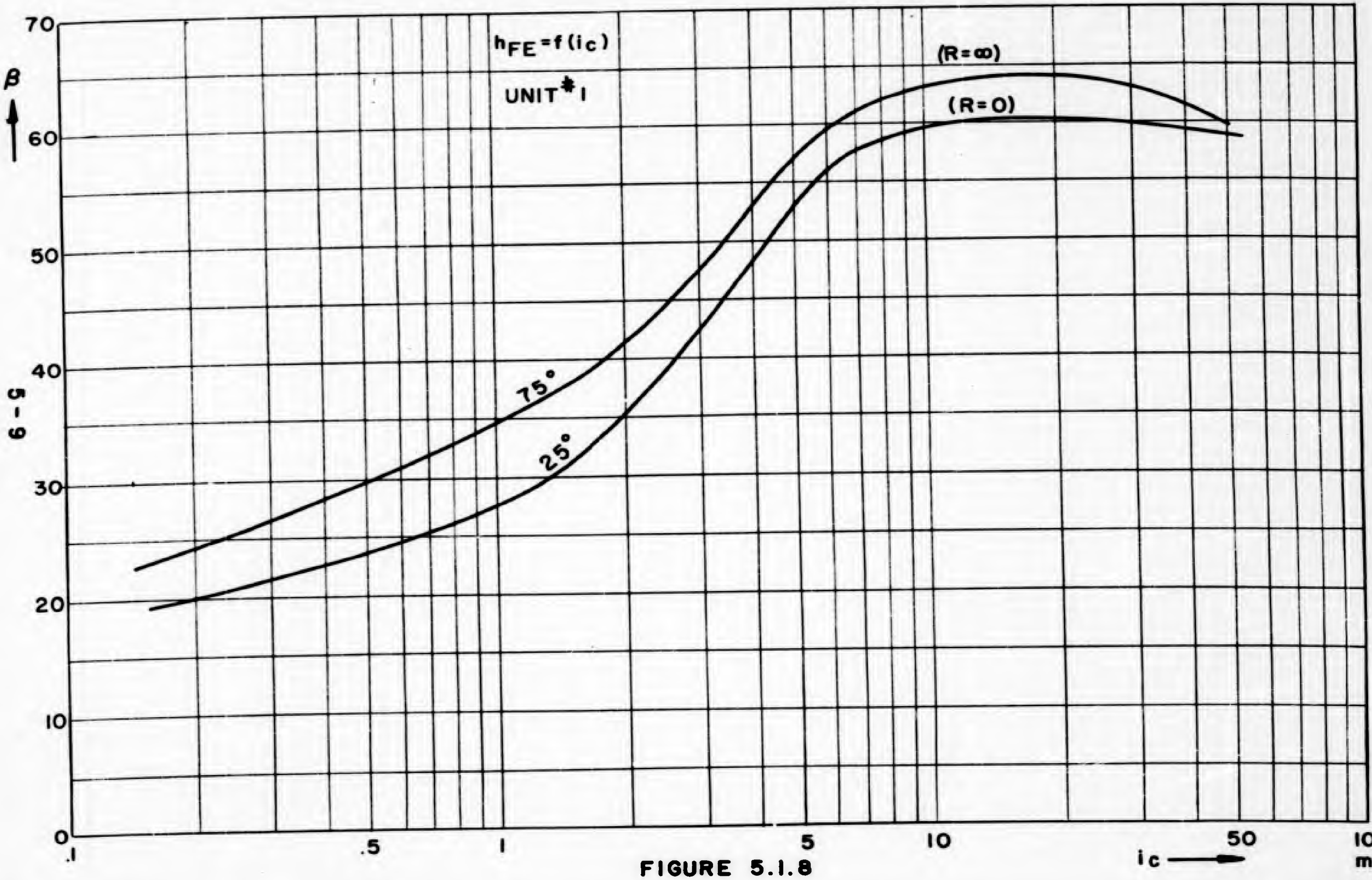


FIGURE 5.1.8

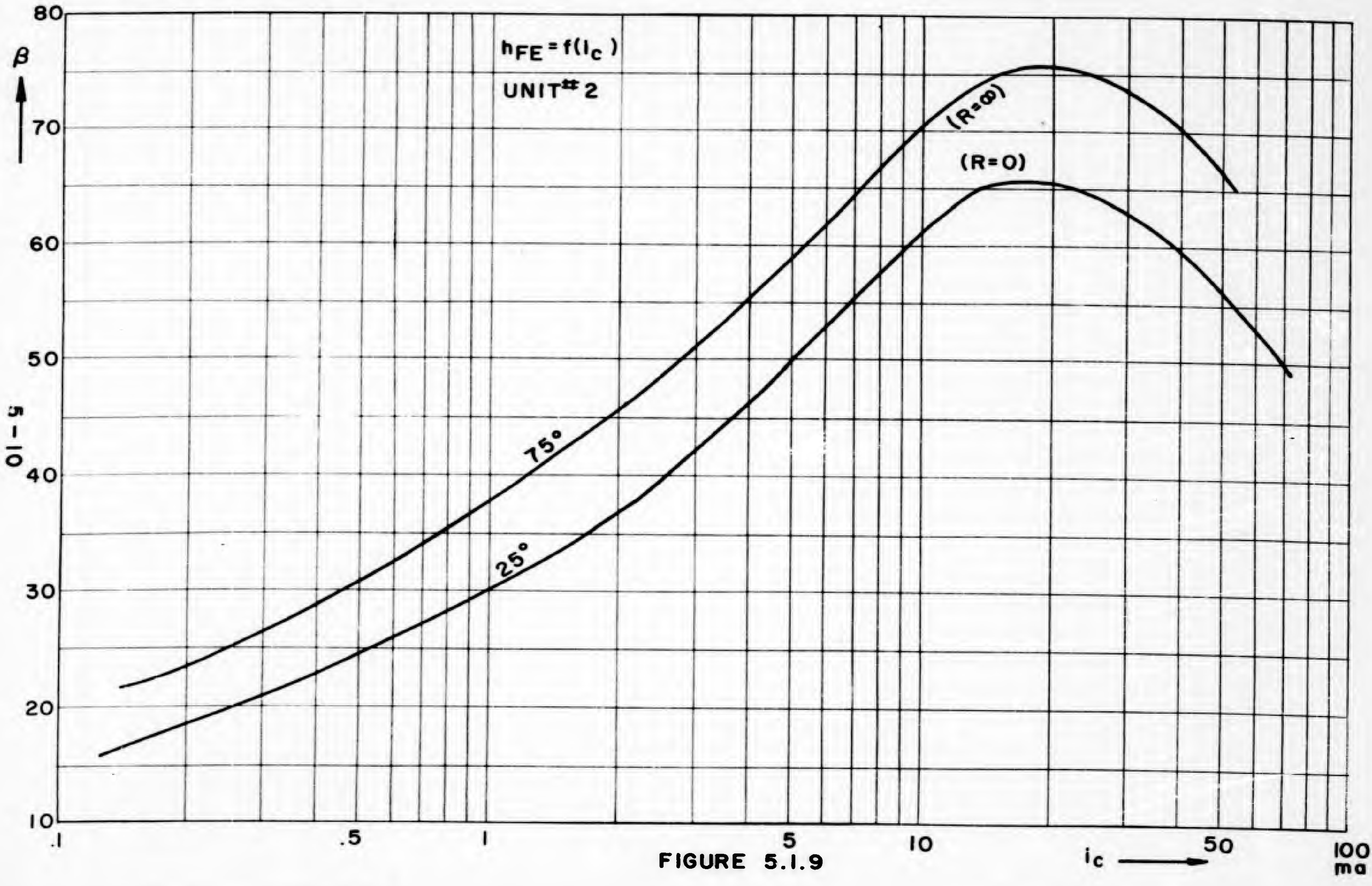


FIGURE 5.1.9

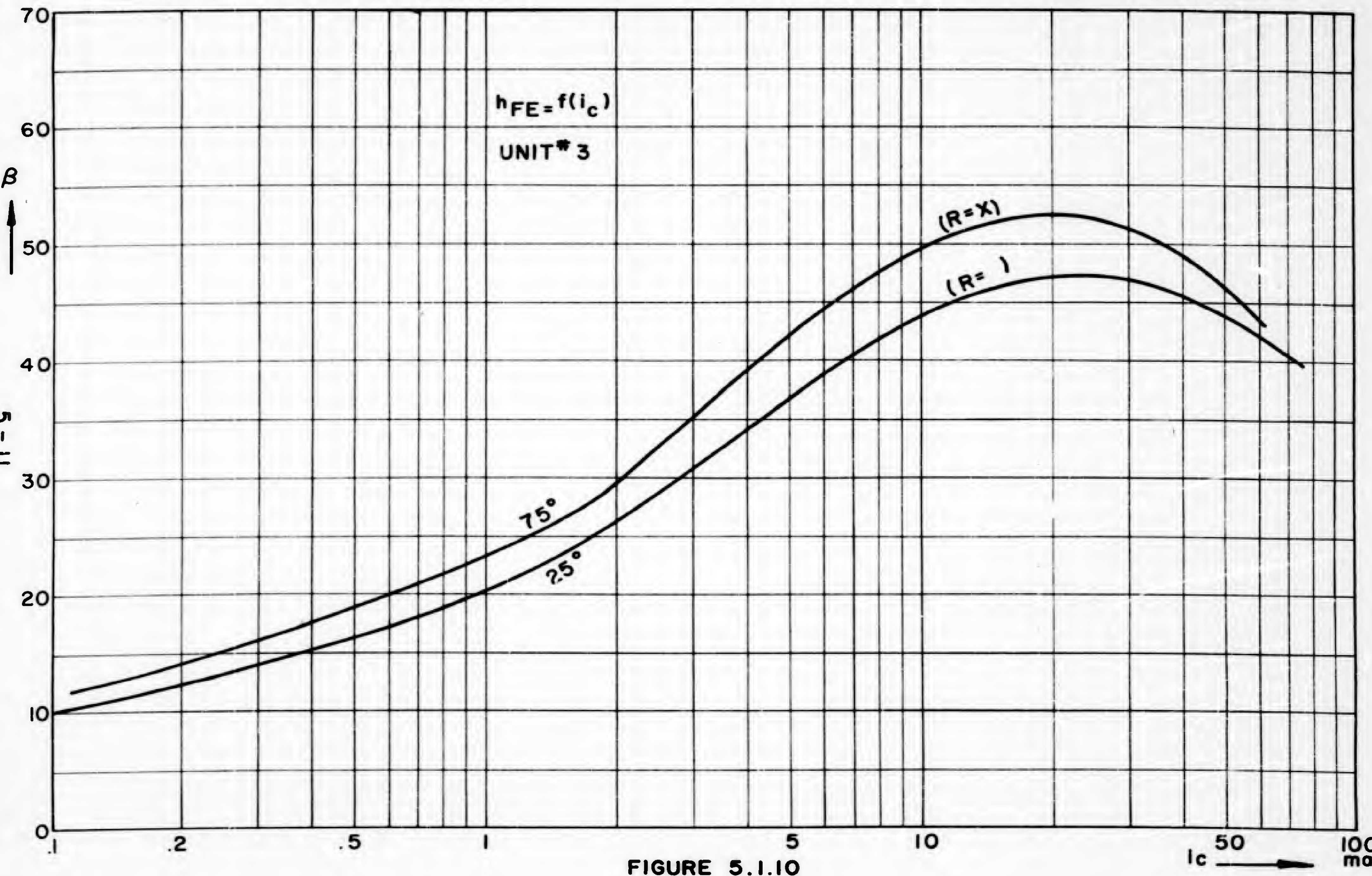


FIGURE 5.1.10

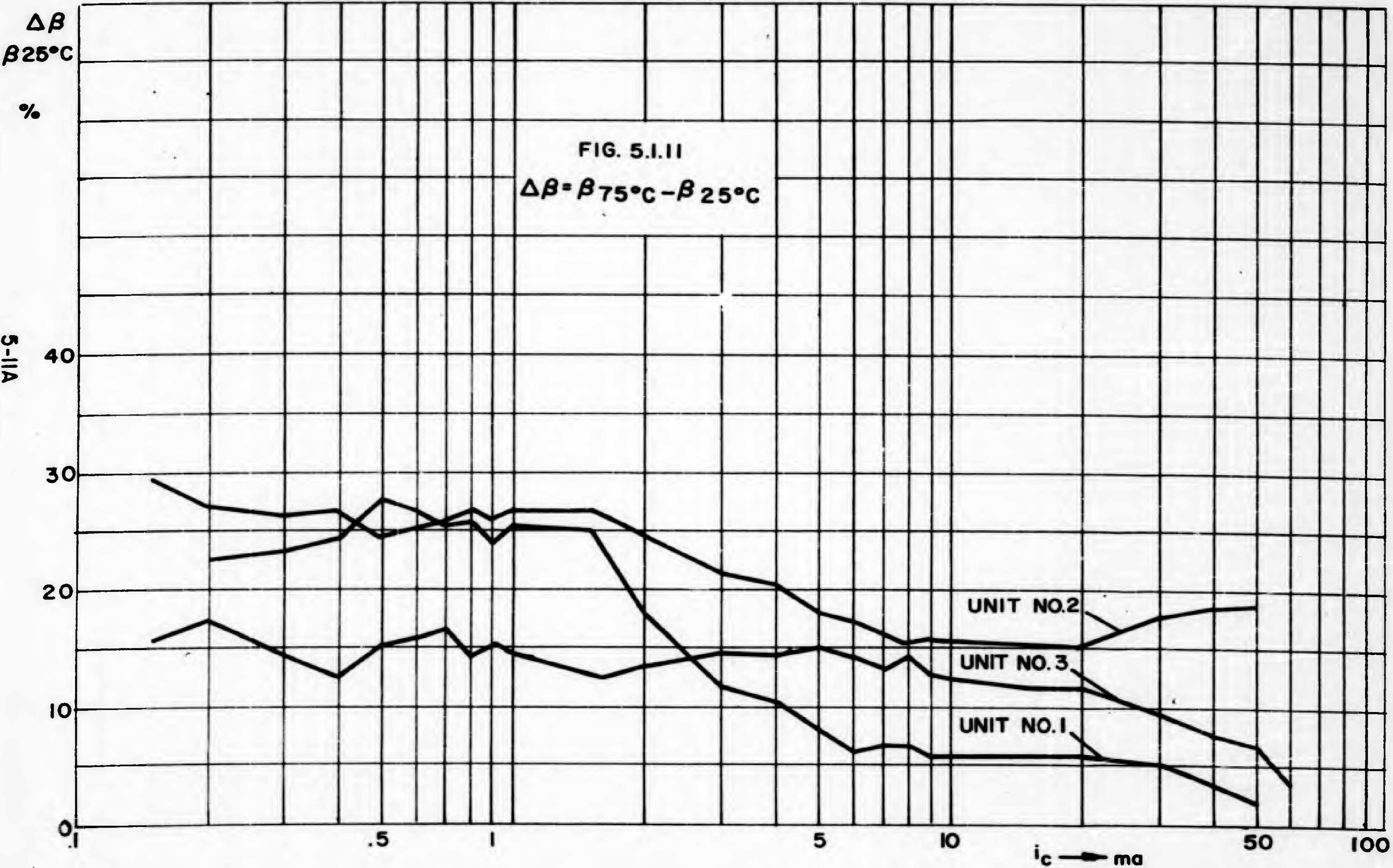

$\frac{\Delta\beta}{\beta_{25°C}}$
%
FIG. 5.1.11
$\Delta\beta = \beta_{75°C} - \beta_{25°C}$
40
30
20
10
0
.1
.5
1
5
10
50
100
$i_c$ ⟶ ma
UNIT NO.2
UNIT NO.3
UNIT NO.1

compensation is to be achieved by this method.

## 5.2 Two Transistors in Parallel Circuit

The circuit of Figure 5.2.1 was constructed with two 2N697 transistors externally connected to provide an analogue of the ultimate device. Figures 5.2.2, and 5.2.3 show curves of the parallel combination as a function of temperature. This data is abstracted in Figure 5.2.4 ; 5.2.5 shows the compensation achieved by use of open and short circuit to simulate the effect of a thermistor or a positive coefficient resistor. The center curves show $R = \infty$ at room temperature and $R = 0$, i.e. both transistors in parallel at 75°C, where the analogue of the changing resistance is simulated at the extremes and proves that $h_{FE}$ compensation is indeed possible as indicated in Section 3.4.

In Figure 5.2.4 the variation in $h_{FE}$ at less than 0.1 ma between the two devices is attributed to variations in surface treatment.

In Appendix VII additional measurements are shown with a thermistor to show the combination variation with temperature. Better compensation is achieved at low current levels, and again a compromise must be struck between

## TWO TRANSISTORS IN PARALLEL CIRCUIT

The two emitters are connected by the extreme impedance $R = 0$ (b) or $R = \infty$ (a).

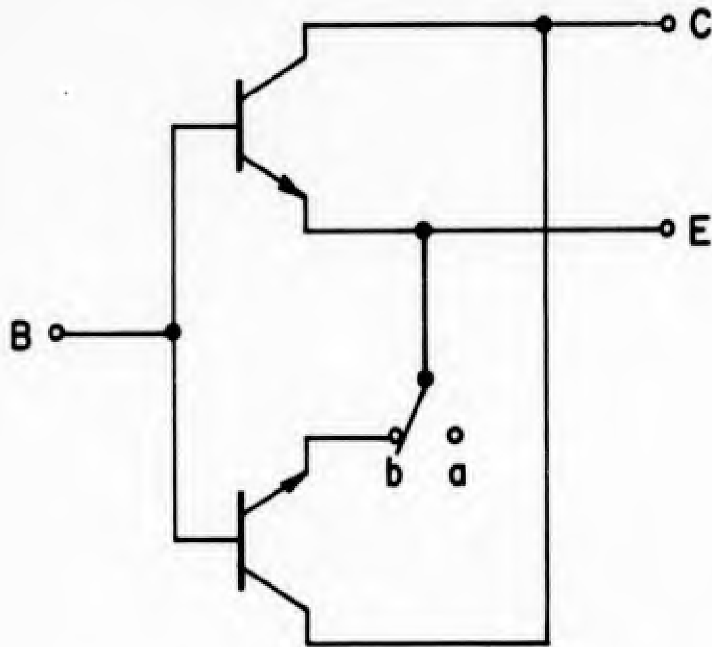


C = COLLECTOR

E = EMITTER

B = BASE

Fig. 5.2.1

UNIT #1

25°C

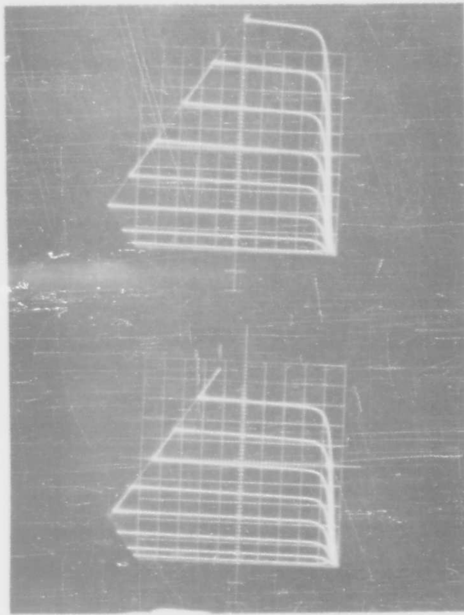

$i_c$

0.2 ma / div

R = ∞

R = 0

$V_{CB}$ ← 0.2 V/div

a

75°C

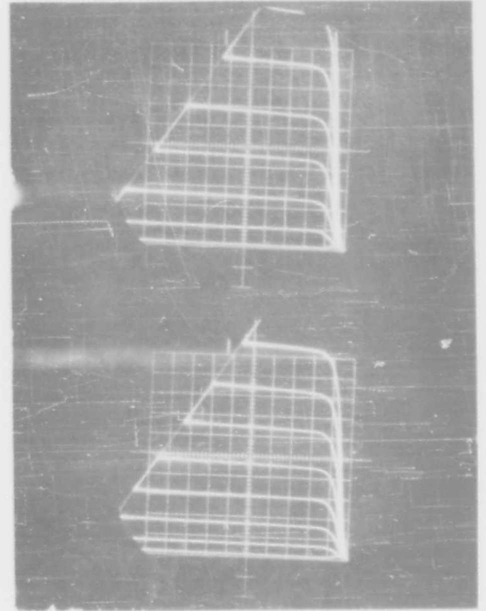

$i_b$

0.01 ma / step

R = ∞

R = 0

$V_{CB}$ ← 0.2 V/div

b

25°C

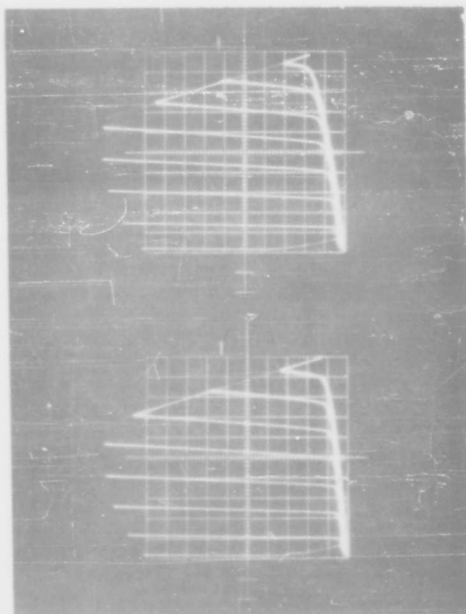

$i_c$

10 ma / div

R = ∞

R = 0

$V_{CB}$ ← 0.5 V/div

c

75°C

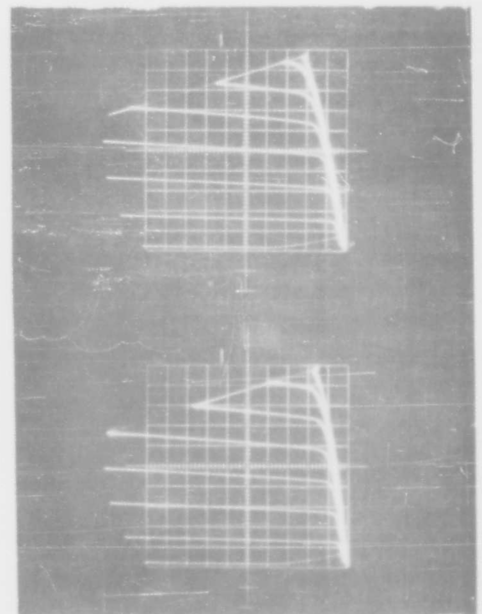

$i_b$

0.2 ma / step

R = ∞

R = 0

$V_{CB}$ ← 0.5 V/div

d

Fig. 5.2.2

UNIT #2

25°C

75°C

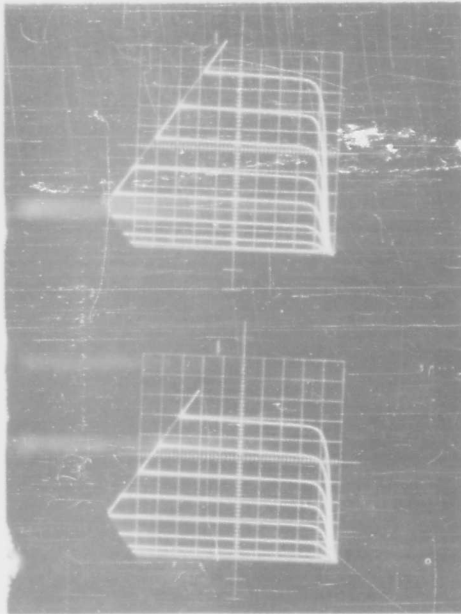

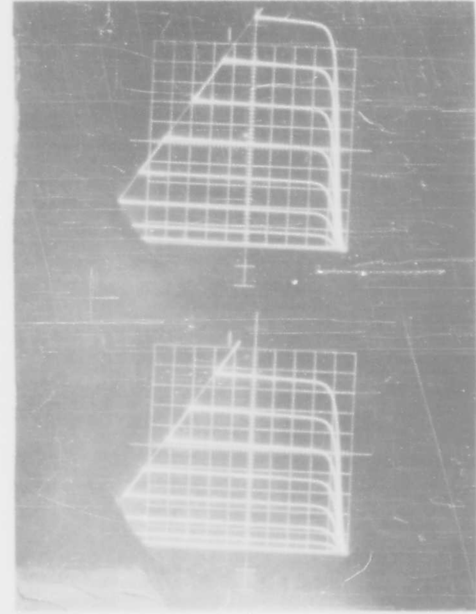



Fig. 5.2.3

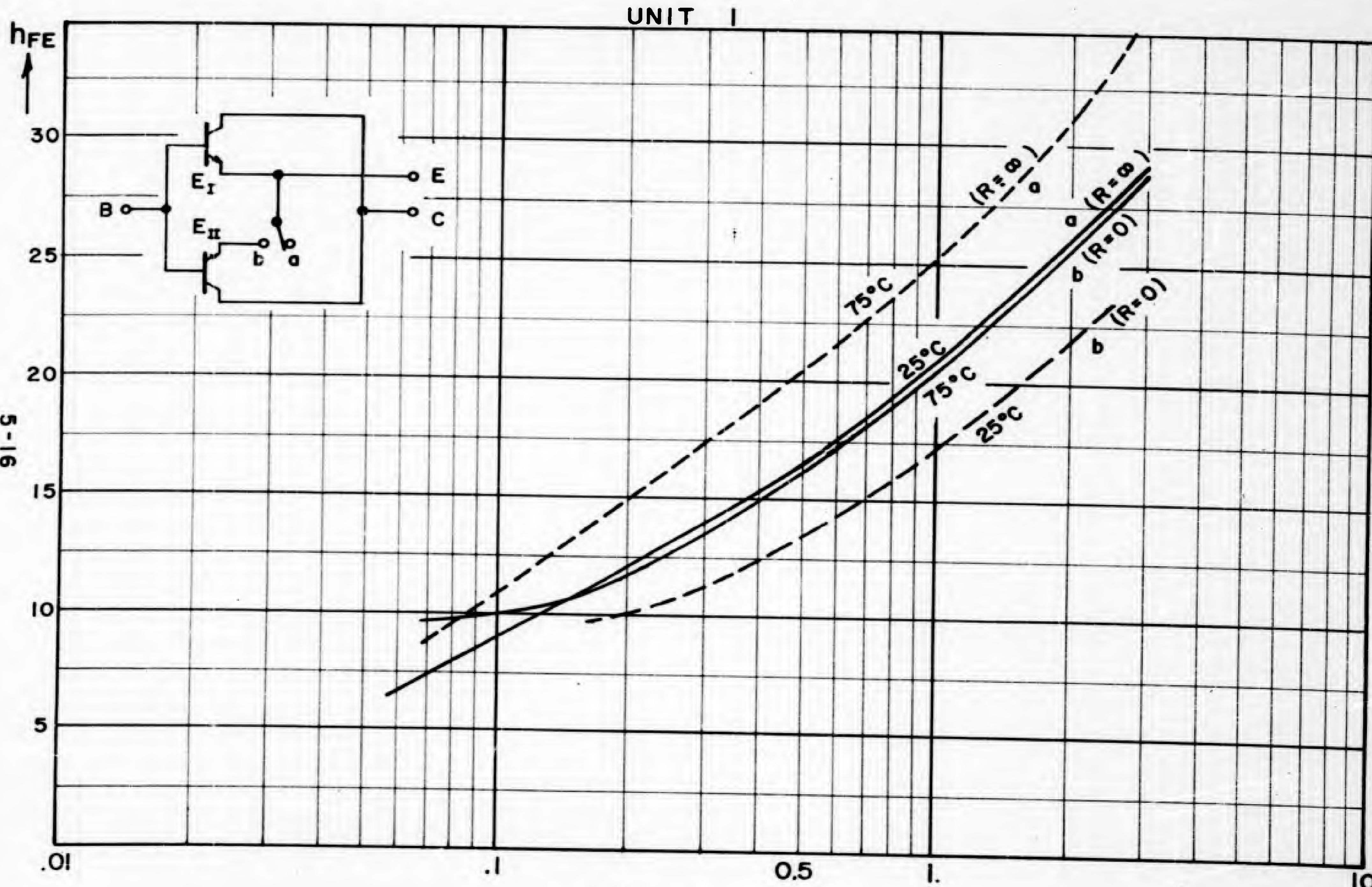


FIG. 5.2.4

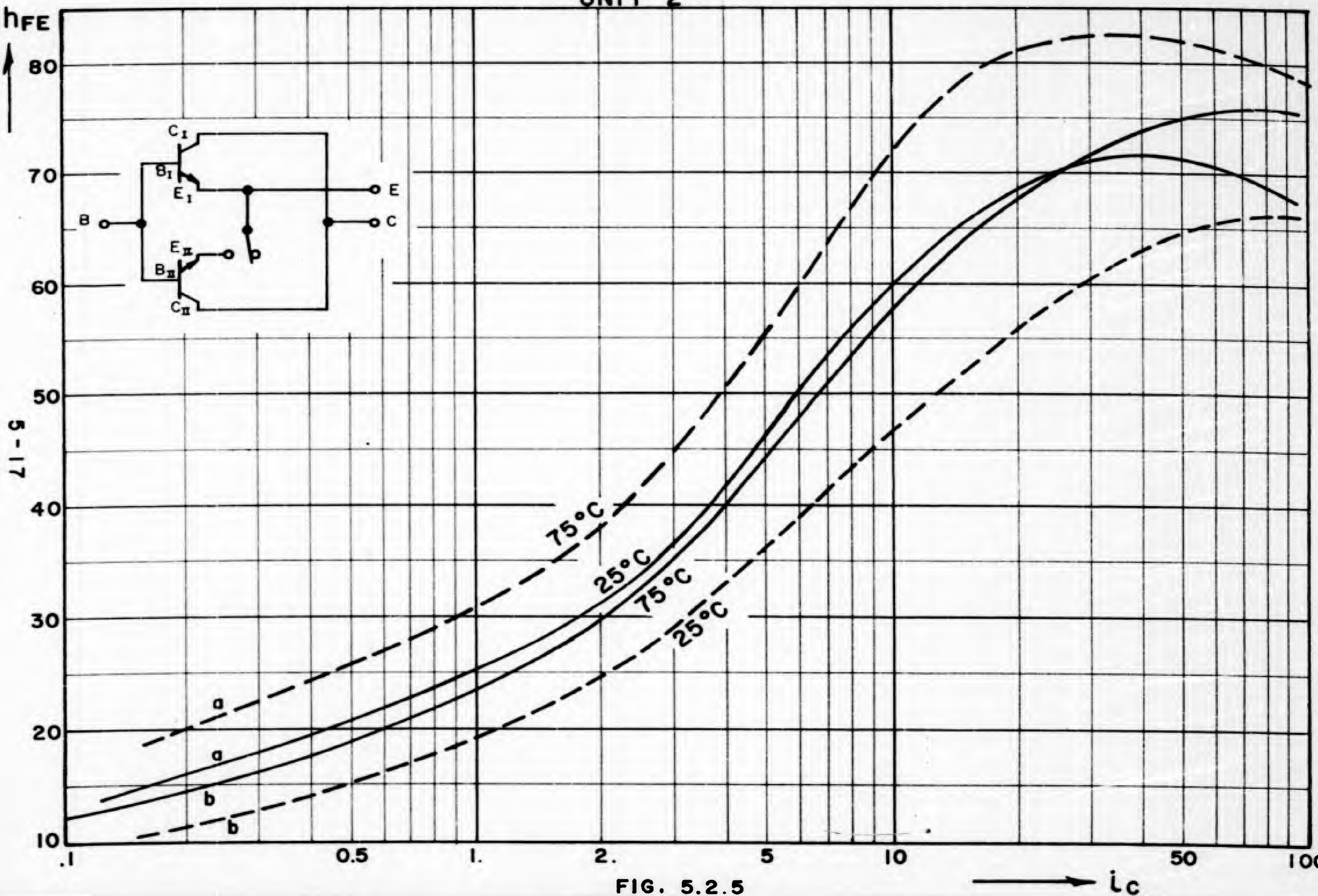


FIG. 5.2.5

performance and compensation. In Figure VII-1 and 2 the sharp increase at 65°C was due to a defective unit which had a poor surface and not due to lack of compensation. At higher current levels this effect is swamped out. This point emphasizes the necessity for surface control.

In Figures VII-3 and 4 the compensation at higher current levels can be seen.

5.3 Diode in Parallel With the Emitter Junction

The circuit of Figure 5.3.1 was constructed to provide an analogue device to study the effect of a diode on $h_{FE}$ compensation. The curves of Figures 5.3.2 and 5.3.3 depict the actual results and are abstracted in Figure 5.3.4.

In Figure 5.3.4 the curve shows the combination of diode and transistor at room temperature as curve a. It should be noted that the transistor was a 2N697, and the diode was the emitter of a second 2N697 to simulate the conditions of actual assembly where the diode and transistor would be fabricated by the same series of diffusions. Curve b shows the increase of $h_{FE}$ due to heating, while the diode was held at 25°C. Curve c shows the effect of heating the diode with transistor at 25°C, and curve d shows the

**TRANSISTOR WITH FORWARD BIASED DIODE IN PARALLEL CIRCUIT TO THE EMITTER JUNCTION**

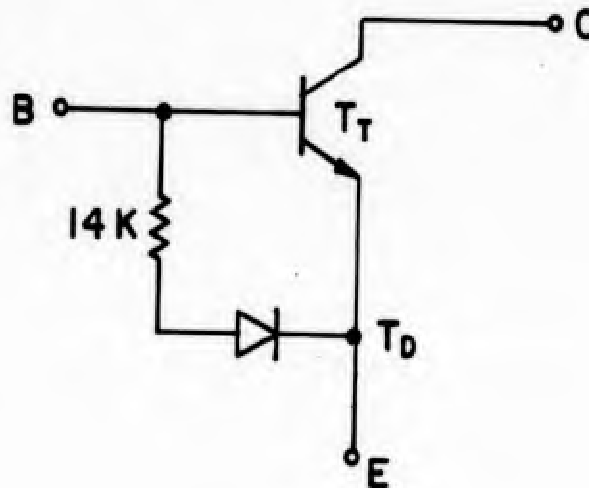


$T_T$ = TRANSISTOR TEMPERATURE

$T_D$ = DIODE TEMPERATURE

a. $T_T = T_D = 25°C$

b. $T_T = 75°C$ $T_D = 25°C$

c. $T_T = 25°C$ $T_D = 75°C$

d. $T_T = T_D = 75°C$

Fig. 5.3.1

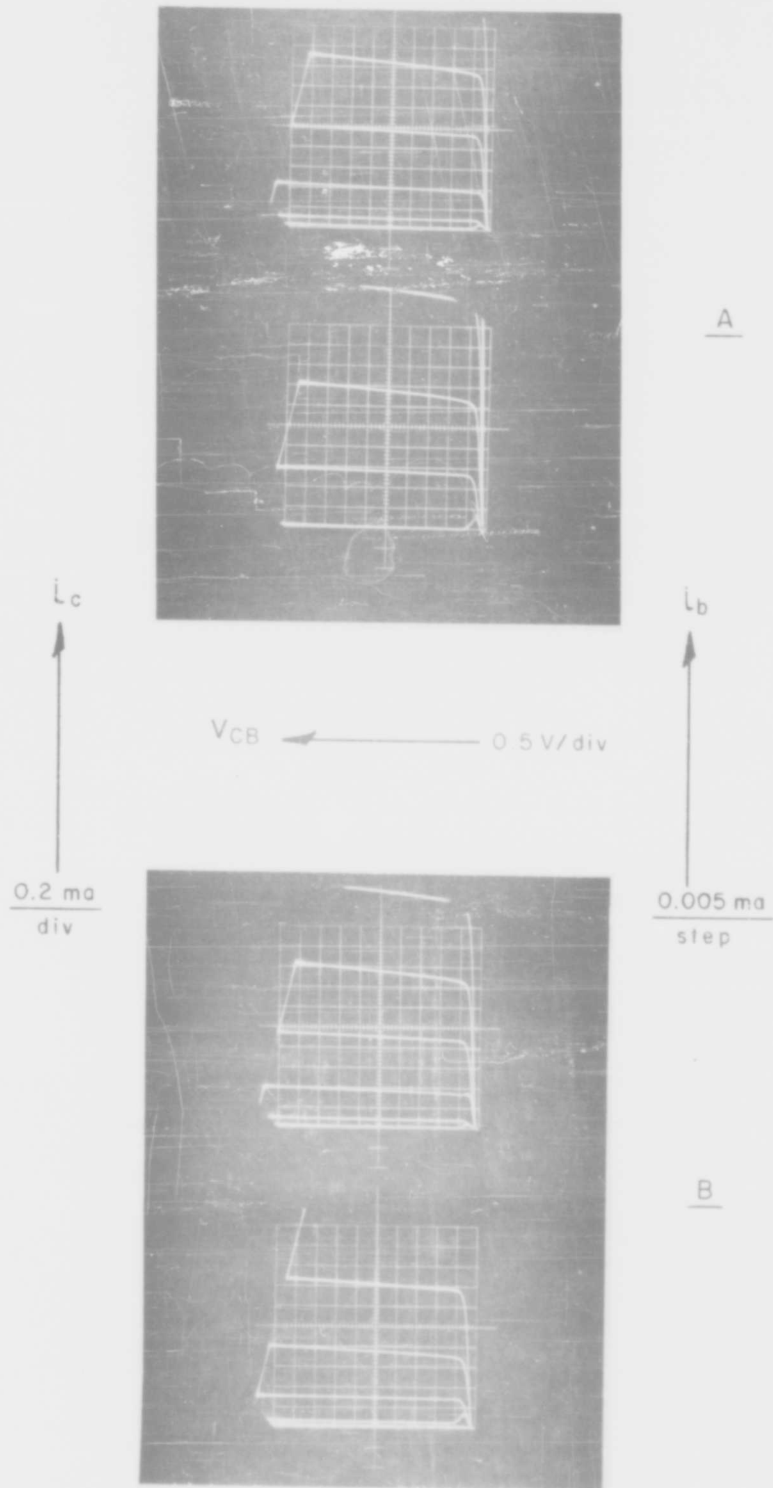


Fig. 5.3.2

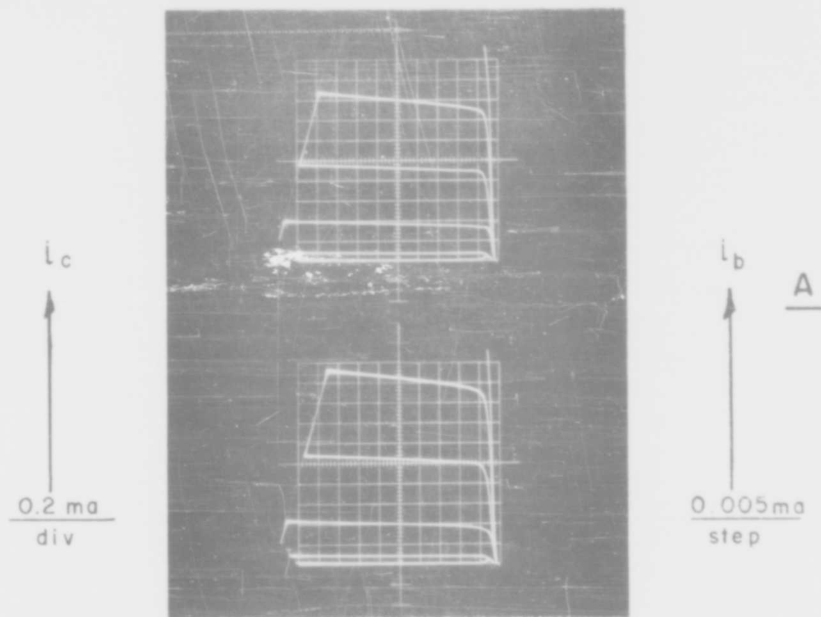


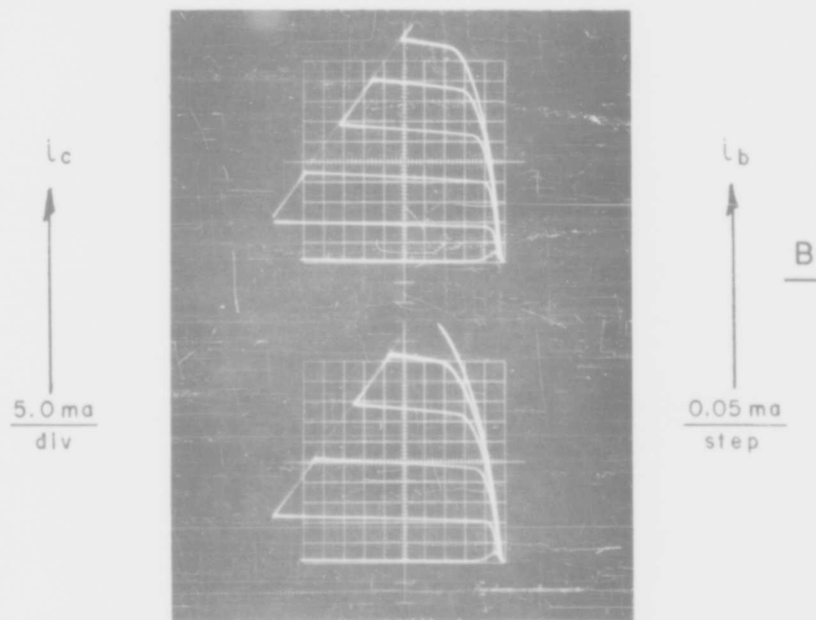


Fig. 5.3.3

## TEMPERATURE DEPENDENCY OF D.C. CURRENT GAIN $h_{FE}$

a. $T_T = T_D = 25°C$
b. $T_T = 75°C$
   $T_D = 25°C$
c. $T_T = 25°C$
   $T_D = 75°C$
d. $T_T = T_D = 75°C$

$T_D$ = DIODE TEMPERATURE

$T_T$ = TRANSISTOR TEMPERATURE

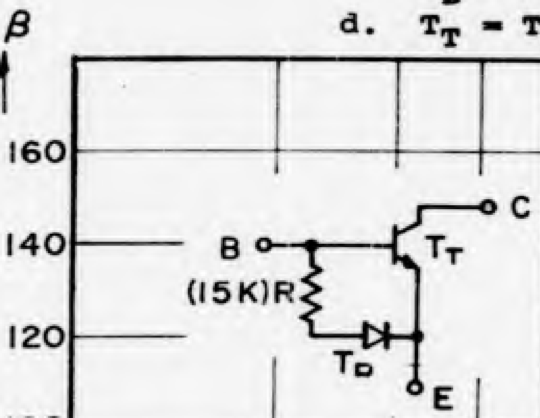


$h_{FE} = f(I_C)$

β
160
140
120
100
80
60
40
20
.01
.1
1
b
d
a
c
$I_C$

FIG. 5.3.4

compensation with diode and transistor hot, compared to curve a with the diode and transistor cold.

The compensation in this case is excellent. See for example Section 3.5 and Appendix III.

Appendix VI depicts the measurement circuit, Figure VI-1A, and additional data showing temperature compensation with resistors of different values. As the value of R increases, the degree of compensation decreases, and the device performance increases. A compromise is necessary for a single device structure between $h_{FE}$ compensation and magnitude. The compensation here is better at low current levels than at high current levels. Note also that the relative change of $h_{FE}$ with the parallel diode is sharply reduced.

5.4 Inverted Transistor Measurements

In order to explore the inverted transistor temperature behavior, devices were inversely connected and a very low value of $h_{FE}$ resulted with no temperature variation.

This effect was explained in Section 3.5. In the current flow map (Fig. 3.5.1), it can be seen that a large amount of the injected emitter current is not collected by the collector due to the geometry of the inverted device.

These minority carriers recombine and cause a large increase of the base current and, therefore, decrease the $h_{FE}$. This additional current comes from a forward biased diode in an equivalent parallel circuit with the transistor emitter junction.

Although the $h_{FE}$ from a conventional device is too low to be useful, this concept will be explored further.

## 6.0 CONCLUSIONS

An investigation of the Webster equation, Fletcher effect, and Shockely space charge recombination phenomena has led to at least four possible approaches for the design and construction of a transistor with an $h_{FE}$ which is compensated for temperature change over the range 0°C to 80°C.

The feasibility of these approaches has been partially tested by the construction of circuit analogues and observation of the desired compensation of $h_{FE}$ with temperature.

It can be concluded that a so-called "planar" or oxide masked structure will be required to achieve the desired results, that a geometry which can vary the effective emitter conduction will provide $h_{FE}$ compensation at high current densities, and that a parallel "distributed" transistor with an f(T) resistive connection between emitters can provide compensation at low current levels as well as a diode in parallel with the emitter-base region of the transistor. An f(T) resistor between two parallel transistors with $\beta_1 \neq \beta_2$ can provide compensation at higher current levels.

Since in general the $h_{FE}$ increases with temperature, compensation can be achieved by a "feed-back" of part of the increased gain to offset the change.

A judicious combination of elements presented in this report appears feasible which can result in temperature compensation of $h_{FE}$ without any sacrifice of device performance.

It further appears that the final device will be distributed in nature.

## 7.0 PROGRAM FOR NEXT INTERVAL

The development of the theory will be continued with the emphasis being on re-examining the gain equation for geometries more akin to those currently under consideration and to include the effects of space charge recombination for the low current density case.

The exploration of the offset collector and distributed device geometries will continue. Surface recombination control will be considered further.

Practical methods of building such devices will be developed more fully, especially the "built-in" temperature sensitive resistors, and preliminary procedures will be resolved.

Calculation of the base resistance will be extended to more complex geometries.

Analogue maps of carrier patterns will be considered as an aid to theory development and extension.

## 8.0 LIST OF REFERENCES


1. On the Variation of Junction-Transistor Current Amplification Factor With Emitter Current, Proc. IRE, Vol. 42, pp. 914 - 920, June (1951).

2. W. W. Gärtner, Transistors Principles, Design and Applications, pp. 86 - 88, Van Nostrand, (1960).

3. Op. Cit. Gartner, pp. 45.

4. E. M. Conwell, Properties of Silicon and Germanium, Proc. IRE, 40, pp. 1330, Nov. (1952).

5. Biondi, Transistor Technology, Vol. II, pp. 410.

6. W. W. Gärtner, Temperature Dependence of Junction Transistor Parameters, Proc. IRE, Vol. 45, pp. 669, Fig. 11, May (1957).

7. N. H. Fletcher, Self-Bias Cutoff Effect in Power Transistors, Proc. IRE, Vol. 43, p. 1669, Nov. (1955).

8. N. H. Fletcher, Some Aspects of the Design of Power Transistors, Proc. IRE, pp. 551 - 559, May (1955).

9. W. Shockley, Bell System Tech. Jrnl., Vol. 28, p. 138, July (1949).

10. Sah, Noyce, & Shockley, Carrier Generation and Regeneration in P-N Junctions and P-N Junction Characteristics, Proc. IRE, Vol. 45, pp. 1228 - 1243, Sept. (1957).

11. V. H. Grinich, R. N. Noyce, & R. T. Kikoshima, Paper presented at IRE Wescon, August 18, 1959.

12. The standard test circuits use a 1 KΩ resistor in series with the base. The transistor base spreading resistor is usually much smaller than 1 KΩ, which justifies the assumption $I_e$ = const.

13. C. T. Sah, "A New Semiconductor Tetrode", Wescon Convention paper #32/2, San Francisco, Aug. (1961).

14. W. W. Gärtner, Op. Cit, Ref. 2, p. 87.

15. V. H. Grinich, R. N. Noyce, & R. T. Kikoshima, "Silicon Mesa Transistors for Use as Saturating Switches," IRE Wescon (1959).

16. G. Backenstoss, Evaluation of the Surface Concentration of Diffused Layers in Silicon, Bell System Tech. Jrnl., Vol. 37, pp. 699 - 712, May (1958).

17. E. Tannenbaum, Detailed Analysis of Thin Phosphorous Diffused Layers in P-Type Silicon, Solid-State Electronics, Vol. 2, pp. 123 - 132, Pergamon Press (1961).

18. Biondi, Transistor Technology, Vol. III, p. 72, Fig. 4, Van Nostrand (1958) - (Article by C. S. Fuller, Diffusion Techniques).

19. F. M. Smits, Formation of Junction Structures by Solid State Diffusion, Proc. IRE, Vol. 46, pp. 1049 - 1061, June (1958).

# APPENDIX I.

Temperature Insensitive Transistor

R. F. Q. Specs

| | | | |
|---|---|---|---|
| $h_{FE}$ | >50 | $I_c$ = 0.5 mA | $V_{CE}$ = 5v |
| $h_{FE}$ | >70 | $I_c$ = 2.0 mA | $V_{CE}$ = 5v |
| $h_{FE}$ | >50 | $I_c$ = 20 mA | $V_{CE}$ = 5v |
| $V_{CE}$ sat | < 0.7v | $I_c$ = 20 mA | $I_b$ = 1 mA |
| $I_{CBO}$ | < 1.0μA | $V_{cb}$ = 30 v | |
| $f_{\alpha B}$ | >20Mc/s | $V_{cb}$ = 5v | $I_c$ = 2 mA |

Variation at all bias points not to vary by more than 10% of $0^\circ$C value in the range 0 - 75°C.

Additional Requirements From Statement of Work

| | | | |
|---|---|---|---|
| $I_{cbo}$ | <0.1μA | $V_{cb}$ = 15v | |
| $V_{cbo}$ | >50v | $I_{cb}$ = 100μA | |
| $V_{CER}$ | >30v | $I_{CE}$ = 10 mA | $R_{bE}$ = 10 Ω |
| $V_{CE}$ sat | < 0.6v | $I_c$ = 10 mA | $I_b$ = 1 mA |
| $V_{bE}$ sat | < 0.9v | $I_c$ = 10 mA | $I_b$ = 1 mA |

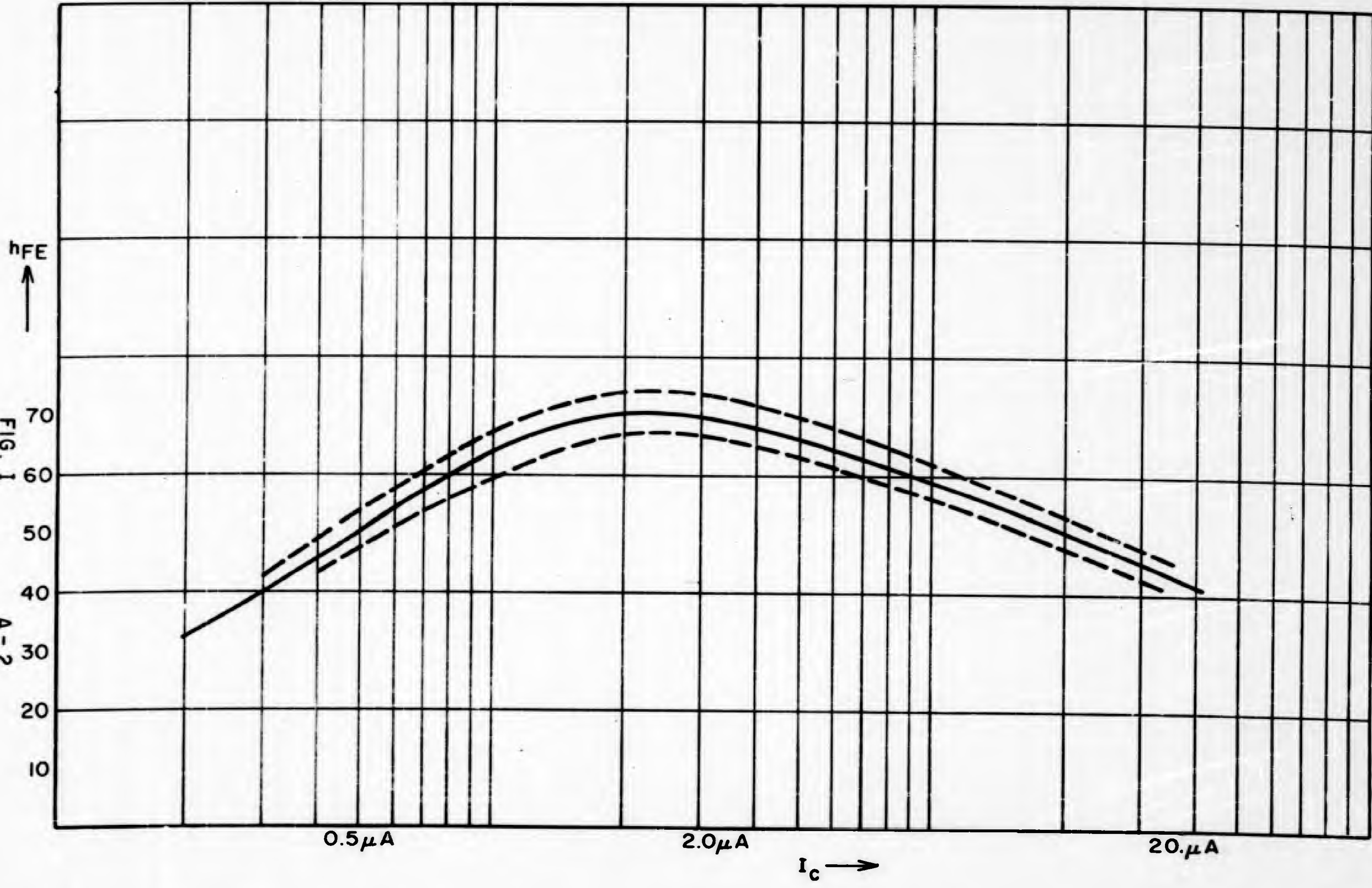

FIG. I

A - 2

## APPENDIX II

**Two Transistors in Parallel Circuit** (R = 0)

1. $\beta_1 = I_{C_1}/I_{B_1}$ current gain of first transistor

2. $\beta_2 = I_{C_2}/I_{B_2}$ current gain of second transistor

3. $\beta = I_{C_1} + I_{C_2}/I_{B_1} + I_{B_2}$ current gain of both transistors in parallel circuit

4. $I_{E_1}/I_{E_2} = \left[(\beta_1 + 1)\ \beta_2/(\beta_2 + 1)\ \beta_1\right]\ I_{C_1}/I_{C_2}$

$$= D_{n_1}\ N_{o_1}\ L_{n_2}/D_{n_2}\ N_{o_2}\ L_{n_1} = C^* \qquad (V_{EB_1} = V_{EB_2})$$

5. $I_{C_1}/I_{C_2} = C^* \left[(\beta_2 + 1)\ \beta_1/(\beta_1 + 1)\ \beta_2\right]$

$$C^* = \frac{1}{C}$$

6. $I_{C_2}/I_{C_1} = C \left[(\beta_1 + 1)\ \beta_2/(\beta_2 + 1)\ \beta_1\right]$

---

Eq. 2 + Eq. 1 = Eq. 7 $$I_{B_1} + I_{B_2} = \frac{\beta_2\ I_{C_1} + \beta_1\ I_{C_2}}{\beta_1\ \beta_2}$$

Eq. 7 + Eq. 3 = Eq. 8 $$\beta = \left(\frac{I_{C_1} + I_{C_2}}{\beta_2\ I_{C_1} + \beta_1\ I_{C_2}}\right) \beta_1\ \beta_2$$

Eq. 8 + Eq. 6 = Eq. 9 $$\beta = \frac{(1 + I_{C_2}/I_{C_1})}{(\beta_2 + \beta_1\ I_{C_2}/I_{C_1})}\ \beta_1\ \beta_2$$

$$\beta = \frac{\left\{1 + C\ \left[(\beta_1 + 1)\ \beta_2/(\beta_2 + 1)\beta_1\right]\right\}}{\beta_2 + C\beta_1\ \left[(\beta_1 + 1)\ \beta_2/(\beta_2 + 1)\beta_1\right]}\ \beta_1\ \beta_2$$

$$\beta = \frac{1 + C\ [\ldots\ldots]}{(\beta_2/\beta_1) + C\ [\ldots\ldots]}\ \beta_2$$

10. $$\frac{(\beta_1 + 1)\, \beta_2}{(\beta_2 + 1)\, \beta_1} = A$$

11. $$\beta = \beta_2 \cdot \left( \frac{1 + CA}{\beta_2/\beta_1 + CA} \right)$$

**Discussion of 11.**

Assumption $C = 1$

$$\beta = \beta_2 \left( \frac{1 + A}{\beta_2/\beta_1 + A} \right)$$

a) $\underline{\beta_1 = \beta_2}$ $\quad A = 1,\ \beta = \beta_2$

b) $\underline{\beta_1 >> \beta_2}$ $\quad \beta_2 >> 1,\ A = 1$

$\beta = 2\beta_2$

c) $\underline{\beta_2 >> \beta_1}$ $\quad \beta_1 >> 1,\ A = 1$

$\beta = 2\beta_1$

d) $\underline{\beta_1 = 2\beta_2}$ $\quad \beta_2 >> 1,\ A = \frac{2\,\beta_2 + 1}{2\,(\beta_2 + 1)}$

$\beta = \frac{4}{3}\beta_2$

e)

| | | | |
|---|---|---|---|
| $\beta_1 = 50$ | $\beta_2 = 30$ | $\beta = 37.5$ | $(A \approx 1)$ |
| $\beta_1 = 70$ | $\beta_2 = 50$ | $\beta = 58$ | $(A \approx 1)$ |
| $\beta_1 = 100$ | $\beta_2 = 60$ | $\beta = 75$ | $(A \approx 1)$ |

## APPENDIX III

**Diode Parallel to Emitter-Base Junction** (Common Emitter)

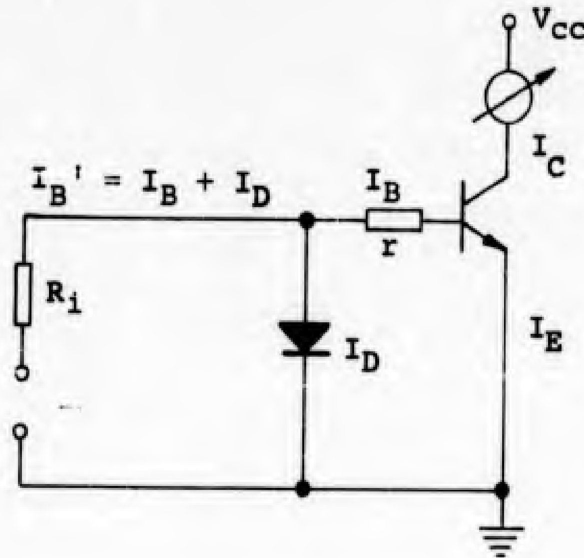


1. $$\beta_O = \frac{I_C}{I_B}$$

2. $$\beta = \frac{I_C}{I_B'} < \beta_O$$

$$\frac{1}{\beta} = \frac{I_B + I_D}{I_C} = \frac{1}{\beta_O} + \frac{I_D}{I_C}$$

3. $$\frac{1}{\beta} = \frac{1}{\beta_O} + \frac{I_D}{I_C} = \frac{1}{\beta_O} \left(1 + \frac{I_D}{I_B}\right)$$

Changing of $\beta$ with temperature:

$$\frac{\partial}{\partial T}\left(\frac{1}{\beta}\right) = \frac{\partial}{\partial T}\left(\frac{1}{\beta_O}\right) + \frac{\partial}{\partial T}\left(\frac{I_D}{I_C}\right) \quad \text{or}$$

4. $$\frac{\partial}{\partial T}\left(\frac{1}{\beta}\right) = \left(1 + \frac{I_D}{I_B}\right) \frac{\partial}{\partial T}\left(\frac{1}{\beta_0}\right) + \frac{1}{\beta_0} \frac{\partial}{\partial T}\left(\frac{I_D}{I_B}\right)$$

<u>Discussion</u>:

a. $\frac{\partial}{\partial T}\left(\frac{1}{\beta_0}\right)$.

$\beta_0$ increases with temperature, therefore, $\frac{1}{\beta_0}$ decreases.

b. $\frac{\partial}{\partial T}\left(\frac{I_D}{I_B}\right)$.

$$\frac{\partial}{\partial T}\left(\frac{I_D}{I_B}\right) = \frac{\partial}{\partial T}\left(\frac{I_D}{I_E\ (1-\alpha)}\right) \approx \frac{I_D}{I_E} \frac{\partial}{\partial T} \beta_0$$

$I_E$, $I_D$, and $\alpha$ increase with temperature. The whole expression $\frac{I_D}{I_E\ (1-\alpha)}$ increases.

We get a temperature independent $\beta$ if

$$\left(1 + \frac{I_D}{I_B}\right) \cdot \left|\frac{\partial}{\partial T}\left(\frac{1}{\beta_0}\right)\right| = -\frac{1}{\beta_0}\left|\frac{\partial}{\partial T}\left(\frac{I_D}{I_E\ (1-\alpha)}\right)\right|.$$

or

$$\left(1 + \frac{I_D}{I_B}\right)\left|\frac{\partial}{\partial T}\left(\frac{1}{\beta_0}\right)\right| \approx -\frac{1}{\beta_0}\left(\frac{I_D}{I_E}\right)\left|\frac{\partial}{\partial T} \beta_0\right|$$

# APPENDIX IV

**Emitter Efficiency $\gamma$ :**

$$\gamma = \left(1 - \frac{W}{L_n} \cdot \frac{\sigma_B}{\sigma_E}\right)$$

According to Gärtner: (minority carrier diff. length)[6].

$L_{Emitter} \approx 1 \times 10^{-3}$ cm $(\sim 10\mu)$

$L_{Coll.} \approx 2.5 \times 10^{-2}$ cm

$L_{Base} \approx 2.0 \times 10^{-2}$ cm

Beside this we know:

$W \approx 1 \times 10^{-4}$ cm

$$\frac{W}{L_{Base}} \approx \frac{10^{-4}}{2 \times 10^{-2}} = 5 \times 10^{-3} .$$

**Calculation of $\sigma_B$, $\sigma_E$, and $\sigma_C$:**

$$\sigma_C \approx \frac{1}{0.85} \Omega cm^{-1} = 1.18 \left[\Omega cm\right]^{-1}$$

$$\sigma_B \approx \frac{1}{\rho_s^* \cdot W} = \frac{1}{6.12 \times 10^3 \times 10^{-4}} = \frac{1}{0.612} = 1.63 \left[\Omega cm\right]^{-1}$$

$$\sigma_E \approx \frac{1}{\rho_s X_j} \quad \text{because } L_E > X_j$$

$$\sigma_E \approx \frac{1}{2 \times 2 \times 10^{-4}} = 2.5 \times 10^3 \left[\Omega cm\right]^{-1}$$

Using the equation $\gamma = \left(1 - \frac{W}{L_n} \cdot \frac{\sigma_B}{\sigma_E}\right)$ we get

$$\gamma = \left(1 - 5 \times 10^{-3} \times \frac{1.63}{2.5 \times 10^{3}}\right) = (1 - 3.26 \times 10^{-6}) \approx \underline{\underline{1.00}}$$

for the inverted transistor:

$$\gamma_i = \left(1 - 5 \times 10^{-3} \cdot \frac{1.18}{1.63}\right) = (1 - 3.62 \times 10^{-3}) = \underline{\underline{0.9964}}$$

---

$$\alpha = \gamma \left(1 - \frac{A_s W}{D A_e}\right) \left[1 - \frac{1}{2}\left(\frac{W}{L_n}\right)^2\right]$$

$$\alpha = \gamma \cdot K$$

$$K = \left(1 - \frac{A_s W}{D A_e}\right) \left[1 - \frac{1}{2}\left(\frac{W}{L_n}\right)^2\right]$$

1. Assumption: $\underline{K = 0.99}$

$\alpha_I = 0.99$ $\qquad$ $\beta_I = 99$

$\alpha_{II} = 0.99 \times 0.99 = 0.98$ $\qquad$ $\beta_{II} = 49$

2. $\underline{K = 0.98}$

$\alpha_I = 0.98$ $\qquad$ $\beta_I = 49$

$\alpha_{II} = 0.98 \times 0.99 = 0.97$ $\qquad$ $\beta_{II} = 32$

3. $\underline{K = 0.97}$

$\alpha_I = 0.97$ $\qquad$ $\beta_I = 32$

$\alpha_{II} = 0.97 \times 0.99 = 0.96$ $\qquad$ $\beta_{II} = 24$

$\alpha_{II}$, $\beta_{II}$ = inverted current gain.

The experiments give, on the other hand, inverted $h_{FE}$'s in the order of one. That means the geometry effect must be responsible for the low $h_{FE}$'s.

## APPENDIX V.

### Explanation of $a = (\tan \phi_2 - \tan \phi_1)$

The expression for a regular linear graded junction (Fig. V-1) is

$$(1) \qquad V_i - V_a = \frac{4}{3} \sqrt{\frac{2 E_M^3}{10^{-7} \tan \phi}}$$

$V_i$ = built-in voltage

$V_a$ = applied voltage

In the following it is shown that (1) can also be used for a double linear diffused junction (Fig. V-2) (i.e., emitter junction of a transistor) simply by substitution $\tan \phi$ by $(\tan \phi_2 - \tan \phi_1)$.

In Figs. V-1, 2, 3 the terms are defined as:

$N_o(x) = N_B$ = const.
the n-type background doping

$N_1(x)$ = linear p-type distribution
(Boron, Gallium)

$N_2(x)$ = linear n-type distribution
(Phosphorus)

$N_3(x) = N_2(x) + N_B$
The total n-type doping

To get (1) we have to integrate Poisson's equation

Emitter junction of
n-p-n transistor

N
p-type
$N_B$
$\phi$
$N_O(X)$
n-type
$x_j$ (emitter junction)
X →

Fig. V-1

N
$N_1(x)$ (p-type)
$N_3(x) = N_2(x) + C_B$
$N_2(x)$ n-type
$N_B$
$N_o(x)$
n-type
$x_j$ (emitter junction)
X →

Fig. V-2

N
$N_B$
$N(o)$
$\phi_1$
$\phi_2$
$N_1(x)$
$N_2(x)$
0
X
X →

Fig. V-3

(2) $\frac{\partial^2 V}{\partial x^2} = - \frac{q \cdot \Delta N}{\varepsilon \varepsilon_o}$ , whereby

(3) $\Delta N = N_1 (x) - \left[ N_2(x) + N_B \right]$ Fig. V-2

(4) $N(O) - N_1(x) = x \tan \phi_1$

(5) $N(O) - \left[ N_2 + N_B \right] = x \tan \phi_2$

(5) - (4) = (6)

$$\Delta N = N_1 - \left[ N_2 + N_B \right] = x \left[ \tan \phi_2 - \tan \phi_1 \right]$$

(6) in (2)

(7) $\frac{\partial^2 V}{\partial x^2} = - \frac{q}{\varepsilon \varepsilon_o} \left[ \tan \phi_2 - \tan \phi_1 \right] x$

(8) $\frac{\partial^2 V}{\partial x^2} = - \frac{q}{\varepsilon \varepsilon_o} \tan \phi \; x$

A comparison of (7) and (8) shows that because $\tan \phi$, $\left[ \tan \phi_2 - \tan \phi_1 \right]$ are constant, we can use the integral of (8) by substituting $\tan \phi$ by $\left[ \tan \phi_2 - \tan \phi_1 \right]$.

(9) $V_i - V_a = \frac{4}{3} \sqrt{\frac{2 \, E_M^3}{10^{-7} \tan \phi_2 - \tan \phi_1}}$

## APPENDIX V-a

Dimension of $K$:

$$K = \frac{q}{\varepsilon \varepsilon_o} \cdot \tan \phi$$

q [coulomb] coulomb = ampere x sec.

$\varepsilon$ number (for Si $\varepsilon = 12$)

$\varepsilon_o$ [A sec./V cm]

$\tan \phi$ $[cm^{-4}]$

so,

$$K \left[\frac{A \text{ x sec. x } cm^{-4}}{A \text{ x sec./V cm}}\right] = K\left[V\ cm^{-3}\right]$$

Proof:

$$w = \left(\frac{3}{2}\ \frac{V}{K}\right)^{1/3}$$

w [cm]

$$\frac{V}{K}\ \left[\frac{V}{V\ cm^{-3}}\right] = \left[cm^3\right]$$

$$\left(\frac{V}{K}\right)^{1/3} = cm$$

2.2.1 $$\tan \phi = \frac{N_s}{(\pi Dt)^{1/2}}\ e^{-\left(\frac{x_j^2}{4Dt}\right)}$$

$$N_B = N_s \text{ erfc } \frac{x_j}{(4Dt)^{1/2}}$$

# APPENDIX VI

Experimental Data for Section 3.5

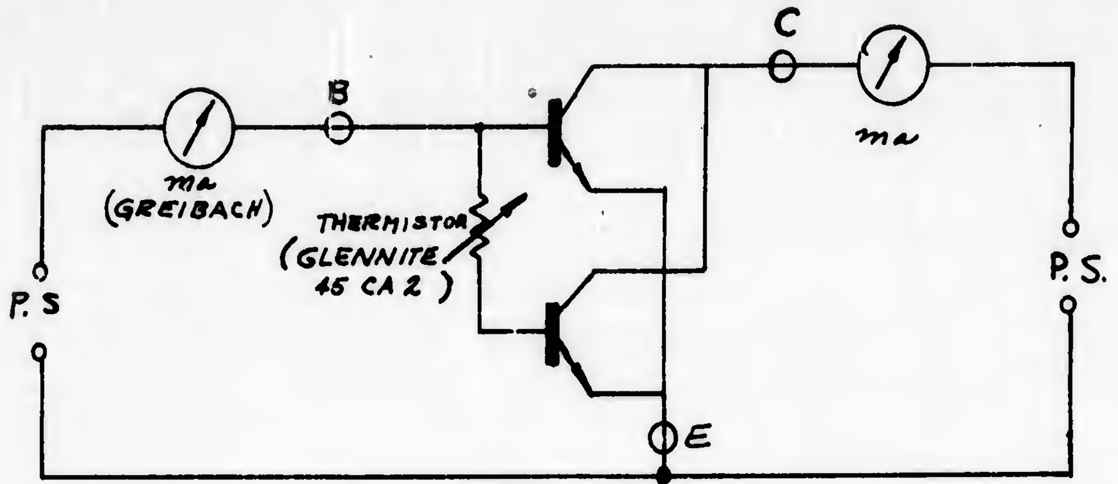


FIG. VII-1B

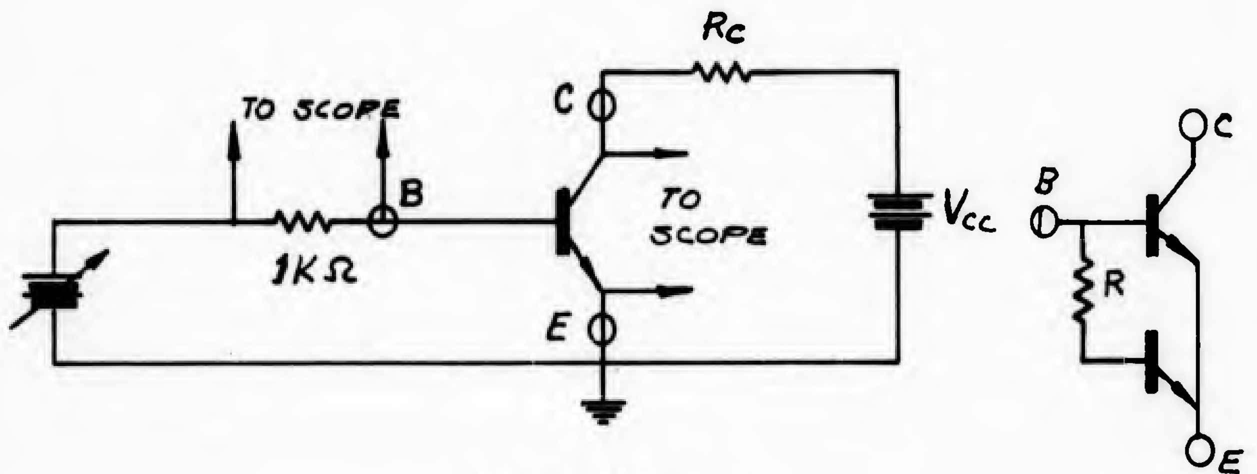


FIG. VI-1B

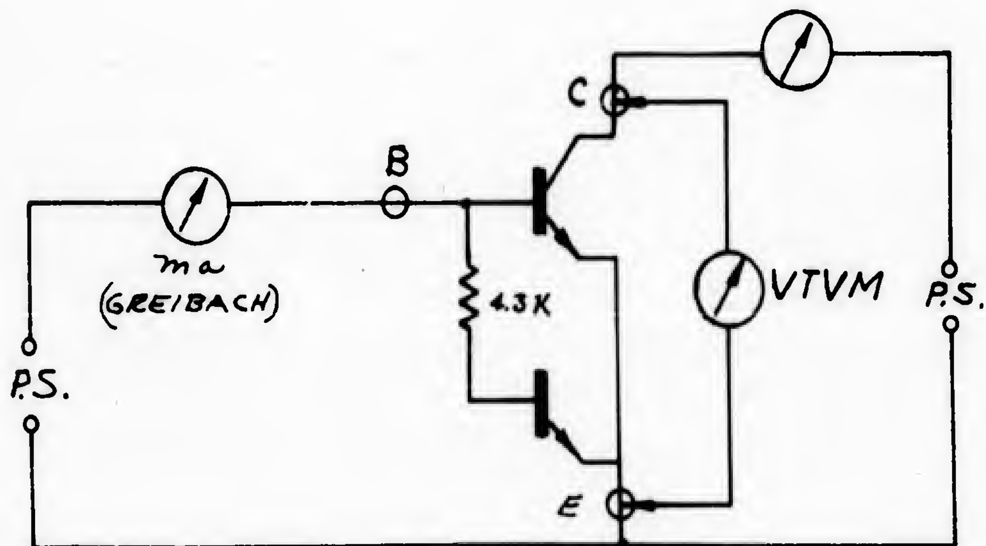


FIG. VI-1A

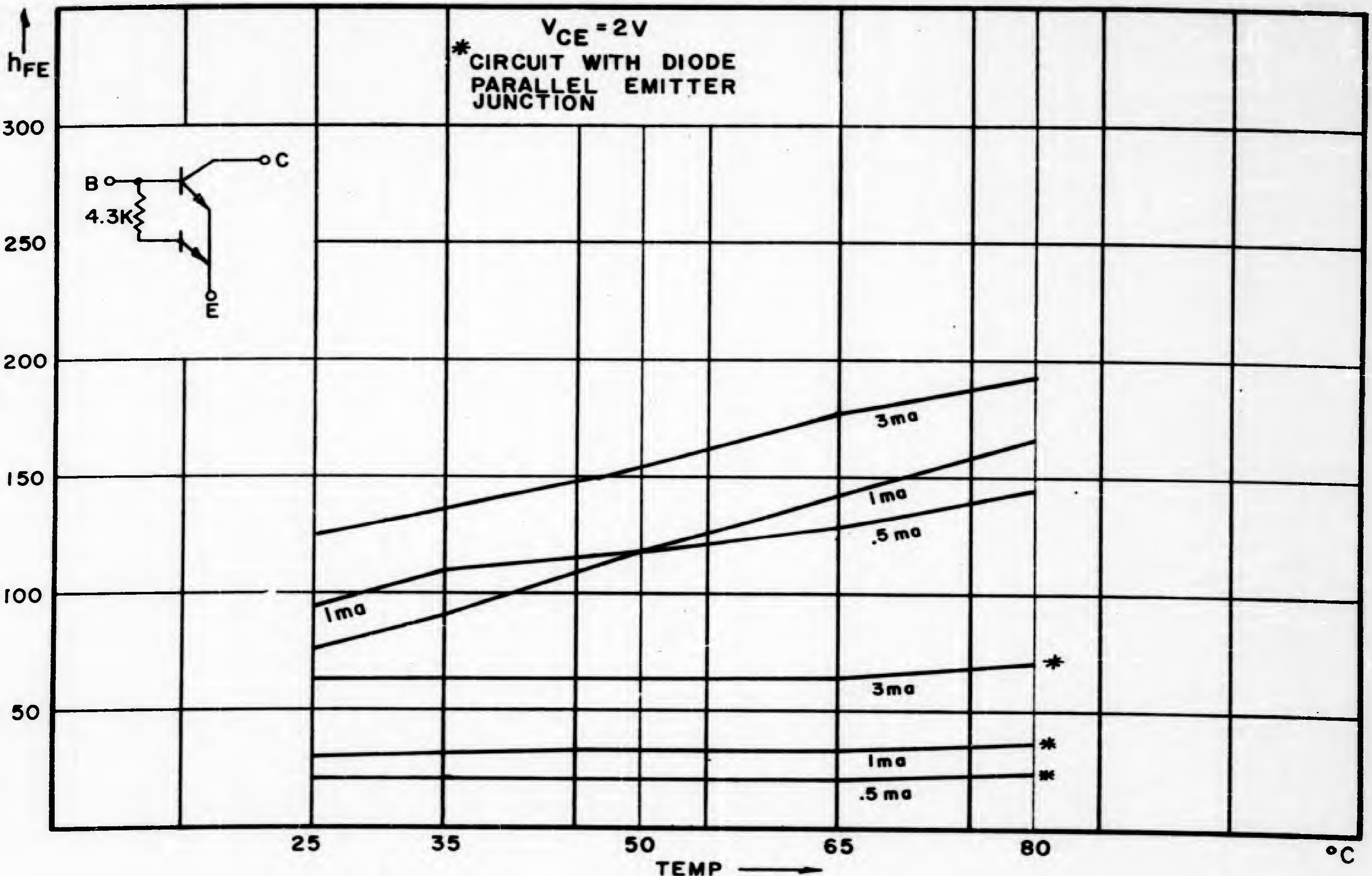

Fig. VI - 1

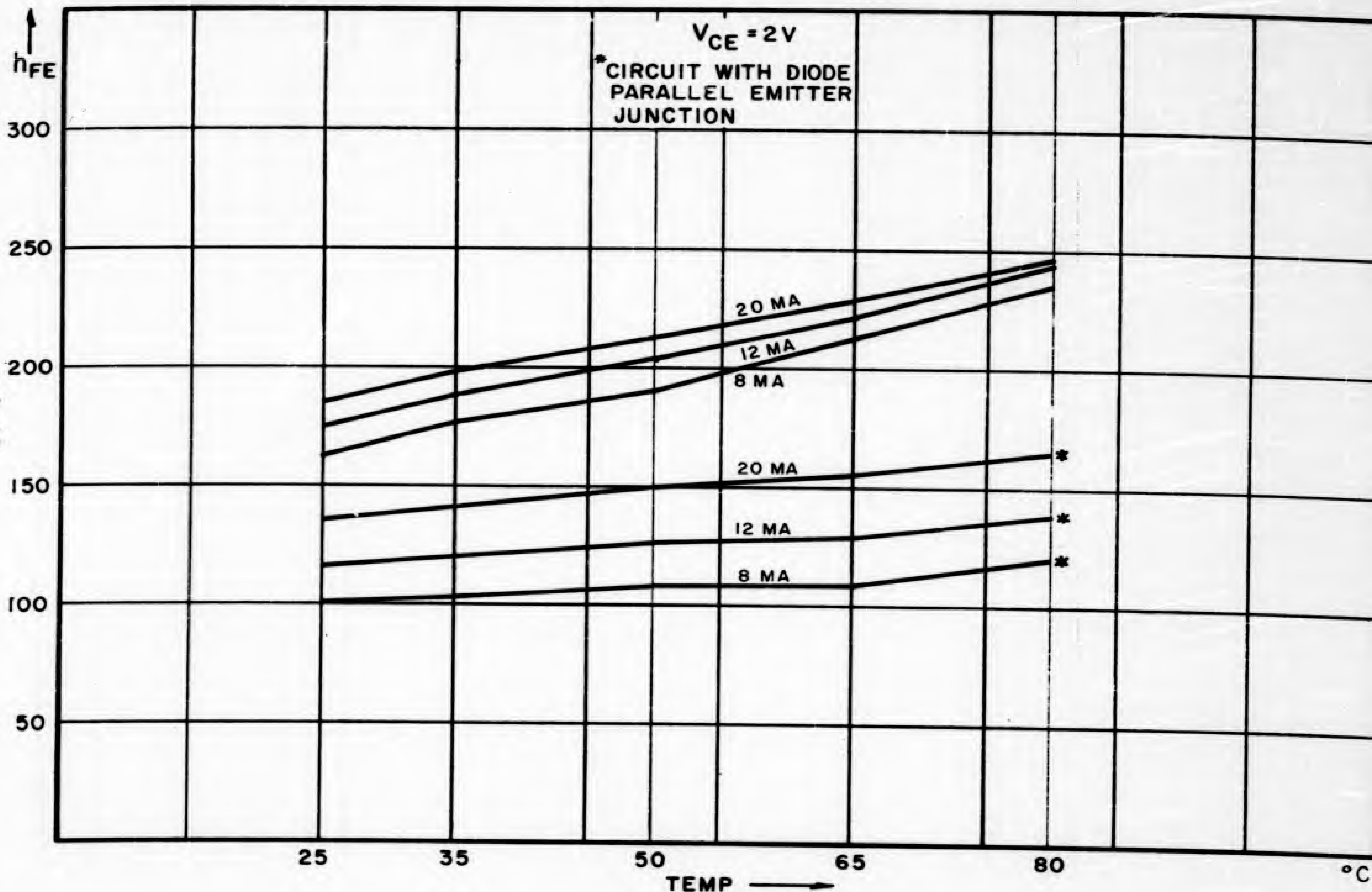


Fig. VI-2

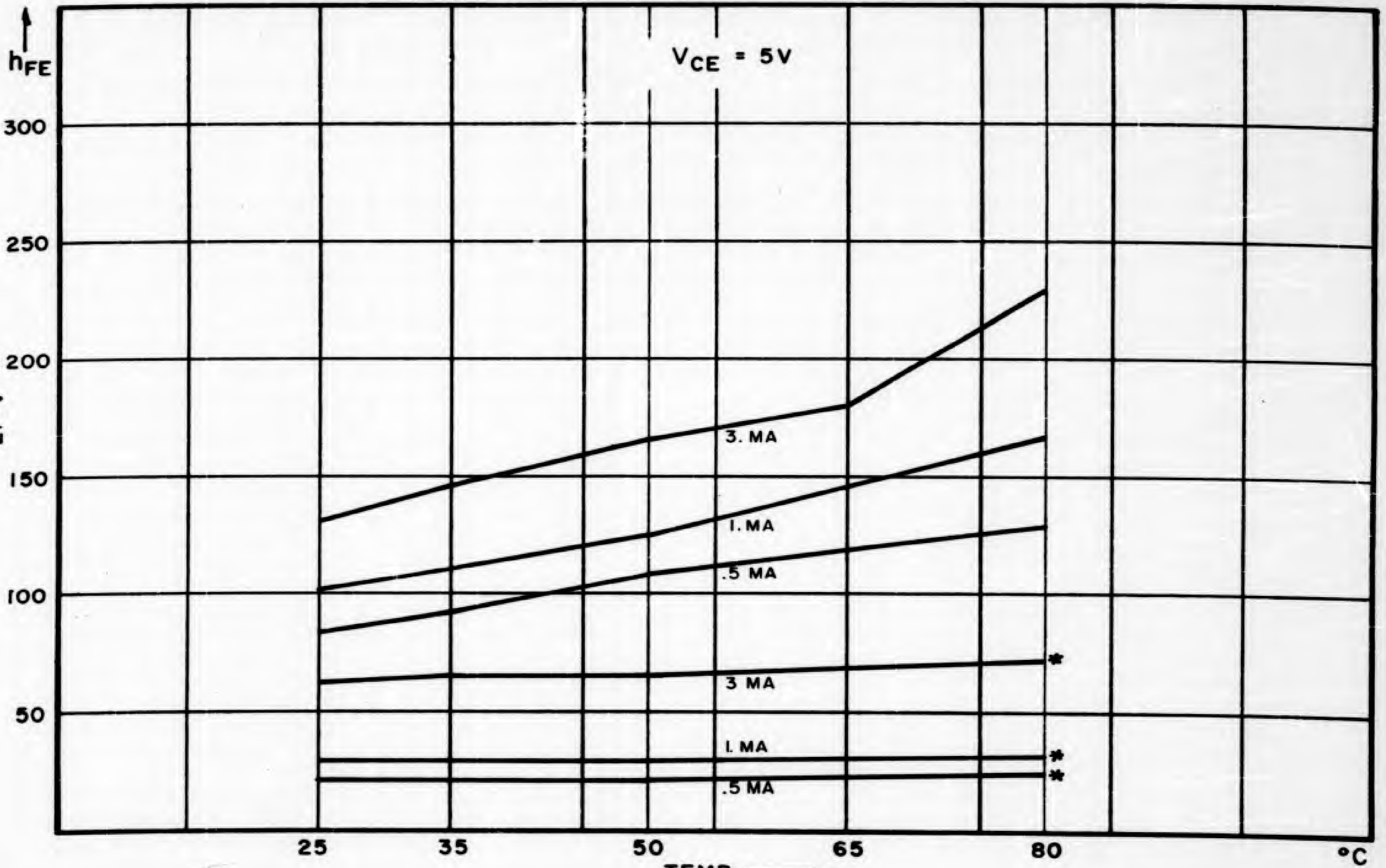


Fig. VI -3

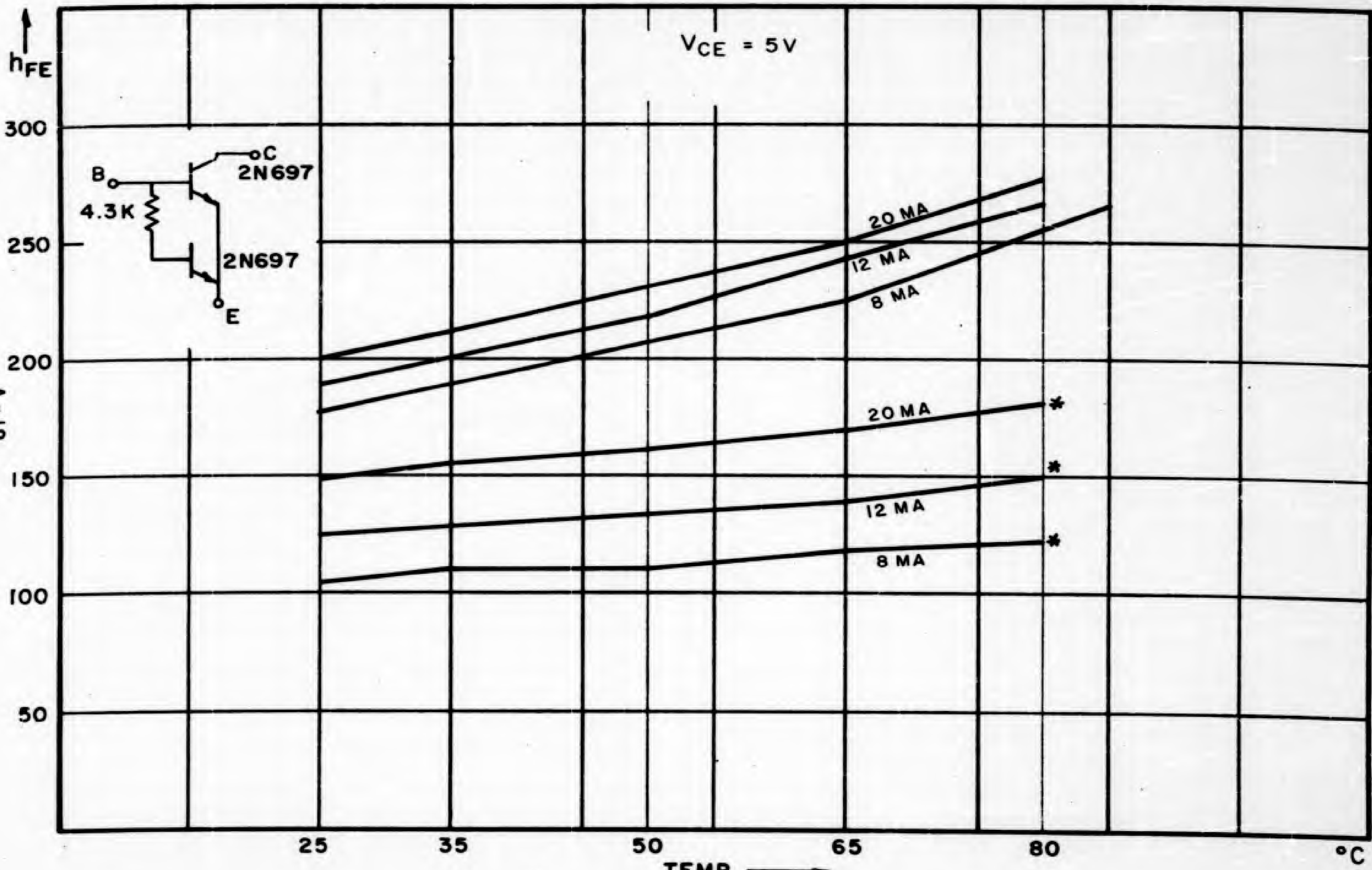


Fig. VI-4

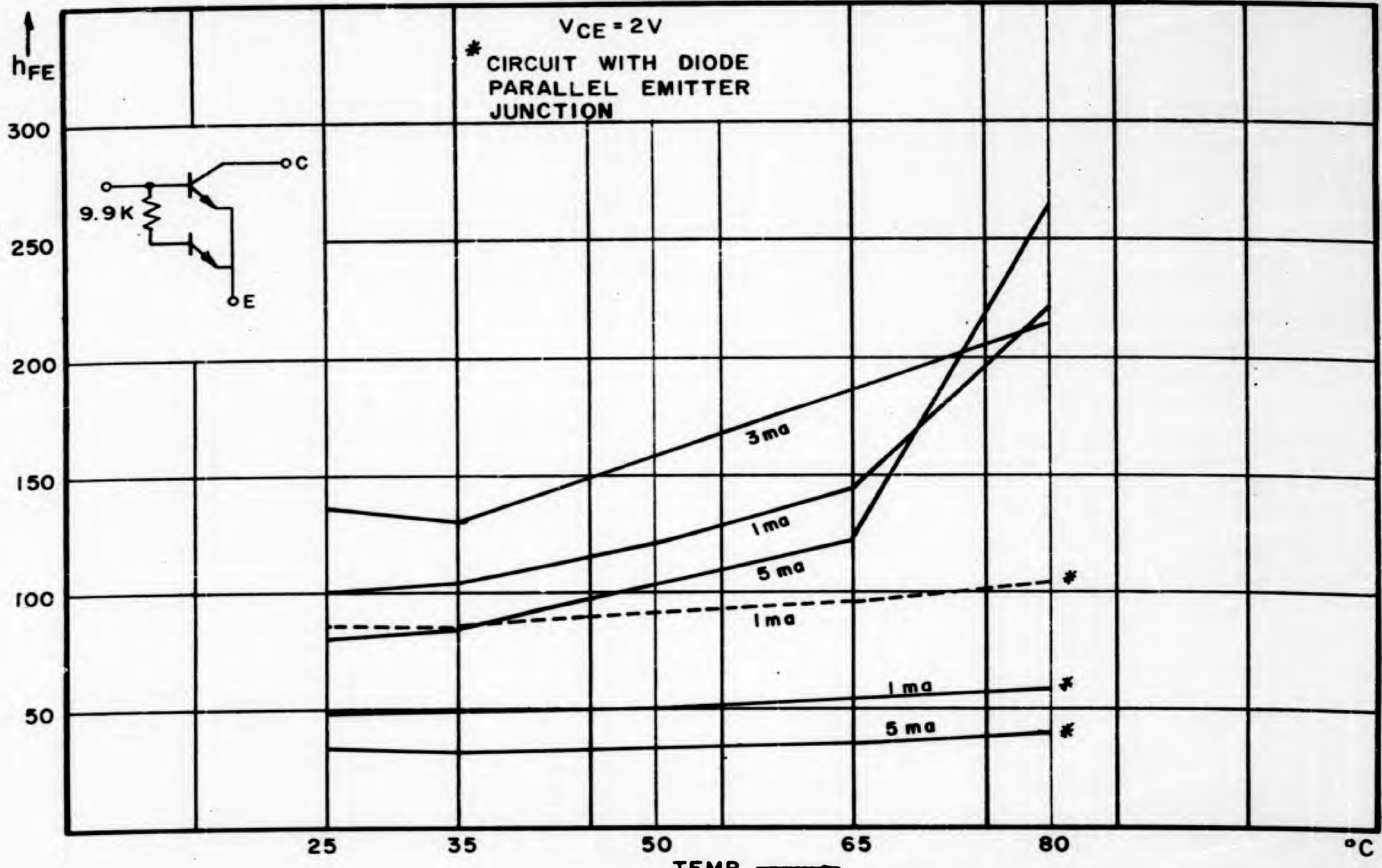


Fig. VI-5

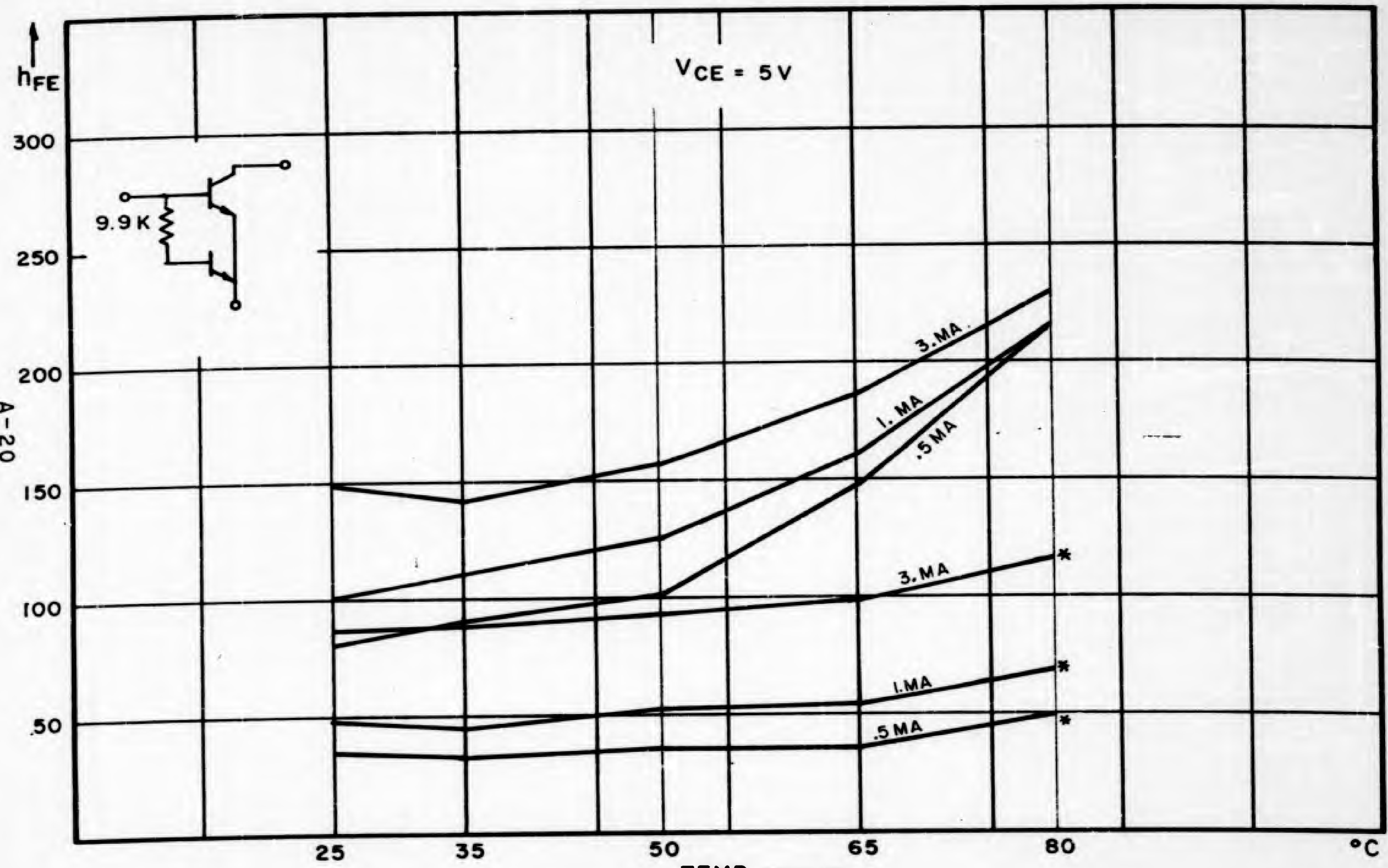


Fig. VI-6

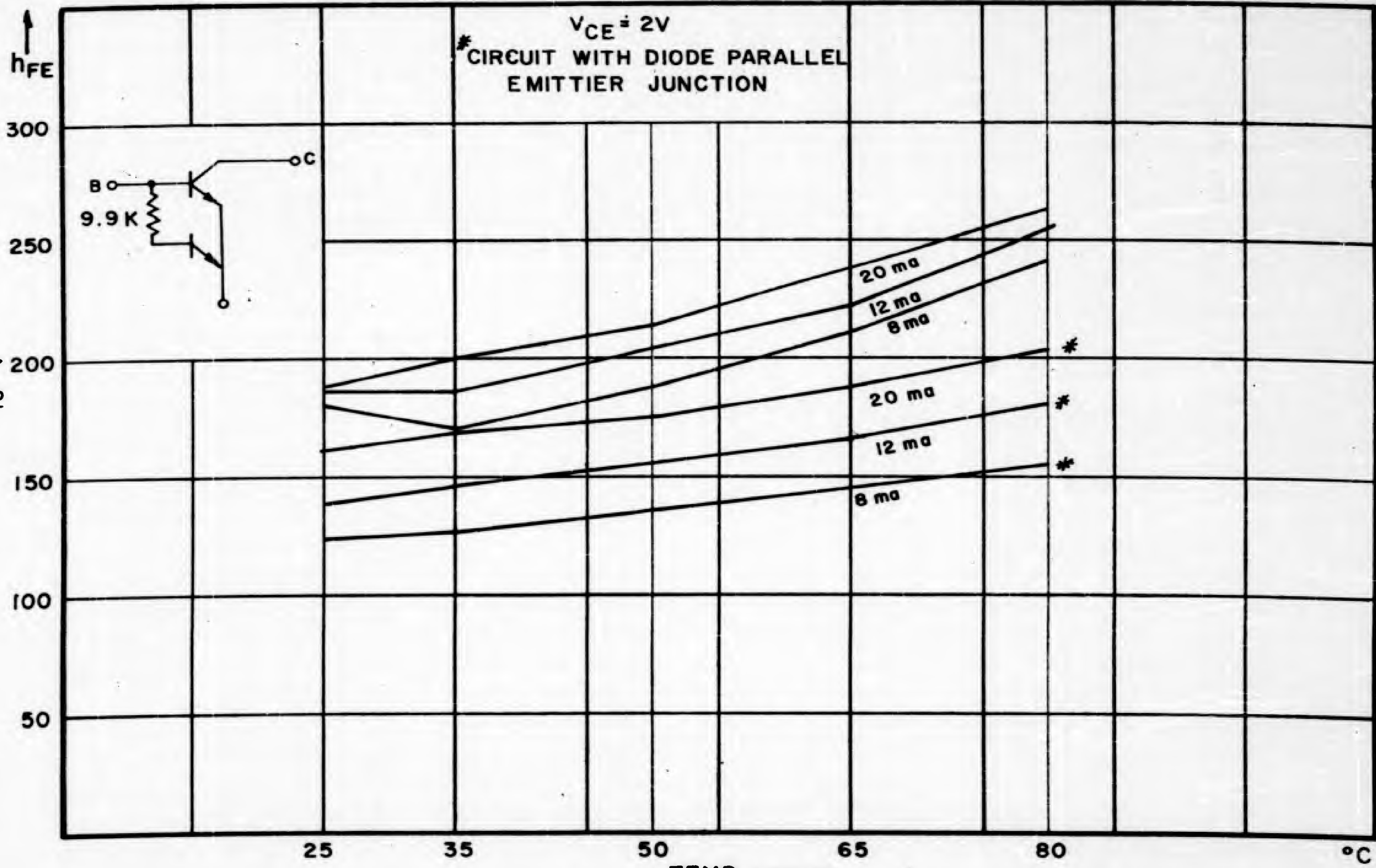


Fig. VI-7

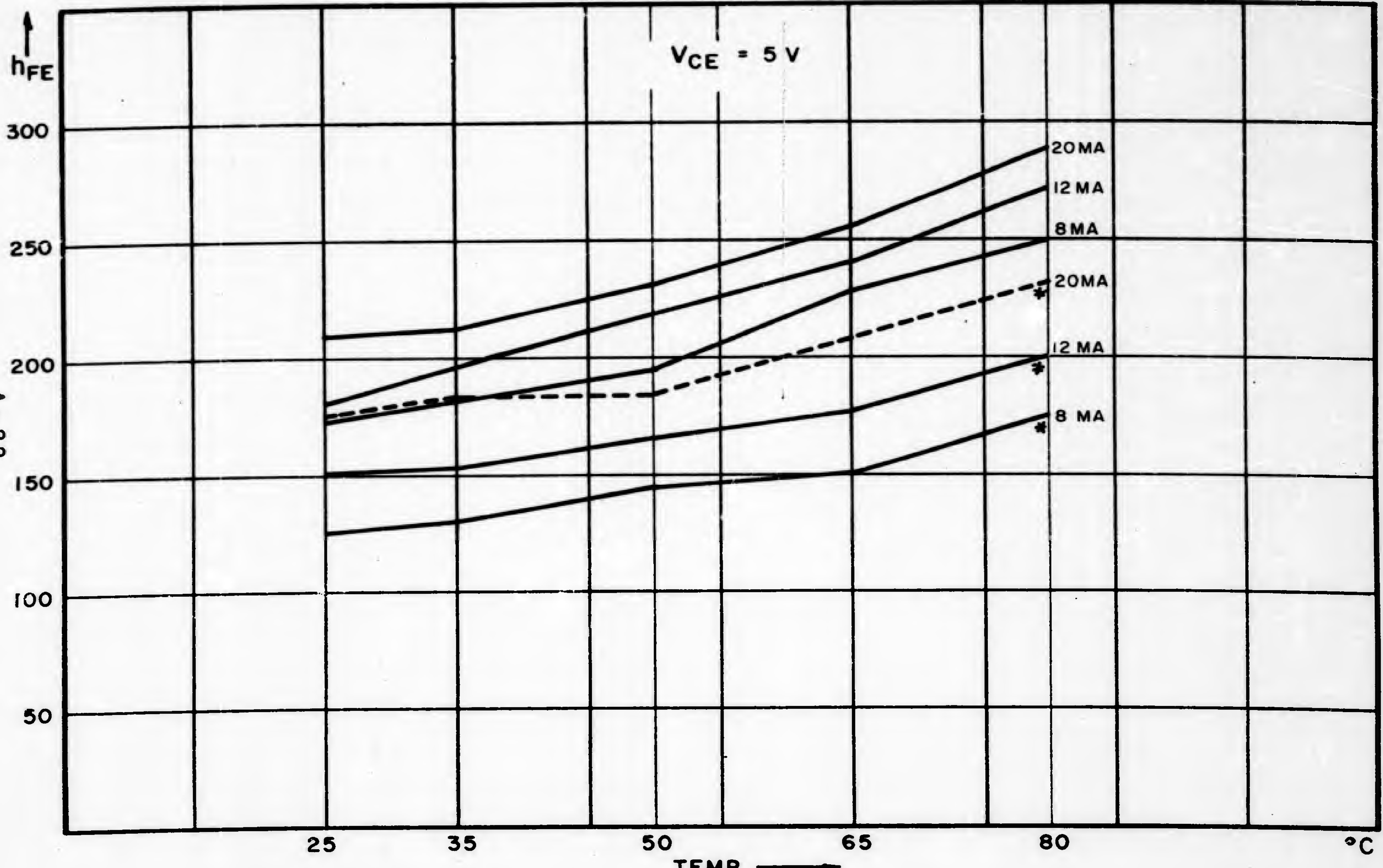


Fig. VI-8

# APPENDIX VII

Experimental Data for Section 3.4

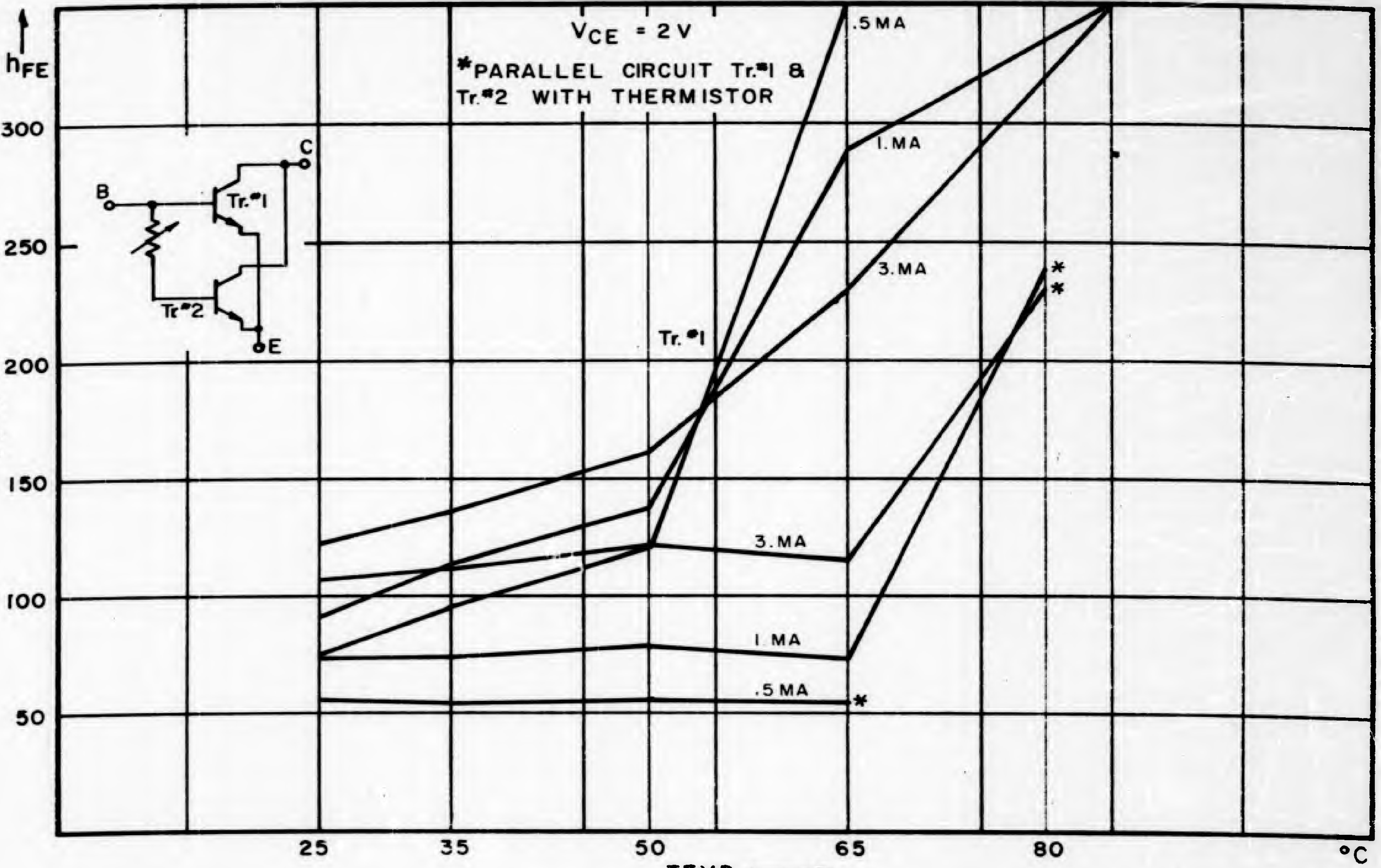


Fig. VII -1

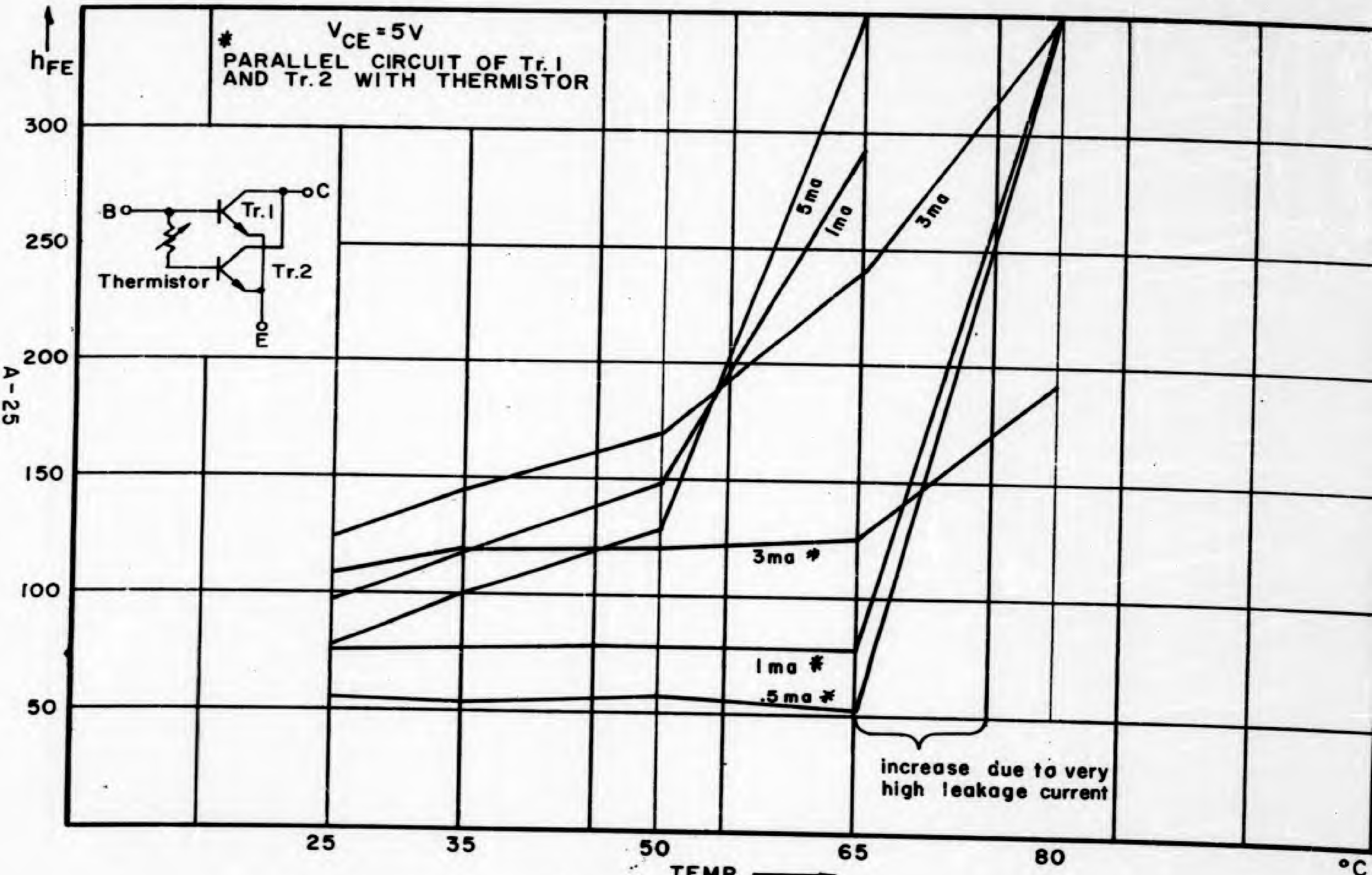

Fig. VII - 2

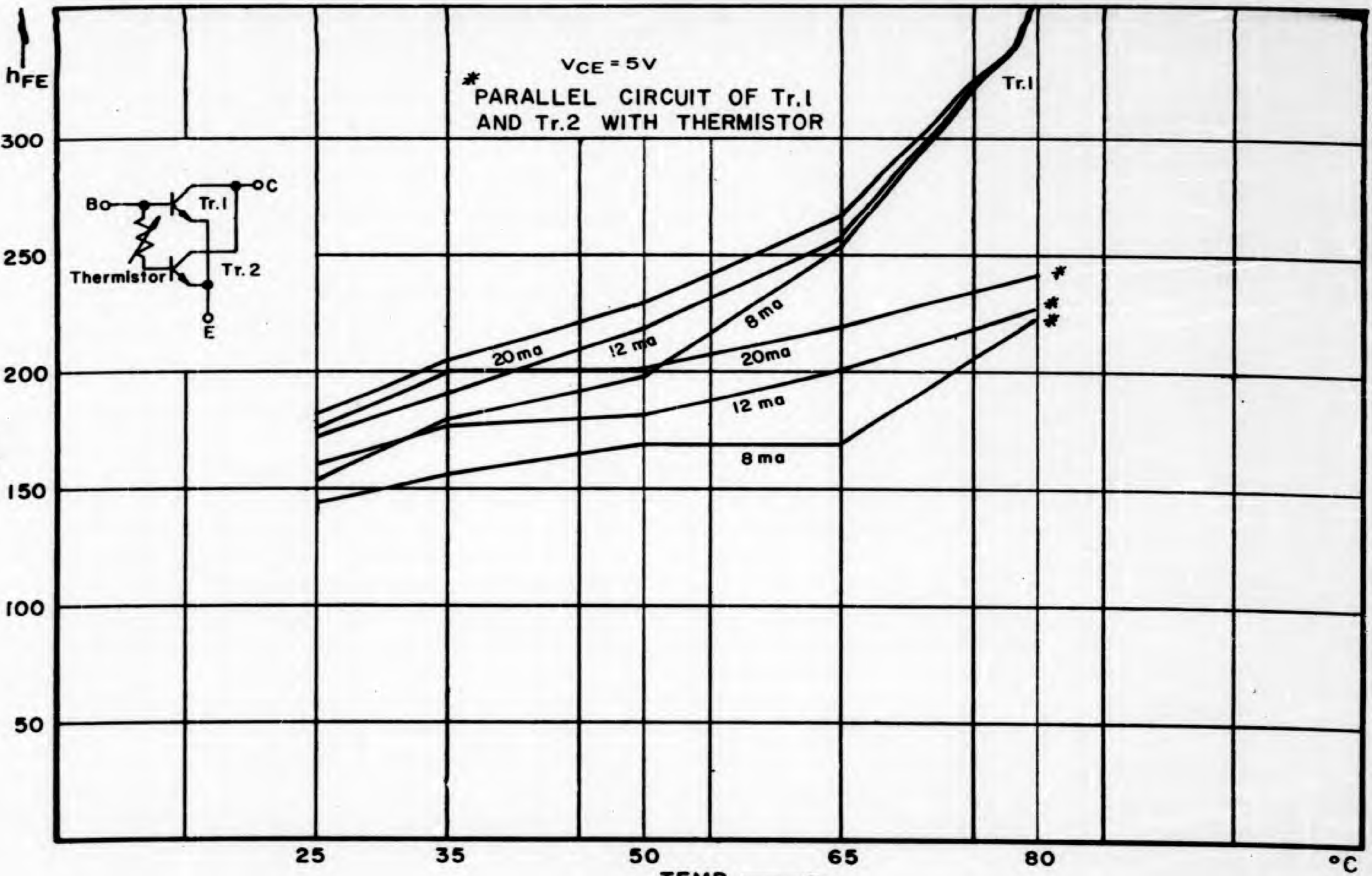


Fig. VII - 4

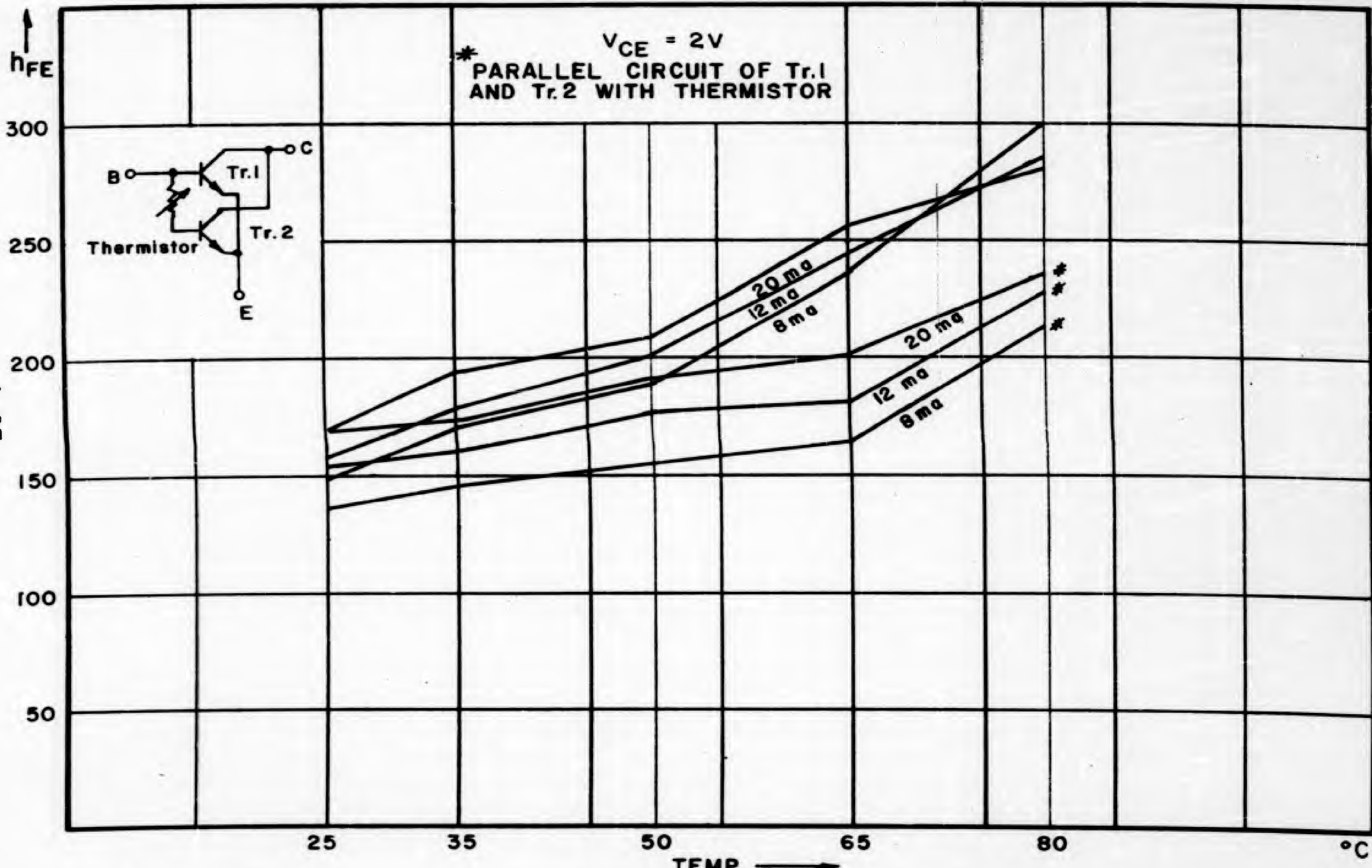


Fig. VII - 3

## APPENDIX VIII

### Identification of Key Personnel

| | |
|---|---|
| Technical Director | Dr. P. N. Russell |
| Project Supervisor | J. Spanos |
| Senior Personnel | Dr. R. Epple |
| | H. Stuy |
| | Dr. F. Woitsch |
| Engineers | D. Johnson |
| | G. Koen |
| | L. Garasi |
| | N. Long |
| | P. Muschinske |
| Junior Personnel | S. Purdy |
| | B. Jackson |
| | P. Soo |
| | F. Marentes |
| | R. Gomez |

UNCLASSIFIED

UNCLASSIFIED